

Aus dem Zentralinstitut für Seelische Gesundheit  
der Medizinischen Fakultät Mannheim  
(Direktor: Prof. Dr. med. Andreas Meyer-Lindenberg)

**Corticostriatal circuitry function and plasticity during  
working memory learning**

Inauguraldissertation  
zur Erlangung des medizinischen Doktorgrades  
der  
Medizinischen Fakultät Mannheim  
der Ruprecht-Karls-Universität  
zu  
Heidelberg

vorgelegt von  
Lena Sophie Geiger-Primo (geb. Geiger)  
aus  
Tscheljabinsk, Russland  
2021

Dekan: Herr Prof. Dr. med. Sergij Goerd

Doktormutter: Frau Prof. Dr. phil. Dr. med. Heike Tost

"The brain is a monstrous, beautiful mess. Its billions of nerve cells – called neurons – lie in a tangled web that displays cognitive powers far exceeding any of the silicon machines we have built to mimic it."

William F. Allman<sup>1</sup>

---

<sup>1</sup> Allman, W. F. (1989). *Apprentices of Wonder: Inside the Neural Network Revolution*: Bantam Books.

# Table of contents

ABBREVIATIONS.....	V
<b>1. INTRODUCTION.....</b>	<b>1</b>
1.1 A BRIEF INTRODUCTION INTO CORTICOSTRIATAL CIRCUIT ANATOMY AND FUNCTION .....	1
1.2 BASAL GANGLIA FUNCTION .....	4
1.3 STRIATAL NEUROCHEMISTRY & GENETIC INFLUENCES.....	5
1.4 BASAL GANGLIA DYSFUNCTION .....	8
1.5 MEMORY AND LEARNING.....	10
1.6 AIMS.....	15
<b>2. EMPIRICAL STUDIES .....</b>	<b>17</b>
2.1 STUDY 1: NOVELTY MODULATES HUMAN STRIATAL ACTIVATION AND PREFRONTAL–STRIATAL EFFECTIVE CONNECTIVITY DURING WORKING MEMORY ENCODING .....	17
2.1.1 <i>Abstract</i> .....	17
2.1.2 <i>Methods</i> .....	17
2.1.3 <i>Results</i> .....	24
2.1.4 <i>Supplemental analyses</i> .....	29
2.2 STUDY 2: LONGITUDINAL BEHAVIORAL AND BRAIN FUNCTIONAL EFFECTS OF A PLASTICITY-RELATED VARIANT IN BDNF ON VERBAL WORKING MEMORY LEARNING.....	31
2.2.1 <i>Abstract</i> .....	31
2.2.2 <i>Methods</i> .....	32
2.2.3 <i>Results</i> .....	39
<b>3. DISCUSSION .....</b>	<b>47</b>
3.1 RESULTS OF THE CROSS-SECTIONAL STUDY (STUDY 1) .....	47
3.2 RESULTS OF THE LONGITUDINAL STUDY (STUDY 2) .....	50
3.3 STERNBERG WORKING MEMORY TASK AND CORTICOSTRIATAL CIRCUITRIES.....	53
3.4 LIMITATIONS AND FURTHER DIRECTIONS .....	54
<b>4. SUMMARY .....</b>	<b>56</b>
<b>5. REFERENCES.....</b>	<b>58</b>
<b>6. SUPPLEMENTAL TABLES .....</b>	<b>73</b>
<b>7. CURRICULUM VITAE.....</b>	<b>78</b>
<b>8. ACKNOWLEDGMENTS .....</b>	<b>81</b>

## Abbreviations

AAL	Automated anatomical labeling
AMPA	$\alpha$ -Amino-3-Hydroxy-5-Methyl-4-Isoxazolpropionacid
ANOVA	Analysis of variance
AU	Arbitrary units
BA	Brodmann area
BDNF	Brain-derived-neurotrophic factor
BG	basal ganglia
BMS	Bayesian model selection
BPA	Bayesian Parameter Averaging
BR	Brain response
CA	Cornu Ammonis
CI	Confidence interval
COMT	Catechol-O-methyltransferase
DAT	Dopamine transporter
DCM	Dynamic causal modeling
DLPFC	Dorsolateral prefrontal cortex
EOI	Effects of interest
EN	Encoding novel
EP	Encoding practice
EPI	Echo planar imaging
FC	Functional connectivity
fMRI	Functional magnetic resonance imaging
FoV	Field of view
FWE	Family-wise error
FWHM	Full-width at half-maximum
GABA	Gamma-aminobutyric-acid
GLM	General linear models
GPe	Globus pallidus external part
GPI	Globus pallidus internal part
gPPI	Generalized psycho-physiological interaction
GoF	Goodness of fit
GRAPPA	Generalized autocalibrating partially parallel acquisition

HRF	Hemodynamic response function
iPAT	Integrated parallel imaging techniques
LDA	Linear discriminant analysis
LRT	Likelihood ratio test
LTM	Long-term memory
LTP	Long-term potentiation
Met	Methionine
MNI	Montreal Neurological Institute
MSN	Medium spiny neuron
MR	Magnetic resonance
NMDA	N-methyl-D-aspartate
PET	Positron emission tomography
RMS	Root mean squared
RN	Retrieval novel
ROI	Region of interest
RP	Retrieval practice
RT	Reaction time
SEM	Standard error of the mean
SMA	Supplementary motor area
sFC	sustained functional connectivity
SNc	Substantia nigra pars compacta
SNr	Substantia nigra pars reticulata
SPM	Statistical Parametric Mapping
SPSS	Statistical Package for the Social Sciences
STM	Short term memory
STN	Subthalamic nucleus
STR	Striatum
TE	Echo time
tmFC	Task-modulated functional connectivity
TR	Repetition time
Val	Valine
VOI	Volume of interest
WM	Working memory

# 1. Introduction

## 1.1 A brief Introduction into corticostriatal circuit anatomy and function

The basic anatomy and functions of corticostriatal circuits are well established and have been the subject of numerous textbooks and review articles (Alexander, DeLong, & Strick, 1986; DeLong, 1990; Gerfen & Surmeier, 2011; Haber, 2003; Nelson & Kreitzer, 2014; O'Reilly & Frank, 2006; Parent & Hazrati, 1995; Seger, 2006). Briefly, human corticostriatal circuits subserves goal-directed and habitual behaviors and are organized in several multisynaptic loops, which connect a particular area of the cortex with a specific area of the basal ganglia (BG) and the thalamus, whose efferents project back to the cortex. The BG play a key role within corticostriatal circuits and consist of five subcortical nuclei, namely, nucleus caudatus (caudate), putamen, globus pallidus (pallidum), substantia nigra and subthalamic nucleus. The nucleus caudatus and putamen are also known as the striatum and form the BG input relay and an integrative hub for information processing across species (McCutcheon, Abi-Dargham, & Howes, 2019; Nelson & Kreitzer, 2014). Further, the area where the striatum is continuous is known as the ventral striatum or nucleus accumbens.

The original description of corticostriatal circuits consisted of five loops, i.e., motor, oculomotor, dorsolateral prefrontal, lateral orbitofrontal, and anterior cingulate loop (Alexander et al., 1986), a model that has been later revised to four major loops (Bohlin & Janols, 2004), thereby merging the oculomotor and the anterior cingulate loop (Chudasama & Robbins, 2006; Seger, 2006), illustrated in figure 1. The anatomy and function of corticostriatal loops are both highly regular and complicated: On the one hand, these loop-shaped neural networks run in parallel and functionally segregated from each other. At the same time, by exchanging and channeling information between nodes, they also work in an integrative fashion (Draganski et al., 2008; McCutcheon et al., 2019; Schroll & Hamker, 2013). Each loop follows a basic design and receives input from multiple cortical areas, which pass through specific regions of the striatum, pallidum, substantia nigra, thalamus subnuclei, and afterwards "closing the loop" by projecting back to its cortical origin, see figure 1 (Alexander et al., 1986; Seger, 2006).

The original description of corticostriatal circuits (Alexander et al., 1986) included a tripartite model of basal ganglia, where specific anatomical subregions are linked to certain cortical regions, e.g., caudate with prefrontal cortical regions. More research in this field has extended the original work and demonstrated a topographical segregation even within basal ganglia subregions (Kemp & Powell, 1970; Parent, 1990; Parent & Hazrati, 1995). Further, the segregation is assumed more a continuum

with overlapping boundaries than a distinct division (Draganski et al., 2008; Kim, Park, & Park, 2013). In general, there is a “rostro-caudal” and a “dorso-ventral” gradient of projections. For example, within the striatum, rostral areas are connected to cognitive domains of the cortex, e.g., prefrontal cortex, whereas more caudal areas are connected to motor areas, e.g., M1. In addition, the ventral area of the striatum, also known as nucleus accumbens, plays an important role in motivation or aversion (Draganski et al., 2008; Haber, 2003; Kim et al., 2013).

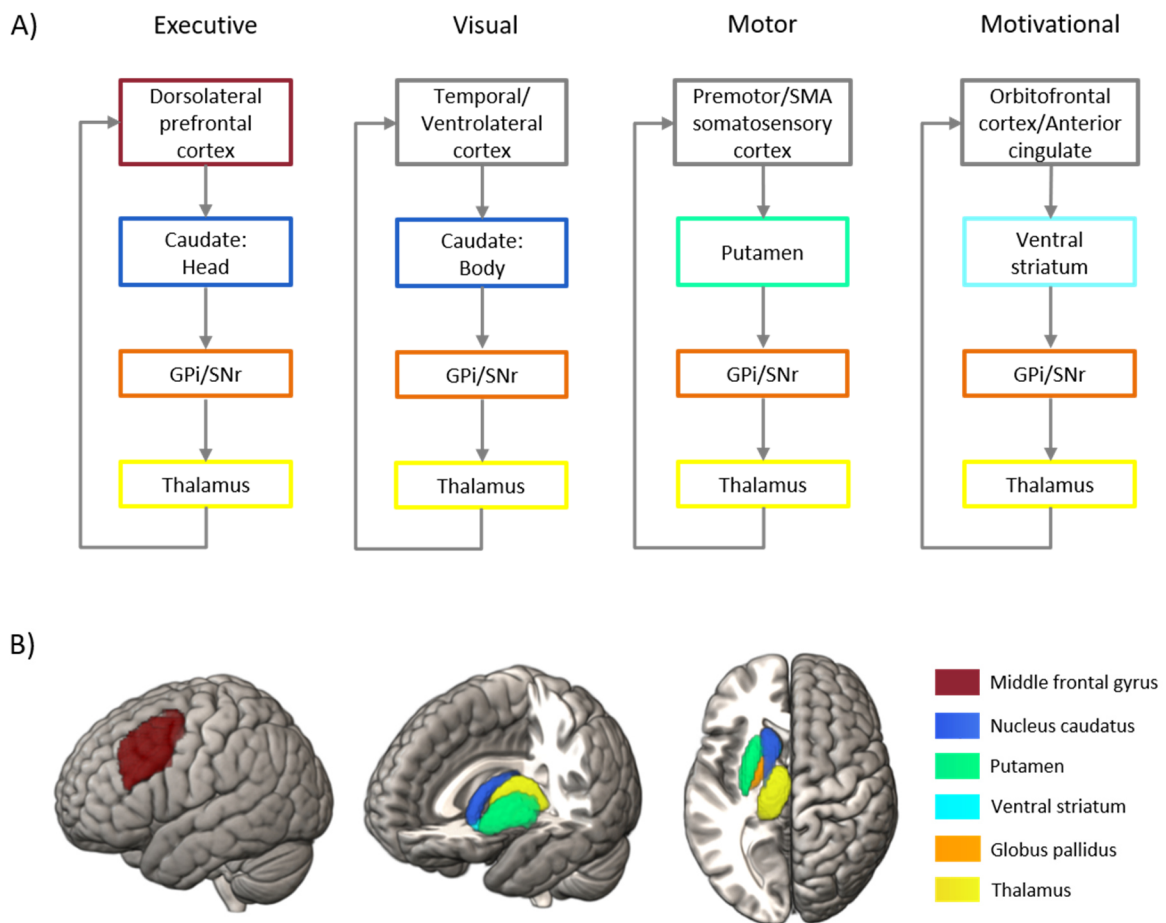


**Figure 1: Revised version of the corticostriatal circuitries.**

Panel A: conceptually modified illustration from Seger (2006), demonstrating the revised four corticostriatal circuitries subserving different functional domains in humans, e.g., cognition or motor control. Within each loop, input from cortical areas passes through a particular region of the striatum, then through pallidum or substantia nigra, and afterwards through the thalamus. Eventually, the information is projected back to the original cortical area. Panel B: Own anatomical illustration of the executive loop with cortical and subcortical structures (using MRICronGL; anatomical labeling according to the automated anatomical labeling (AAL) atlas, Tzourio-Mazoyer et al., (2002)). Abbreviations: GPI = Globus pallidus internal part, SNr = substantia nigra pars reticulata, SMA = supplementary motor area.



Within each corticostriatal loop, there is a direct and indirect pathway (Albin, Young, & Penney, 1989; DeLong, 1990), which is displayed in figure 2. In both pathways, cortical pyramidal neurons (from layer five) provide excitatory (glutamatergic) projections to the striatum. Striatal medium spiny neurons (MSN) provide inhibitory (GABAergic) projections to globus pallidus internus (GPi) and externus (GPe) and “form” a direct and indirect pathway. Direct pathway-forming MSNs express dopaminergic D1 receptors and project to GPi, while indirect pathway-forming MSNs express D2 receptors and project via several synapses (through GPe and subthalamic nucleus) indirectly to GPi (Gerfen & Surmeier, 2011; Girasole & Nelson, 2015). Further, the projections from GPi to the thalamus are GABAergic. However, thalamic projections back to the cortex are excitatory, i.e., glutamatergic (Chevalier & Deniau, 1990; Deniau & Chevalier, 1985).

Through the direct pathway, which is assumed to facilitate cortical activity, e.g., in the motor cortex, firing from cortex and striatal neurons results in an inhibition of GPi and thus in a disinhibition of the thalamus. Proposed functions of the direct pathway are, for example, motor facilitation, working memory gating and maintenance, and precise initiation of responses (Schroll & Hamker, 2013). Within the indirect pathway, cortical input passes to the striatum and GPe and additionally with an inhibitory projection to the subthalamic nucleus (STN). Projections from STN to the thalamus are excitatory, resulting in an inhibition of GPi and an inhibition of the thalamus. Thus, the indirect pathway is considered the inhibitory pathway, and suggested functions are the inhibition of motor programs or the termination of executed responses (Schroll & Hamker, 2013).

Of importance is the modulation of cortical glutamatergic signals at the striatal level by dopaminergic projections arising from the ventral midbrain. The ventral midbrain includes components such as substantia nigra (pars compacta and pars reticulata), ventral tegmental area, or the retrorubral field. Within the substantia nigra, the pars compacta (SNc) is the primary source of dopaminergic (DA) projections to the striatum (nigrostriatal pathway), the pars reticulata is part of the cortico-striatal circuits, and projections are GABAergic (see figure 2). Dopamine modulates glutamate signaling of cortical inputs at the level of the MSN within the striatum via D1 (direct pathway) and D2 receptors (indirect pathway), which is displayed in figure 2 (Gerfen, 2000; Gerfen & Surmeier, 2011; Girasole & Nelson, 2015).

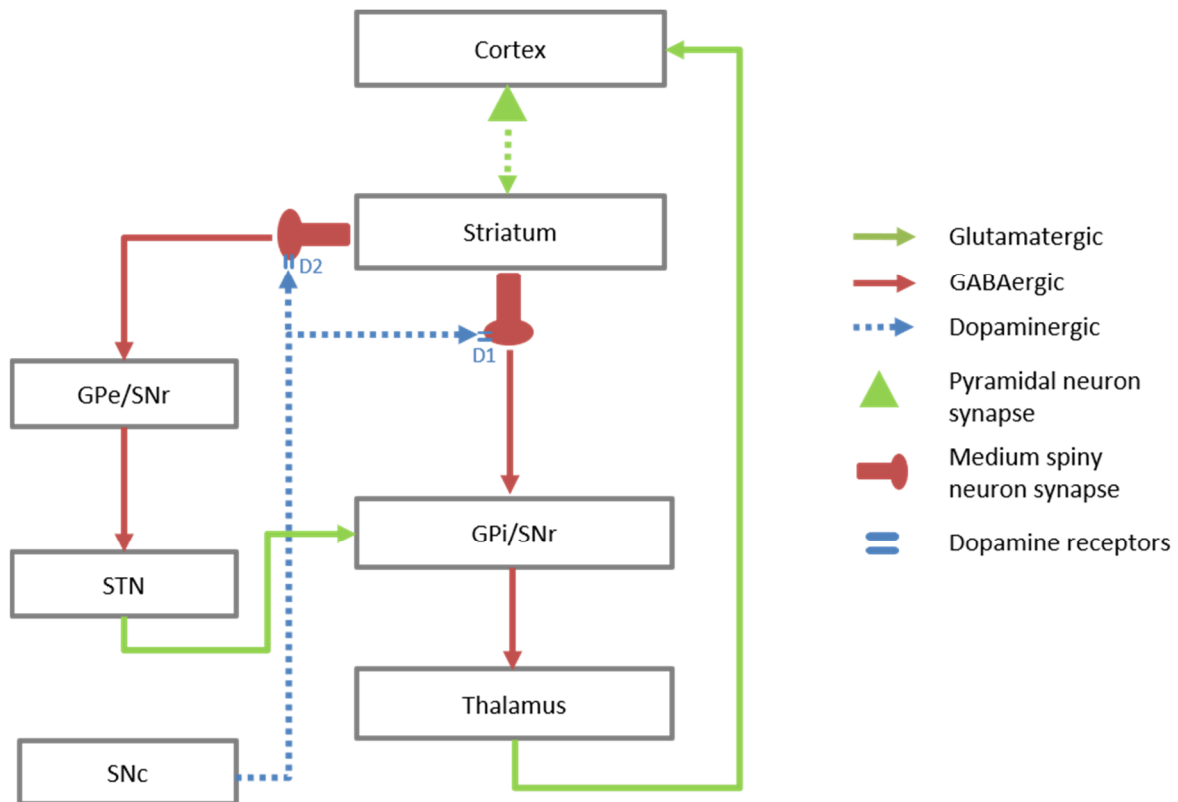


**Figure 2. The direct and indirect pathways within corticostriatal circuitries.**

Own illustration conceptually based on Gerfen (2000) and O'Reilly & Frank (2006). Green arrows indicate excitatory connections via glutamate, red arrows indicate inhibitory connections via GABA, blue arrows demonstrate the modulatory effect of dopamine via D1 (excitatory) or D2 (inhibitory) receptors. Abbreviations: GPe = Globus pallidus externus, GPi = Globus pallidus internus, SNr = substantia nigra pars reticulata, SNc = substantia nigra pars compacta; STN = subthalamic nucleus.

## 1.2 Basal ganglia function

BG contribute to a wide range of cognitive and behavioral functions. Over the last decades, a role as a selective gating mechanism within the motor system has been well established (Frank, Loughry, & O'Reilly, 2001a; Hikosaka, Takikawa, & Kawagoe, 2000; Mink, 1996; Schroll & Hamker, 2013). In detail, BG have been associated with gating adequate movement programs to the motor cortex while preventing the execution of less appropriate and competing motor plans (movement control), the performance of sequences, or controlling eye movements (Chevalier & Deniau, 1990; Mink, 1996; Schroll & Hamker, 2013).

Growing evidence from recent fMRI studies showed that BG are not only primarily engaged in the control function of the motor system but also within other corticostriatal circuits. In this context, it has been proposed that the BG, in particular the striatum, filter internal cognitive and emotional states

(Schroll & Hamker, 2013; Trapp, Schroll, & Hamker, 2012). Within the cognitive (executive) loop, the striatum was associated with the control of working memory (WM) processes (e.g., WM gating), especially during the encoding process of a working memory task phase (Chang, Crottaz-Herbette, & Menon, 2007; McNab & Klingberg, 2008; Moore, Li, Tyner, Hu, & Crosson, 2013; O'Reilly & Frank, 2006; Schroll & Hamker, 2013). Other data suggest that the striatal “gating” mechanism during working memory encoding may extend to other task-relevant stimulus attributes, including the novelty or increased cognitive demands of the stimulus (Chang et al. 2007; Landau et al. 2004; Nee and Brown 2013). Further, striatal activation was associated with the ability to suppress irrelevant or distractive information (McNab & Klingberg, 2008), especially under high memory load (Chang et al., 2007), and to control salience-driven attention switching (van Schouwenburg, den Ouden, & Cools, 2010). Overall, the studies mentioned above reported increased recruitment of striatal regions during working memory tasks, independent of task modality and particularly pronounced during the encoding process, supporting the BG gating mechanism. However, little is known about the relative contributions of the striatum to working memory function in the encoding relative to the retrieval process and for different degrees of stimulus novelty. Moreover, the proposed corticostriatal control mechanism that supports the gating mechanism during working memory encoding is still underexplored.

### **1.3 Striatal neurochemistry & genetic influences**

As previously introduced in section 1.1, the most critical transmitters within the corticostriatal circuits are glutamate, GABA, and dopamine. The interaction between glutamate and GABA (cholinergic system) results either in an excitatory (direct pathway) or in an inhibitory (indirect pathway) output within the individual corticostriatal circuits (Albin et al., 1989; DeLong, 1990). A detailed description is given in section 1.1.

There are four subtypes of glutamatergic receptors: N-methyl-D-aspartate (NMDA) receptor  $\alpha$ -Amino-3-Hydroxy-5-Methyl-4-Isoxazolpropionacid (AMPA) receptor, Kainate receptors, and metatropic receptors. Previous studies indicated that NMDA receptors are critical for WM and plasticity (Driesen et al., 2013). Studies using NMDA receptor antagonists, e.g., ketamine, showed impaired WM performance and reduced task-related activation in areas of the lateral prefrontal cortex or ventral striatum during a WM task as well as reduced connectivity of brain areas involved in WM (Driesen et al., 2013; Francois et al., 2016). In addition, impaired learning and decreased connectivity as a result of experimental NMDA antagonism were also reported within the motor domain (Zang et al., 2018).

Within the dopaminergic system, five subtypes of dopaminergic receptors, namely, D1, D2, D3, D4, and D5, have been identified, among which D1 and D2 play a particularly crucial role within the corticostriatal circuits. For example, the well-studied motor gating mechanism has been associated with the interplay between D1 and D2 receptors of medium spiny neurons (MSN). The activation of excitatory MSN via D1 receptors leads to disinhibition of the corticostriatal loop, which results in facilitating information flow into the prefrontal cortex. On the contrary, the inhibition of MSN via D2 receptors blocks the corticostriatal information flow (Chatham & Badre, 2015; Frank, Loughry, & O'Reilly, 2001b; Gerfen, 2000; Shepherd, 2013). For more details, see figure 2 in section 1.1. Further, dopaminergic impacts have been associated with long-term potentiation (LTP) via facilitating the direct pathway (D1 receptors) and long-term depression via the indirect pathway (D2 receptors), thus modulating synaptic plasticity within a corticostriatal circuitry (Gerfen, 2000; Gerfen et al., 1990; Schroll & Hamker, 2013; W. Shen, Flajolet, Greengard, & Surmeier, 2008). Even the specific location of the dopaminergic receptor within the striatum seems to have an impact. For instance, rodent studies have revealed that dopamine signaling in dorsal regions is associated with novelty and intensity of a stimulus and threat-related information, while ventral regions seem to be more linked to stimulus value (McCutcheon et al., 2019; Menegas, Akiti, Amo, Uchida, & Watabe-Uchida, 2018; Menegas, Babayan, Uchida, & Watabe-Uchida, 2017). Another noteworthy mechanism of the dopaminergic neurons is the ability to co-release. Most dopaminergic neurons can co-release GABA and a smaller section also glutamate (McCutcheon et al. 2019), allowing to moderate the interaction between the dopaminergic and cholinergic system, depending on their location within the striatum (Chuhma, Mingote, Moore, & Rayport, 2014).

Aside from neurotransmitters themselves, the genetic regulation of their signaling plays a fundamental role. There are numerous candidate genes among those Catechol-O-methyltransferase (COMT) and brain-derived-neurotrophic factor (BDNF) are crucial in the field of memory and learning. Both the *COMT* and the *BDNF* genes have functional single nucleotide polymorphism (SNP), resulting in an amino acid substitution from valine [Val] to methionine [Met] at a specific codon, 158 for *COMT* (*COMT Val158Met* (nucleotide rs4680)) and codon 66 for *BDNF* (*BDNF Val66Met* (nucleotide rs6265)), leading to a significant decrease in enzymatic activity (Meyer-Lindenberg et al., 2006). The dopamine-regulating gene, *COMT*, controls the presynaptic reuptake in the prefrontal cortex or modulates striatal dopamine activity and has been extensively studied in the past decades. The *COMT* risk variant (*Val158Met*), which reduces the thermostability of the encoded enzyme, has been associated with impaired prefrontal functioning in WM or reward tasks and has also been linked to an increased risk of psychiatric disorders such as schizophrenia (Brehmer et al., 2009; Bruder et al., 2005; J. Chen et al.,

2004; Egan et al., 2001; Frank & Fossella, 2011; Goldberg & Weinberger, 2004; Meyer-Lindenberg et al., 2005; Wang et al., 2015).

BDNF protein, as a member of the neurotrophin family of growth factors, has become the most widely studied neurotrophin (Notaras & van den Buuse, 2019). BDNF receptors are widely distributed among the human brain but notably highly expressed in regions essential for learning and memory, such as the cortex, striatum, and hippocampus (Hariri et al., 2003; von Bastian & Oberauer, 2014).

Prior behavioral studies demonstrated poorer performance among risk allele carrier (Met allele carrier) in several cognitive fields such as WM (Baig et al., 2010; Egan et al., 2003; Hariri et al., 2003; Harris et al., 2006; Hashimoto et al., 2008; Kambeitz et al., 2012; Karnik, Wang, Barch, Morris, & Csernansky, 2010), verbal learning (O. Gruber et al., 2012; Schofield et al., 2009), episodic memory (Hashimoto et al., 2008) as well as long-term memory (Montag et al., 2014). The substitution of valine to methionine at codon 66 within the BDNF pro-domain interferes with a Sortilin binding. As a consequence, intracellular trafficking and the activity-dependent release of BDNF is disrupted (Chen et al., 2015; Z. Y. Chen et al., 2004; Chiaruttini et al., 2009; Notaras, Hill, & van den Buuse, 2015; Notaras & van den Buuse, 2019), which might result in inefficient LTP (Figurov, Pozzo-Miller, Olafsson, Wang, & Lu, 1996; Jovanovic, Czernik, Fienberg, Greengard, & Sihra, 2000; Y. X. Li, Zhang, Lester, Schuman, & Davidson, 1998; Notaras et al., 2015; Tyler & Pozzo-Miller, 2001). Unfortunately, most behavioral studies on *BDNF* were conducted in a cross-sectional design. Only a few pre-post training studies have been performed, with varying time intervals ranging from one day (Goldberg et al., 2008) to several days (Montag et al., 2014) or months (LeMoult, Carver, Johnson, & Joormann, 2015). These studies showed poorer memory performance in Met allele carriers, which was compensated for after several repetitive training days in very few studies (Freundlieb et al., 2015; McHughen, Pearson-Fuhrhop, Ngo, & Cramer, 2011).

In the field of imaging studies, Met allele carrier showed increased activation and inefficient functional connectivity in prefrontal regions in WM or cognitive control tasks (Dennis et al., 2011; Egan et al., 2003; Jabbi et al., 2017; Schweiger et al., 2019) and reduced grey matter volume, e.g. in the prefrontal cortex (Soltesz et al., 2014). Similarly, reduced grey matter (Dennis et al., 2011; Soltesz et al., 2014) and abnormal activation have been reported in the hippocampus (Hariri et al., 2003; Hashimoto et al., 2008; Notaras et al., 2015). Likewise, most imaging genetic studies with *BDNF Val66Met* have followed a cross-sectional or a pre-post longitudinal approach, thus not reflecting the time course of learning and the corresponding neural correlates, e.g. reduced activation in striatal and frontal regions.

Overall, this section demonstrates that genetic predispositions affecting transmitter and neurotrophic action in corticostriatal circuits are linked to individual differences in memory and learning and further emphasizes the importance of interaction among different neurotransmitters and their regulating genes. BDNF activity-dependent secretion in corticostriatal areas is performed via NMDA receptors (Gibon & Barker, 2017; Park, Popescu, & Poo, 2014), which are essential for LTP and thus plasticity. Besides, BDNF influences striatal dopamine release and thus interacts with COMT, which also plays an important role in the corticostriatal circuitries, especially within the frontostriatal loop (von Bastian & Oberauer, 2014; Wang et al., 2015; Wang et al., 2014).

While these findings collectively suggest that genetic predispositions related to BDNF contribute to individual differences in learning and memory, a comprehensive longitudinal characterization of BDNF effects, including the behavioral and neural level, has to my knowledge, not been conducted yet.

#### **1.4 Basal ganglia dysfunction**

Irregularities in corticostriatal circuitries facilitate neurological diseases or psychiatric disorders such as Parkinson's disease, Huntington's disease, schizophrenia, or substance abuse (Peters, Dunlop, & Downar, 2016).

Parkinson's disease is a neurodegenerative disease characterized by a progressive cell loss of dopaminergic neurons, especially in the brain stem nuclei and the substantia nigra, leading to a decreased amount of striatal dopamine. In short, the output via the direct pathway decreases while the output via the indirect pathway increases (followed by decreased activity in GPe and an increase in GPi). For a detailed explanation of the pathways, see section 1.1 and figure 2. This imbalance within the dopaminergic system causes the cardinal motor symptoms of bradykinesia, rigidity, and resting tremor (Parkinsonism) (Kreitzer & Malenka, 2008; Nelson & Kreitzer, 2014). In addition, knowing that the direct pathway is involved in movement selection and initiation explains other symptoms such as difficulties in initiating movements, e.g., freezing or performing movements, e.g., reduced swinging of arms, hypomimia, micrographia. As the disease progresses, psychiatric and cognitive symptoms such as personality changes, depression, apathy, or memory impairment progress and emphasize the involvement of BG in non-motor fields.

Another neurodegenerative disease related to BG dysfunction is Huntington's disease, an autosomal dominant genetic disease with high penetrance caused by a pathological trinucleotide repeat expansion (Marreiros, Cagnan, Moran, Friston, & Brown) in the huntingtin gene, resulting in a successive striatal and later prefrontal cortical cell loss. Within the striatum, preferentially neurons of the indirect pathway seem to be affected (Reiner, Dragatsis, & Dietrich, 2011), leading to a reduced amount of inhibitory control causing the main symptoms chorea and hyperkinesia. Cell loss in prefrontal areas is associated with cognitive deficits, affect dysregulations, depression, and in later stage dementia (Peters et al., 2016).

Among psychiatric diseases, schizophrenia is a relatively common and well-investigated chronic illness, associated with positive symptoms (such as hallucinations and delusions), negative symptoms (such as flattened affect and lack of motivation) as well as cognitive symptoms (such as lack of concentration, WM deficits) (Gaebel & Zielasek, 2015; Girdler, Confino, & Woesner, 2019). The dopaminergic system plays an important role in the etiology of schizophrenia. Early models proposed a dysfunction within the dopaminergic system, which causes hyperdopaminergia (Creese, Burt, & Snyder, 1976; Seeman & Lee, 1975; Seeman, Lee, Chau-Wong, & Wong, 1976; Snyder, 1976). Later research specified the abnormal dopamine signaling to specific regions, i.e., subcortical hyperdopaminergia and prefrontal hypodopaminergia (Davis, Kahn, Ko, & Davidson, 1991; Peters et al., 2016). Recent imaging studies, using fMRI or PET, emphasize the role of dorsal striatal regions (McCutcheon et al., 2019), showing that greater activity in dorsal striatum or increase in striatal dopamine correlates with psychotic symptoms (McCutcheon et al., 2019; Sorg et al., 2013). Other symptoms of schizophrenia such as WM deficits are linked to lower levels of dopamine or hypoactivation in frontal regions, as well as disconnectivity between BG and prefrontal regions (Fusar-Poli et al., 2010; O. Howes, McCutcheon, & Stone, 2015; O. D. Howes, McCutcheon, Owen, & Murray, 2017; McCutcheon et al., 2019; Meyer-Lindenberg, 2010; Meyer-Lindenberg & Weinberger, 2006; Tost, Alam, & Meyer-Lindenberg, 2010).

Aside from schizophrenia, accumulating evidence has highlighted the involvement of the dopaminergic system in substance abuse. Dopamine plays an important role in the addiction cycle (Koob & Volkow, 2010), and its dysfunctions have been associated with drug-seeking behavior and impulsivity (Koob & Volkow, 2010; Menon, 2011; Peters et al., 2016).

To summarize, this section emphasizes the central role of corticostriatal circuitries in the onset of several psychiatric disorders or neurological diseases.

## 1.5 Memory and Learning

Memory is a fundamental function in human cognition. Conceptually, it can be seen as a storing and processing unit where existing knowledge is updated and previously acquired experiences are compared (Robertson, 2002). It can be divided into two major types, i.e., explicit memory (including facts and events) and implicit memory (including skills, habits, unconscious learning). Historically, Hebb proposed a distinction (for explicit memory) into short-term memory (STM) system and a long-term memory system (LTM) (Baddeley, 2003; Hebb, 1949; Robertson, 2002). Later, several revised memory models arose, e.g., Atkinson & Shiffrin Model, and most studies classified memory according to time into three different types: STM, WM, and LTM (Atkinson & Shiffrin, 1968; Baddeley, 2003; Robertson, 2002). Briefly, STM can be considered as a temporary buffer, where we shortly hold information for seconds, such as a telephone number. If we rehearse and repeatedly use this information, it can be kept in WM for minutes to hours, if not, it will not be consolidated towards forming a long-term memory representation. Depending on the amount of usage and rehearsal, it can be stored in the LTM for years or even a lifetime (Robertson, 2002).

The WM itself was proposed as a three-component WM model including a central executive and two storage systems, namely a phonological loop and visuospatial sketchpad (Baddeley & Hitch, 1974). This WM model has been extended to the multicomponent WM model, including a fourth component, the episodic buffer (Baddeley, 2000). In general, WM is responsible for temporary storage and "online" manipulation of information. Depending on the subcomponent, WM is, among other functions, essential for attention, learning, speech, orientation, and comprehension of stimuli (Baddeley, 2003, 2010). Typically, the capacity of WM is known to be around seven items (Miller's magical number seven) or chunks, which are meaningful units of information (Goh, Beason-Held, An, Kraut, & Resnick, 2013; Guida, Gobet, Tardieu, & Nicolas, 2012; Miller, 1956). In the last decades, neuroimaging and brain lesions studies were able to identify the neural correlates for the individual WM components. Inferior parietal regions (BA 40), Broca's area (BA 6/44), and the SMA (BA 6) were linked to the phonological loop (Baddeley, 2003; Muller & Knight, 2006; G. Vallar, Di Betta, & Silveri, 1997; G. P. Vallar, C., 2002), whereas prefrontal (BA 9/46), inferior frontal (BA 6/44) and parietal (BA 7/40) regions were related to the central executive network (Baddeley, 2003; Braver et al., 1997; Cohen et al., 1997).

In a similar approach, lesion and neuroimaging studies identified critical regions for LTM, including the hippocampus, entorhinal, and parahippocampal cortex. The hippocampus is one of the oldest parts of the human brain and crucial for encoding and retrieval of information (Eichenbaum, 2004; Staresina, Cooper, & Henson, 2013). Similar to corticostriatal circuitries, the hippocampal functions are



represented in a neural circuitry, which is displayed in figure 3. Briefly, the hippocampus receives high-level, diverse, and widespread cortical input, either directly through the entorhinal cortex or indirectly via the parahippocampal or perirhinal cortex. The entorhinal cortex can be seen as a “portal” between the cortex and the hippocampal subregions, i.e., dentate gyrus, cornu ammonis (CA1 - 3), and subiculum (Shastri, 2002). Of particular interest for memory encoding is subregion CA3, which is known as a “conjunctive code,” merging items into memory. Granule cells in the dentate gyrus send “mossy fiber axons” to the CA3 region (Hainmueller & Bartos, 2020; Rebola, Carta, & Mulle, 2017; Shastri, 2002). Cells in this region have recurrent and widespread connections and are mainly glutamatergic. For example, subregion CA3 projects via the “Schaffer collaterals” into subregion CA1, which then projects back to the entorhinal cortex and then returns to the originated cortex. Further, the CA3 region directs information through other complex loops within the hippocampus, including hippocampal areas such as CA2, subiculum, and dentate gyrus (Goode, Tanaka, Sahay, & McHugh, 2020; Hainmueller & Bartos, 2020; Lazarov & Hollands, 2016; Rebola et al., 2017; Shastri, 2002).

The hippocampus is well known for rapid synaptic plasticity or experience-dependent remodeling of the functional efficacy of synaptic connections, also called long-term potentiation (LTP) (Bliss & Collingridge, 1993; Bliss & Lomo, 1973). LTP is the most common cellular model for learning and memory and is highly related to glutamate and NMDA receptors (see section 1.3 for more information). Once glutamatergic synapses are high-frequently stimulated, a rapid and long-lasting increase in strength of transmission between them occurs, which can persist, e.g., for many days or longer (Bliss & Collingridge, 1993; Nicoll, 2017). In addition to glutamate, dopamine is critical for learning and memory formation. Previous studies demonstrated that dopamine antagonists can block LTP, thus emphasizing the role of dopamine in the entry of novel information (Bunzeck & Thiel, 2016). The hippocampus has widespread connections with multiple brain regions such as the prefrontal, temporal or parietal cortex (Robertson, 2002).

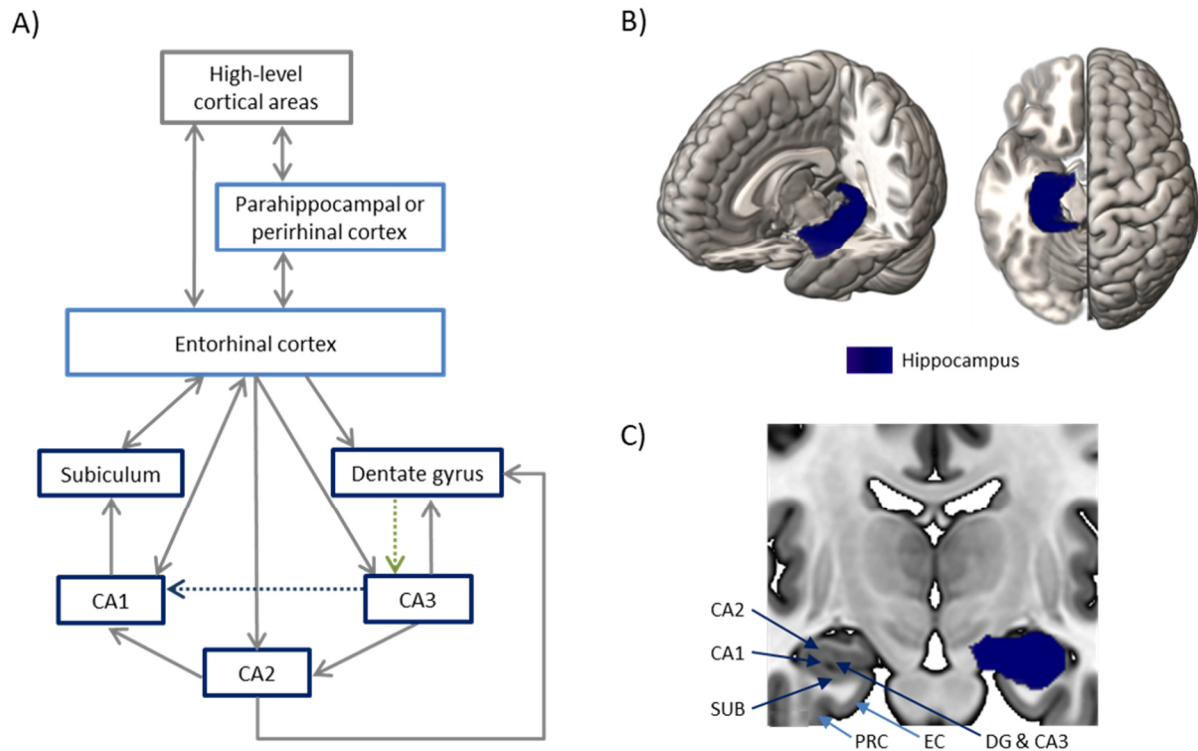


**Figure 3. Hippocampus anatomy and hippocampal circuits.**

Panel A) Own illustration of hippocampal circuits based on Shastri (2002). Panel B) Panel B: Own anatomical illustration of the hippocampus (using MRICronGL; anatomical labeling according to the automated anatomical labeling (AAL) atlas, Tzourio-Mazoyer et al. (2002)). Panel C) Own anatomical mapping (using MRICronGL; anatomical labeling according to Suwabe et al. (2018)). Blue dashed line from CA3 to CA1 = Schaffer collaterals. Green dashed line from Dentate gyrus to CA2 = mossy fiber. Abbreviations: CA = cornu ammonis, SUB = subiculum, PRC = perirhinal cortex, EC = entorhinal cortex, DG = dentate gyrus.

Previous evidence suggested that hippocampal and cortical areas have powerful learning capacities but reflect different stages and mechanisms (McClelland, McNaughton, & O'Reilly, 1995; O'Reilly & Rudy, 2001). For instance, the hippocampus is considered as rapid learning of individual events or episodes, while the cortex is proposed to gradually extract regularities over many experiences. Furthermore, growing evidence supports that repeated activation of the hippocampal-cortical network, e.g., during rehearsal or recall, may provide the basis for an extended consolidation of memories within the cerebral cortex (Eichenbaum, 2004).

A topic closely related and interlinked to memory is the ability to learn and practice. "Practice makes perfect" is a proverbial truism, referring to the observation that practice results in improvement in performance. A long history of behavioral studies described a characteristic shape of performance improvement over time, known as learning curves (Gulliksen, 1934; Mazur & Hastie, 1978; Restle & Greeno, 1970; Thurstone, 1919), which were defined as an exponential, hyperbolic or logistic function. An important aspect is that performance improvement can be described along two dimensions:

learning *speed* and learning *gain* (i.e., the amount of improvement). Newell & Rosenbloom (1981) proposed the term "law of practice," which followed a power function, i.e., log-log linear learning function, also called the power law of practice. While learning curves were historically associated with "skill acquisition" in motor behavior tasks, Newell & Rosenbloom proposed a universal quantitative law that includes all types of cognitive behavior (Newell & Rosenbloom, 1980). More recent research demonstrated that an exponential law of practice could describe learning curves better than a power function (Evans, Brown, Mewhort, & Heathcote, 2018).

In the WM literature, the best-studied mechanism for explaining this "practice effect" is the formation of "chunks" (Guida et al., 2012; Miller, 1956; Newell & Rosenbloom, 1980). A chunk is a meaningful and effective reorganization of information, which is usually accompanied by the compression of information. Early learning studies proposed chunking as the mechanism to acquire expertise in fields such as morse codes or chess play (Bryan & Harter, 1899; Chase & Simon, 1973). Several WM studies demonstrated that the chunking mechanism improves (WM) performance and reduces cognitive load, leading to more efficient WM capacity (Bor, Cumming, Scott, & Owen, 2004; Ericcson, Chase, & Faloon, 1980). The recruitment of lateral prefrontal areas, such as the DLPFC, has been linked to the selection of appropriate chunks (Bor et al., 2004; Bor, Duncan, Wiseman, & Owen, 2003; Goh, An, & Resnick, 2012; Goh et al., 2013). A reasonable explanation might be the usage of long-term memory traces or memory engrams, leading to a functional reorganization and eventually re-facilitating memory processes (Bor et al., 2004; Goh et al., 2013).

In general, learning and practice are examples of plasticity processes, which have been demonstrated in several cross-sectional and longitudinal studies. See figure 4 for an illustration. Typically, the improvement in performance has been quantified by an increase in accuracy and/or a decrease in reaction time, often modeled linearly. The neural correlates of behavioral improvement, e.g., induced by short-term or long-term training, is reduced activation or increase in grey matter, which has been reported within the motor (Draganski et al., 2004; Floyer-Lea & Matthews, 2005; Lehericy et al., 2005) as well as the cognitive systems. In WM tasks, a decrease in activation has been particularly shown in striatal and frontal regions, e.g., DLPFC (Garavan, Kelley, Rosen, Rao, & Stein, 2000; Sankar, Adams, Costafreda, Marangell, & Fu, 2017; van Raalten, Ramsey, Duyn, & Jansma, 2008; van Raalten, Ramsey, Jansma, Jager, & Kahn, 2008). Unfortunately, most of the studies were either conducted in a cross-sectional design or used a simple pre-post longitudinal approach without specific modeling of behavioral improvement and its neural correlates. A more promising approach to investigate plasticity is to characterize learning-induced changes in behavior and brain function by applying an exponential function in the sense of the previously explained "law of practice." So far, only a few studies in the field

of motor learning were conducted, where an exponential function was used to estimate learning parameters, such as movement time, learning speed, or error level (Bassett, Yang, Wymbs, & Grafton, 2015; Kodama et al., 2018). These studies have also found corresponding brain adaptations, e.g., increased hippocampal grey matter volume (Kodama et al., 2018), or decrease in learning-induced integration of cognitive systems (Bassett et al., 2015). Another important aspect in studying the effect of plasticity is the consideration of genetic influences. As previously outlined (see section 1.3), BDNF plays an essential role in synaptic plasticity and has been extensively studied. However, most of the conducted imaging genetic studies with *BDNF Val66Met* have followed either a cross-sectional or a longitudinal design with a simple pre-post approach. A comprehensive longitudinal characterization of *BDNF* effects at the behavioral and neural levels has not been studied extensively, and to my knowledge, at least not in the context of applying exponential learning curves.

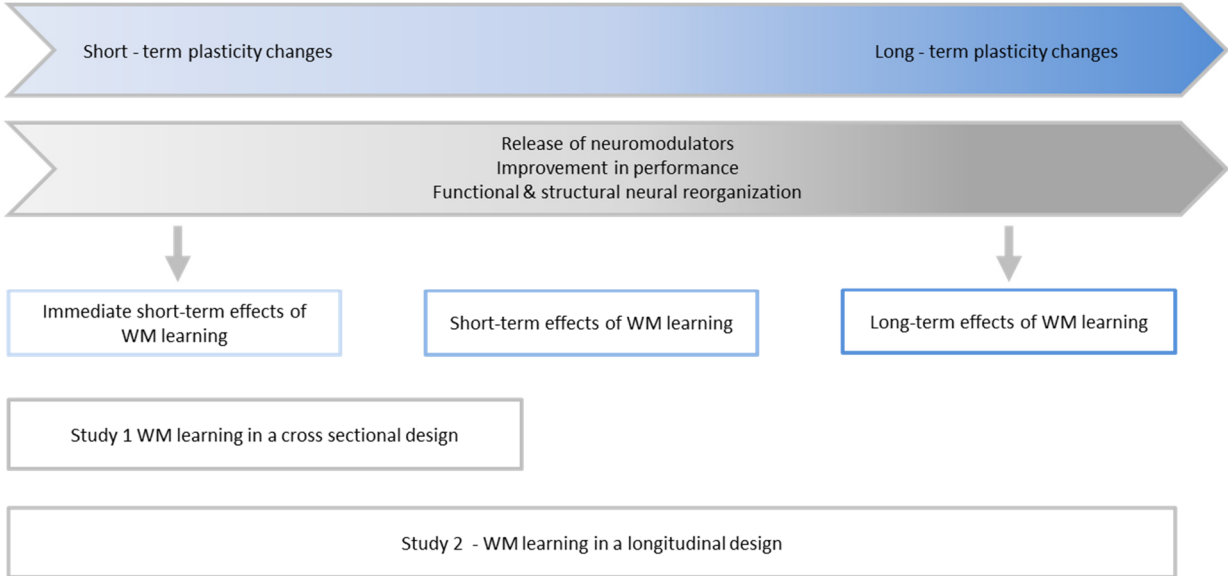


**Figure 4. Illustration of the cross-sectional design (study1) and the longitudinal design (study2) used to investigate plasticity during working memory (WM) learning.**

## 1.6 Aims

As outlined above, corticostriatal circuitries play an essential role in basic and high-level functions of the human brain, such as control of motor function, goal-director behavior, cognition, as well as learning and memory function. The neurotransmitters glutamate and dopamine, as well as the neurotrophin BDNF, are critically involved in the process of memory and learning. Malfunctioning within corticostriatal circuitries is associated with several neurological and psychiatric diseases.

In general, study 1 of this thesis, focuses on short term effects of WM learning. In particular, on defining the underlying effects of striatal gating and possible modulatory influences by frontal areas, thereby following a cross-sectional design. Study 2 of this thesis aims to investigate short-term and long-term effects of corticostriatal functioning and examine possible influences of *BDNF* by applying exponential learning curves. Thus, study 2 was conducted in a longitudinal design. See figure 4 for an illustration.

Study 1 aims to investigate [1] whether striatal activation during working memory varies across task phase (i.e., encoding and retrieval) and novelty of the presented materials, and [2] by which corticostriatal connectivity mechanism the task-phase specific engagement of the striatum during novelty processing is plausibly achieved. Therefore, fMRI activation and connectivity analyses in 74 healthy volunteers, performing a Sternberg working memory task with different task phases and degrees of stimulus familiarity, were performed (section 2.1). Based on the literature mentioned above, more pronounced striatal activations in the encoding (vs. retrieval) phase of the task and during the processing of the cognitively more demanding novel (vs. practiced) Sternberg items are hypothesized. Further, to investigate whether the observed effects are best explained by a model assuming a modulatory influence of stimulus encoding on the information flow between the DLPFC and the striatum, and if so, whether the winning model hypothesizes a top-down, bottom-up, or reciprocal increase in effective connectivity.

While the cross-sectional study 1 focuses on defining the circumstances of striatal gating and possible modulatory influences by DLPFC, the main focus of study 2 is to investigate corticostriatal functioning in a longitudinal design and examine possible influences of *BDNF* by applying exponential learning curves.

Study 2 aims to characterize learning-induced changes in cognitive behavior and brain function during a two-week learning period with consecutive training and fMRI acquisition on a regular basis and the modulation of these learning-induced changes by the plasticity marker BDNF. Therefore, a sample of

23 subjects performing a modified Sternberg working memory task was examined, and exponential decay modeling (learning curves) was used to examine two key dimensions of learning, i.e., the parameters for learning *speed* ( $\tau$ ) and learning *gain* ( $\alpha$ , reflecting the amount of change). Based on prior mentioned work, the following hypotheses were postulated. [1] Carriers of the *BDNF* plasticity risk variant (Met carrier) would show performance deficits, e.g., higher error rates, during longitudinal working memory learning, and [2] display differences in temporal characteristics of working memory learning across the training interval, [3] learning-related behavioral alterations can be linked to neural learning parameters estimated from frontal-striatal activation and connectivity estimates, and [4] these measures of frontal-striatal function would be impacted by *BDNF* genotype.

Please note that several parts of this thesis have already been published or are about to be published by the doctoral candidate as a first author. Therefore, certain sections, tables, or figures of this thesis will be identical to the following publications:

Geiger, L. S., Moessnang, C., Schafer, A., Zang, Z., Zangl, M., Cao, H., van Raalten, T., Meyer-Lindenberg, A., Tost, H. (2018). Novelty modulates human striatal activation and prefrontal-striatal effective connectivity during working memory encoding. *Brain Struct Funct.* doi:10.1007/s00429-018-1679-0

Geiger, L. S., Zang, Z., Melzer, M., Witt, S., Rietschel, M., van Raalten, T. R., Meyer Lindenberg, A., Moessnang, C., Wüstenberg, T. & Tost, H. (2021). Longitudinal behavioral and brain functional effects of a plasticity-related variant in *BDNF* on verbal working memory learning. In presubmission to *Proc Natl Acad Sci U S A (PNAS)*.

## 2. Empirical studies

### 2.1 Study 1: NOVELTY MODULATES HUMAN STRIATAL ACTIVATION AND PREFRONTAL–STRIATAL EFFECTIVE CONNECTIVITY DURING WORKING MEMORY ENCODING<sup>2</sup>

#### 2.1.1 Abstract

The functional role of the basal ganglia in the gating of suitable motor responses to the cortex is well established. Growing evidence supports an analogous role of the BG during working memory encoding, a task phase in which the “input-gating” of relevant materials (or filtering of irrelevant information) is an important mechanism supporting cognitive capacity and the updating of working memory buffers. One important aspect of stimulus relevance is the novelty of working memory items, a quality that is understudied with respect to its effects on corticostriatal function and connectivity. To this end, functional magnetic resonance imaging (fMRI) was applied in 74 healthy volunteers performing an established Sternberg working memory task with different task phases (encoding vs. retrieval) and degrees of stimulus familiarity (novel vs. previously trained). Activation analyses demonstrated a highly significant engagement of the anterior striatum, in particular during the encoding of novel working memory items. Dynamic causal modeling (DCM) of corticostriatal circuit connectivity identified a selective positive modulatory influence of novelty encoding on the connection from the dorsolateral prefrontal cortex (DLPFC) to the anterior striatum. These data extend prior research by further underscoring the relevance of the BG for human cognitive function and provide a mechanistic account of the DLPFC as a plausible top-down regulatory element of striatal function that may facilitate the “input-gating” of novel working memory materials.

#### 2.1.2 Methods

##### Participants

Seventy-four healthy right-handed subjects (43 females, age:  $26 \pm 7.0$  years) participated in this study. Informed consent was obtained from all individual participants included in the study. The protocol was approved by the Ethics Committee of the Medical Faculty Mannheim at the University of Heidelberg.

---

<sup>2</sup> Published as: Geiger, L. S., Moessnang, C., Schafer, A., Zang, Z., Zangl, M., Cao, H., van Raalten, T., Meyer-Lindenberg, A., Tost, H. (2018). Novelty modulates human striatal activation and prefrontal-striatal effective connectivity during working memory encoding. *Brain Struct Funct.* doi:10.1007/s00429-018-1679-0

Subjects had no history of neurological illness, psychiatric disorders, or substance abuse. Handedness was assessed using the Edinburgh Handedness Inventory (Oldfield, 1971).

### **fMRI experiment**

Subjects performed a modified Sternberg item recognition task with four task conditions and a total duration of 8.4 minutes (figure 5a). Similar paradigms have been previously used to study brain activations related to the processing of novel and automated stimulus-response relationships during verbal working memory (Jansma JM, 2001; van Raalten, Ramsey, Duyn, et al., 2008; van Raalten, Ramsey, Jansma, et al., 2008). Each trial consisted of an encoding phase (3500 ms) during which a target set of five consonants was presented and had to be memorized. After a variable interstimulus interval (358 ms – 1790 ms, randomly jittered in steps of 358 ms), ten single-letter probes were presented consecutively for 1400 ms each, followed by a fixation cross for 800ms in the retrieval phase (total duration of 26 s). For every single probe, the subjects had to indicate whether the letter was part of the target set (or not) by pressing the left (or right) button on a magnetic-resonance-compatible response pad.

Since this task aimed at investigating memory phase-dependent differences in the neural processing of novel and practiced working memory items, specific stimuli were trained and automatized prior to the fMRI scan. For this, subjects practiced three series of trials consisting of a fixed encoding stimulus set (i.e., FGMPT) and a fixed set of 50 letter probes (i.e., 25 target and 25 non-target probes) that were presented in a pseudo-randomized order in the retrieval phase. During the actual fMRI scan, novel and previously practiced working memory stimuli were presented along with a low-load cognitive control condition and a rest condition. While entirely novel target sets and probes were presented in the novel condition (e.g., DCKWX), the previously practiced target set and practiced probes were shown in the practiced condition. In the low-load cognitive control condition, the target set consisted of five identical vowels (AAAAA), and only two probes (one target and one non-target probe) were presented five times each during retrieval. In the rest condition, the German word for "rest" ("Ruhe") was displayed instead of a target set followed by a fixation cross, and no response was required. All conditions were presented four times in a pseudo-randomized and counterbalanced order. All stimuli were presented at fixed positions on the screen to minimize condition-dependent differences in spatial attention and eye movements. The basic motor and sensory processing demands of the novel and practiced conditions were comparable. Since the analyses were restricted to the direct comparison of novel and practice conditions, the low-load cognitive control condition and the rest condition were not analyzed further in this study.



## Behavioral data analysis

Mean reaction times (RT) for target and non-target stimuli were calculated for the novel and practiced conditions. Accuracy was recorded for each condition as percentage of correctly identified probes. The performance parameters of the novel and practiced task conditions were compared using paired sample t-tests. A significance level of  $p < 0.05$  was applied.

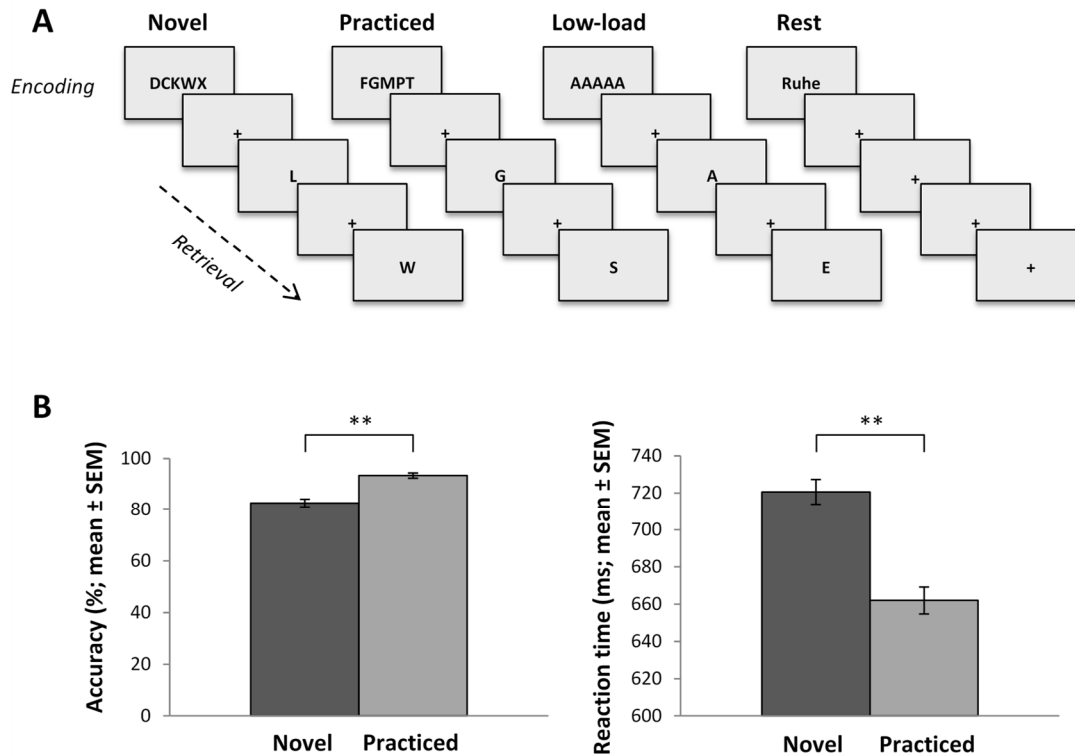


**Figure 5 Sternberg task and behavioral results.**

Panel A: Structure of the Sternberg task consisting of two task phases (encoding, retrieval) and four different task conditions (novel, practiced, low-load cognitive control, and rest). Panel B: Behavioral results of the Sternberg task, with accuracy given in percent correct and reaction time given in milliseconds for the novel and practiced task conditions, respectively (\*\* indicates  $p < 0.001$ ). Abbreviation: SEM = standard error of the mean.

## Image acquisition

Functional data were acquired on a 3 Tesla whole-body MR Scanner (Siemens, Erlangen, Germany), with a 32-channel head coil (parallel imaging; generalized autocalibrating partially parallel acquisition (GRAPPA); iPAT=2). Functional images were acquired in descending order with a gradient-echo echo-planar imaging (EPI) sequence (TR = 1790 ms, TE = 28 ms, flip angle =  $76^\circ$ , 34 axial slices, 3 mm slice thickness, 1 mm gap, matrix size:  $64 \times 64$ , field of view (FoV):  $192 \times 192$  mm; whole brain coverage was ensured by tilting the FoV to  $-25^\circ$  from the individual anterior commissure – posterior commissure line).

### **Image preprocessing**

Data preprocessing was performed using standard routines of the Statistical Parametric Mapping software (SPM8; <http://www.fil.ion.ucl.ac.uk/spm/software/spm8/>). Briefly, this included a two pass realignment procedure (i.e., functional images were registered to the mean of the images after a first realignment to the first image), slice time correction, normalization to the Montreal Neurological Institute (MNI) EPI template (using the mean functional image as the source image and the MNI EPI template as the template image), and spatial smoothing with an 8mm full-width at half-maximum (FWHM) Gaussian kernel. To rule out excessive frame-to-frame motion in the sample, mean framewise displacement was assessed. For this, mean relative RMS (root mean squared) displacement according to (Jenkinson, Bannister, Brady, & Smith, 2002) we computed. The resulting values (mean = .07 mm, SD = .03 mm, min = .03 mm, max = .21 mm) suggest that overall motion in the sample was low (see also Ciric et al. (2017)).

### **Activation analysis**

The activation analysis followed a two-level procedure in SPM8. At the first level, general linear models (GLM) were defined for each subject that included eight separate regressors for each stimulus type (novel, practiced, low-load cognitive control, and rest) and memory phase (i.e., encoding, retrieval). Regressors were modeled using delta (stick) functions for the encoding phases and boxcar functions for the retrieval phases. The six head motion parameters from the realignment step were included as nuisance covariates into the model to account for head motion. During model estimation, the data were high-pass filtered with a cutoff of 128 s, and an autoregressive model of the first order was applied. Contrast images were calculated for each subject to assess the 1) main effect of memory phase (encoding > retrieval, retrieval > encoding), 2) main effect of stimulus type (novel > practiced, practiced > novel), and 3) the encoding specific effect of stimulus type (encoding-novel > encoding-practiced, encoding-practice > encoding-novel). The first-level contrast images were entered into second-level random-effects models using age and sex as covariates of no interest, and one-sample t-tests were calculated for statistical inference at the group level ( $p < 0.05$ , whole brain family-wise error (FWE) corrected). Note that results for the main effect of memory phase are reported in the supplemental material (figure S1, page 30; table S1, page 73 and 74,) since the direct comparison of encoding and retrieval phases is of limited interpretability given profound differences in visual stimulation, task demands, and duration.

### **Dynamic causal modeling (DCM)**

In addition to the activation analysis, DCM was conducted to explore the proposed role of prefrontal-striatal interactions for the regulation of the access of novel information into working memory. In brief, DCM allows clarifying how a specific brain region intrinsically exerts influences on another brain region and how this influence is modulated by the experimental conditions of a task. DCM models three brain dynamics in the context of external stimuli (Friston, Harrison, & Penny, 2003; Stephan, Weiskopf, Drysdale, Robinson, & Friston, 2007): the endogenous coupling between two regions (intrinsic connections), the impact of experimental conditions on the regions themselves (driving inputs) and on the strength of the coupling between the regions (modulatory effects). Based on the published literature (A. J. Gruber, Dayan, Gutkin, & Solla, 2006; O'Reilly & Frank, 2006) and own activation findings, focus was laid on the functional interaction of two key cognitive nodes in the corticostriatal circuitry, the DLPFC and the downstream input node for excitatory projections from the prefrontal cortex at the level of the basal ganglia in the anterior striatum. Specifically, the aim was to examine potential modulatory effects of the encoding phase of novel and practiced items on the DLPFC and its effective connectivity to the striatum in the context of this Sternberg working memory task.

#### *Definition of subject-specific volumes of interest (VOIs)*

Subject-specific VOIs were defined in two steps. First, two anatomical masks from the Automated Anatomical Labeling (AAL) atlas (Tzourio-Mazoyer et al., 2002) representing the DLPFC and the striatum were derived. The DLPFC mask covered the AAL regions of Brodmann area (BA) 46, whereas the striatum mask covered the merged AAL regions of the putamen and caudate nucleus. Due to the focus on the dorsolateral prefrontal loop (executive loop) within the corticostriatal circuits (Alexander et al., 1986), only the anterior part of the putamen and the head of the caudate nucleus were chosen ( $MNI\ y \geq -1$ ). Then, subject-specific VOIs were defined by superimposing the masks to the first-level statistical images of the "encoding-novel > encoding practice" contrast, identifying the peak statistical voxel within each mask, centering 6mm spheres around the peak voxels, and extracting the first eigenvariate from these spheres. The VOI time series were adjusted for the effects of interest (EOI), which accounts for movement artifacts based on the realignment parameters and mean-corrects the data. Following previous literature demonstrating predominantly left hemispheric lateralization for verbal WM items (Nagel, Herting, Maxwell, Bruno, & Fair, 2013) and confirming a higher involvement of the left hemisphere during similar Sternberg tasks (Cairo, Liddle, Woodward, & Ngan, 2004; Chang et al., 2007; van Raalten, Ramsey, Duyn, et al., 2008), VOIs were defined within the left hemisphere. For an illustration of the distribution of individual VOIs, see figure 6.

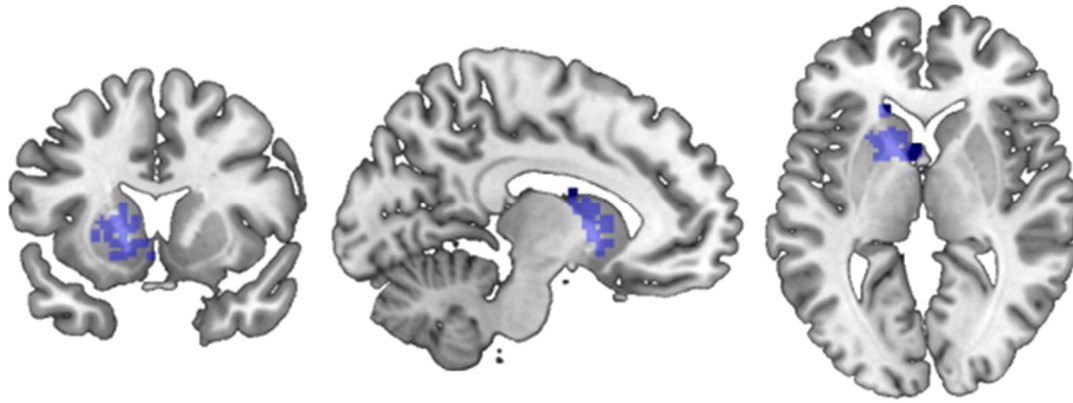


**Figure 6. Illustration of individual peak voxels of the encoding novel > encoding practice contrast images in normalized space.**

Distribution of individual peak voxels within the anatomical striatum mask (ROI mask) superimposed on T1-weighted images. For DCM VOI definition, 6-mm spheres were constructed around individual peaks. Abbreviations: DCM = dynamic causal modeling, ROI/VOI = region/volume of interest.

#### *DCM model space definition and estimation*

DCM12 toolbox implemented in SPM12 (r6685) was used for model definition and estimation of deterministic DCMs. In order to test whether the experimentally induced influence is consistent with a "top-down" and/or "bottom-up" regulatory effect, the following brain dynamics were included in the definition of DCM models. 1) Intrinsic connections: Consistent with the anatomy of corticostriatal circuits (Alexander et al., 1986; Shepherd, 2013), a bidirectional intrinsic connection between the DLPFC and the basal ganglia was assumed. 2) Driving inputs: All four conditions (encoding-novel [EN], encoding-practice [EP], retrieval-novel [RN], retrieval-practice [RP]) were used as driving input to DLPFC, striatum or both (i.e.  $2^4 - 1 = 15$ ; no input at all was ignored). 3) Modulatory effects: The two encoding conditions (EN, EP) were included as modulatory effects, either jointly or separately, on the bidirectional intrinsic connections (i.e., DLPFC to striatum vs. striatum to DLPFC;  $2^4 = 16$ ). Systematic variation of these dynamics resulted in a total of  $2^4 * (2^4 - 1) = 240$  models. An illustration of all brain dynamics taken into account for model definition is provided in figure 7.

In a first step, model families were defined by modulation patterns, resulting in  $2^4 = 16$  families, and compared using random effects Bayesian model selection (BMS) to identify the winning family. In a second step, the individual models within the winning family (15 models) were compared by means of random effects BMS to determine the model that most likely generated the observed data (winning model) assessed by the protected exceedance probability. The protected exceedance probability measures how likely any given model is more frequent than all other models in the comparison set and is, other than the exceedance probability per se, protected against the possibility that the alternative hypothesis is not true (Penny et al., 2010; Rigoux, Stephan, Friston, & Daunizeau, 2014;

Stephan, Penny, Daunizeau, Moran, & Friston, 2009; Stephan et al., 2010). In a last step, Bayesian Parameter Averaging (BPA) was used for a detailed description of the winning model.

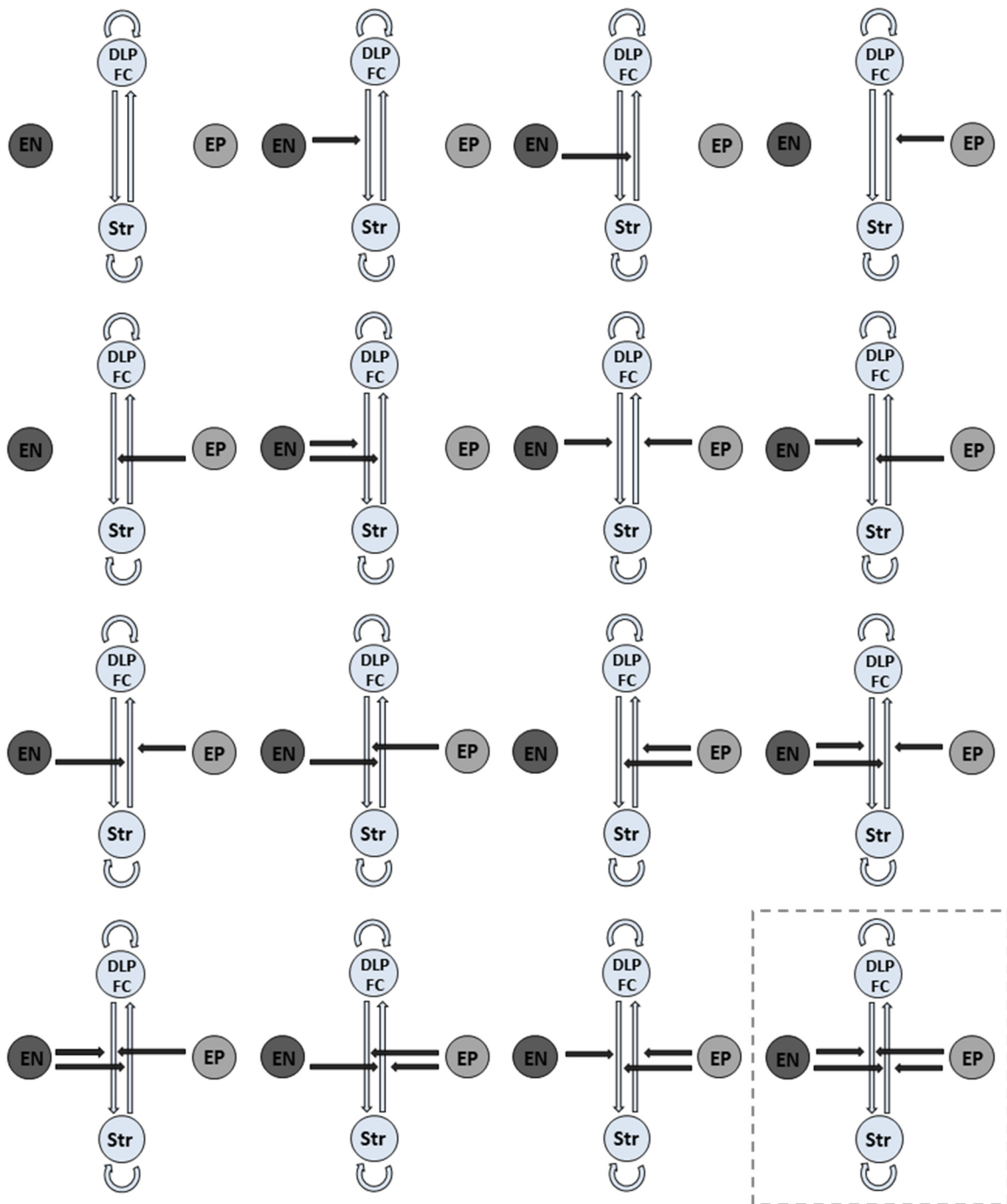


**Figure 7. Illustration of model families.**

Bilateral intrinsic connections (light grey arrows) between DLPFC and striatum were fixed (i.e., not varied) across models. The two encoding conditions (EN, EP) were defined as modulatory effects (black arrows), either jointly or separately, on the bidirectional intrinsic connections (DLPFC to striatum vs. striatum to DLPFC). Model families resulted from the variation of modulatory effects. Dashed box indicates the winning family. Abbreviations: DLPFC = dorsolateral prefrontal cortex, EN = encoding-novel, EP = encoding-practice.

### 2.1.3 Results

#### Behavioral data

During memory retrieval, subjects achieved accuracies of 82 % (standard error of the mean (SEM) = 1.0 %) in the novel condition and of 93 % (SEM = 1.5 %) in the practiced condition. Mean reaction times were 721 ms (SEM = 7 ms) for the novel condition and 662 ms (SEM = 7 ms) for the practiced condition (figure 5B, page 19). The statistical comparison confirmed a significant increase in accuracy ( $t_{[73]} = 8.9$ ,  $p < 0.001$ ) and a decrease in reaction time ( $t_{[73]} = 14.3$ ,  $p < 0.001$ ) during the retrieval of practiced stimuli relative to the retrieval of novel stimuli, consistent with a successful automatization of the trained working memory items prior to the scan.

#### Activation analysis

A significant main effect of stimulus type manifesting as a significant bilateral activation increases in the putamen ( $t_{\max} = 10.26$ ) and DLPFC ( $t_{\max} = 6.1$ ) during the processing of novel relative to practiced stimuli (figure 8A) was detected. Other significant regions included the anterior insula, anterior cingulate cortex, and higher order motor and visual areas. In the opposite contrast, the comparison of practiced to novel items revealed increased activation bilaterally in the angular gyrus and in the left precuneus (table 1).

For the encoding specific effect of stimulus type, a relative increase of activation during encoding of novel relative to practiced stimuli in the putamen ( $t_{\max} = 10.43$ ) and several other cortical and subcortical areas, including the DLPFC (figure 8A), was observed. The opposite contrast revealed activation in the bilateral angular gyrus and left precuneus (table 2).

For all contrasts revealing striatal activations, i.e., contrasts reflecting increased activation during encoding and during the processing of novel items, clusters were located in the anterior putamen, i.e., dorsal and rostral to the anterior commissure. For illustration purposes, figure 8B depicts the response profile of the DLPFC and putamen within the VOIs that were subsequently used for DCM.

#### Dynamic Causal Modeling

BMS analysis of the model families, which varied by modulation pattern, identified a clear winning family (model family # 16; family exceedance probability:  $p = .94$ ). This model family comprised a full modulation pattern, i.e., a modulation of both intrinsic connections (DLPFC to striatum and striatum to DLPFC) by the two encoding conditions (EN, EP; figure 9A).

Within the winning family, the highest protected exceedance probability was observed for the model, including the input from all four conditions exclusively to DLPFC (model # 9; protected exceedance probability:  $p = .86$ ; Figure 9a,b).

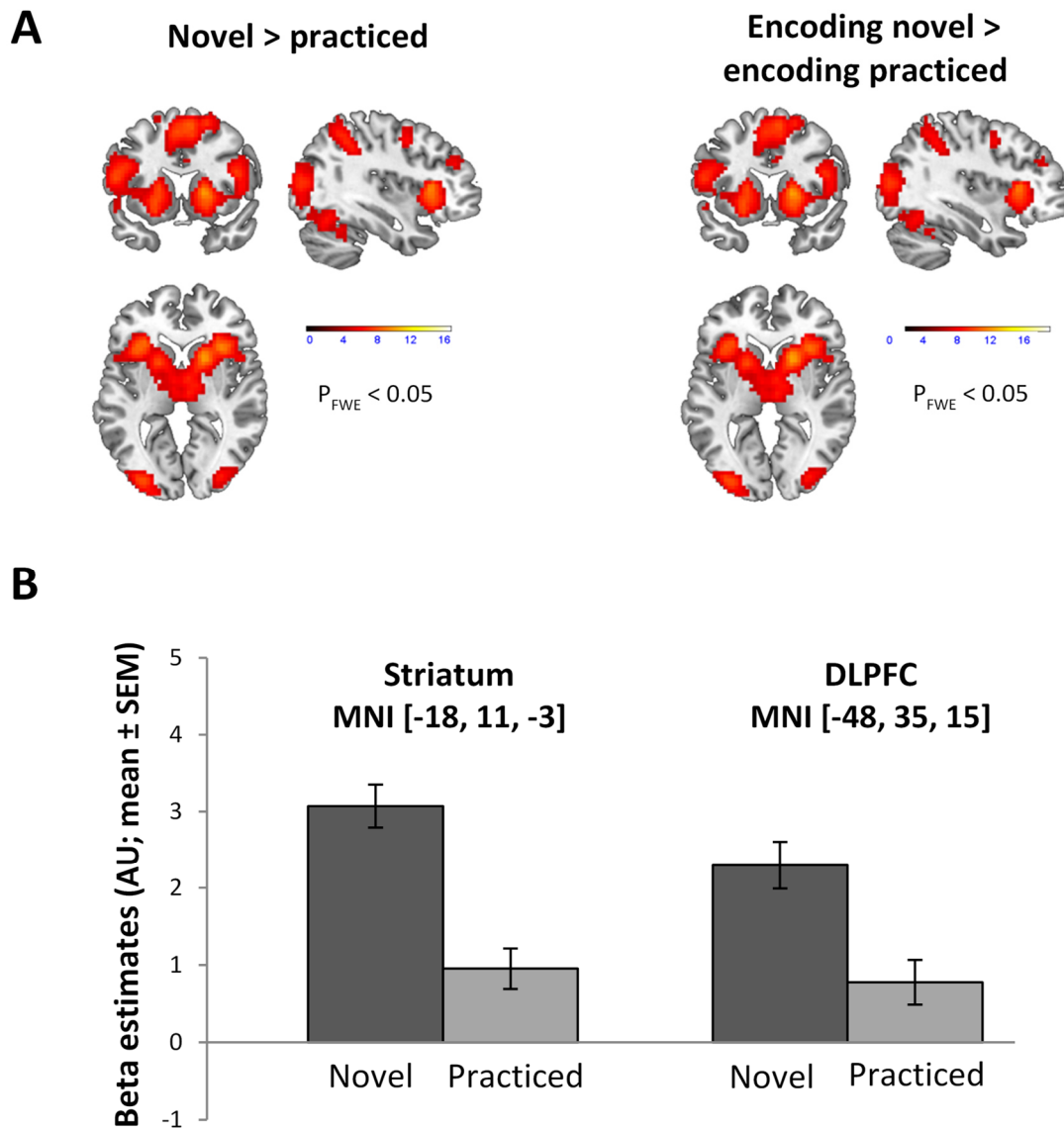


**Figure 8 Brain activations at group level.**

Panel A: Activation maps for the main effect of stimulus type (novel > practice) and the encoding specific effect of stimulus type (encoding-novel > encoding-practiced). All maps are thresholded at  $p < 0.05$ , family-wise error corrected ( $P_{FWE}$ ) for the whole brain. Color bars represent  $t$  values. Panel B: Bar graph illustrations of the mean beta estimates ( $\pm$  SEM) across subjects for the different task conditions within the striatum and DLPFC volumes of interest used for DCM; Abbreviations: DLPFC = dorsolateral prefrontal cortex, AU = arbitrary units, DCM = Dynamic causal modeling.

**TABLE 1:** Regional brain activations related to stimulus type.

Region (Brodmann area)	Cluster size	t value	Peak MNI coordinates		
			x	y	z
<i>Novel &gt; practice</i>					
Insula (BA 13)	4106	10.34	33	23	6
Anterior Putamen		10.26	18	14	6
SMA (BA 6)		9.67	6	8	60
Insula (BA 13)		8.82	-36	23	3
Middle Cingulum (BA 32)		8.49	9	20	36
Anterior Putamen		8.35	-18	8	6
SMA (BA 6)		7.99	-3	11	54
Middle Cingulum (BA 32)		7.99	-6	17	42
Precentral Gyrus (BA 6)		7.82	-42	-7	48
Precentral Gyrus (BA 6)		7.51	48	-1	45
Thalamus		7.22	6	-4	3
Thalamus		6.47	-6	-7	3
DLPFC (BA 10/46)		6.1	-45	32	18
Superior parietal gyrus (BA 7)	1399	8.95	27	-64	45
Parietal inferior gyrus (BA 40)		7.07	45	-40	48
Middle occipital gyrus (BA 18/19)		7.51	36	-85	12
Inferior occipital gyrus (BA 20/37)		8.06	45	-61	-15
Fusiform gyrus (BA 19/37)		8.06	45	-61	-15
Superior parietal gyrus (BA 7)	1560	8.85	-24	-64	54
Middle occipital gyrus (BA 18/19)		8.6	-27	-76	24
Parietal inferior gyrus (BA 40)		7.55	-42	-40	42
Inferior occipital gyrus (BA 20/37)		6.72	-48	-61	-15
Fusiform gyrus (BA 19/37)		7.19	-30	-64	-12
DLPFC (BA 10/46)	39	6.08	39	41	27
Cerebellum	12	5.94	-39	-58	-24
Cerebellum	19	5.72	36	-52	-27
<i>Practice &gt; Novel</i>					
Precuneus (BA 31)	109	6.68	-6	-58	27
Angular gyrus (BA 39/40)	127	6.53	-51	-70	39
Angular gyrus (BA 39/40)	31	6.11	54	-67	36

Note: Regions were classified according to the AAL Atlas (Tzourio-Mazoyer et al., 2002). Coordinates in MNI space and statistical information refer to the peak voxel in the corresponding area. Cluster size is given at  $p < 0.05$  (family-wise error corrected for the whole brain). Abbreviations: Automated Anatomical Labeling (AAL), Montreal Neuroimaging (MNI), supplementary motor area (SMA), dorsal premotor cortex (dPMC), dorsolateral prefrontal cortex (DLPFC).



**TABLE 2: Regional brain activations related to encoding specific effects of the stimulus type.**

Region (Brodmann area)	Cluster size	t value	Peak MNI coordinates		
			x	y	z
<i>Novel (encoding &gt; retrieval) &gt; practiced (encoding &lt; retrieval)</i>					
Anterior Putamen	3536	9.43	21	14	6
Insula (BA 13)		8.8	33	23	6
Pre-SMA (BA 6)		8.23	6	5	63
dPMC/DLPFC (BA 6/9)		7.51	48	-1	45
Anterior Putamen		7.42	-18	8	3
Middle Cingulum (BA 32)		7.38	9	20	36
Insula		7.29	-36	23	3
Middle Cingulum (BA 32)		6.98	-6	17	39
Pre-SMA		6.82	-3	5	63
Inferior frontal Gyrus (BA 44/45)		6.72	-54	8	18
Inferior frontal Gyrus		6.41	48	11	18
dPMC/DLPFC (BA 6/9)		6.03	-51	-1	36
Thalamus		5.41	9	-7	0
Thalamus		5.29	-6	-10	0
Middle occipital gyrus (BA 18/19)	1228	7.76	36	-85	12
Inferior occipital gyrus (BA 20/37)		6.86	45	-64	-6
Parietal inferior gyrus (BA 40)		5.38	45	-37	48
Fusiform gyrus (BA 37)		5.15	39	-61	-12
Middle occipital gyrus (BA 18/19)	1179	7.57	-36	-88	3
Superior parietal gyrus (BA 7)		7.31	-21	-64	54
Fusiform gyrus (BA 37)		6.66	-30	-64	-12
Superior parietal gyrus (BA 7)		6.51	27	-61	51
Inferior occipital gyrus (BA 20/37)		5.62	-45	-73	-6
Parietal inferior gyrus (BA 40)	102	5.34	-39	-40	45
<i>Practice (encoding &lt; retrieval) &gt; novel (encoding &gt; retrieval)</i>					
Angular gyrus (BA 39/40)	100	5.42	-48	-70	42
Precuneus (BA 31)	51	5.36	-6	-58	24
Angular gyrus (BA 39/40)	24	5.22	54	-64	36

Note: Regions were classified according to the AAL Atlas (Tzourio-Mazoyer et al., 2002). Coordinates in MNI space and statistical information refer to the peak voxel in the corresponding area. Cluster size is given at  $p < 0.05$  (family-wise error corrected for the whole brain). Abbreviations: Automated Anatomical Labeling (AAL), Montreal Neuroimaging (MNI), supplementary motor area (SMA), dorsal premotor cortex (dPMC), dorsolateral prefrontal cortex (DLPFC).

Further inspection of the winning model parameters using BPA revealed a significant input from encoding novel and encoding practice to DLPFC as well as a significant top-down connection from DLPFC to striatum. Further, a significant modulatory effect for encoding novel on the top-down connection from DLPFC to striatum ( $p = 1$ ) was found. Bayesian parameter averages, including

posterior probabilities of the winning model, are shown in table 3. The winning model, including significant BPA results, is displayed in figure 9B. In order to rule out an effect of the thalamus on DLPFC-driven top-down modulation of the striatum (Perakyla et al., 2017), a supplemental DCM analysis was performed, which included the thalamus as a VOI and had no impact on the main outcome of the initial analysis (i.e., modulation of the connection from DLPFC to striatum). For more detail, see supplementary results in section 2.1.4 (page 29) and Table S2 in section 6 (page 74).

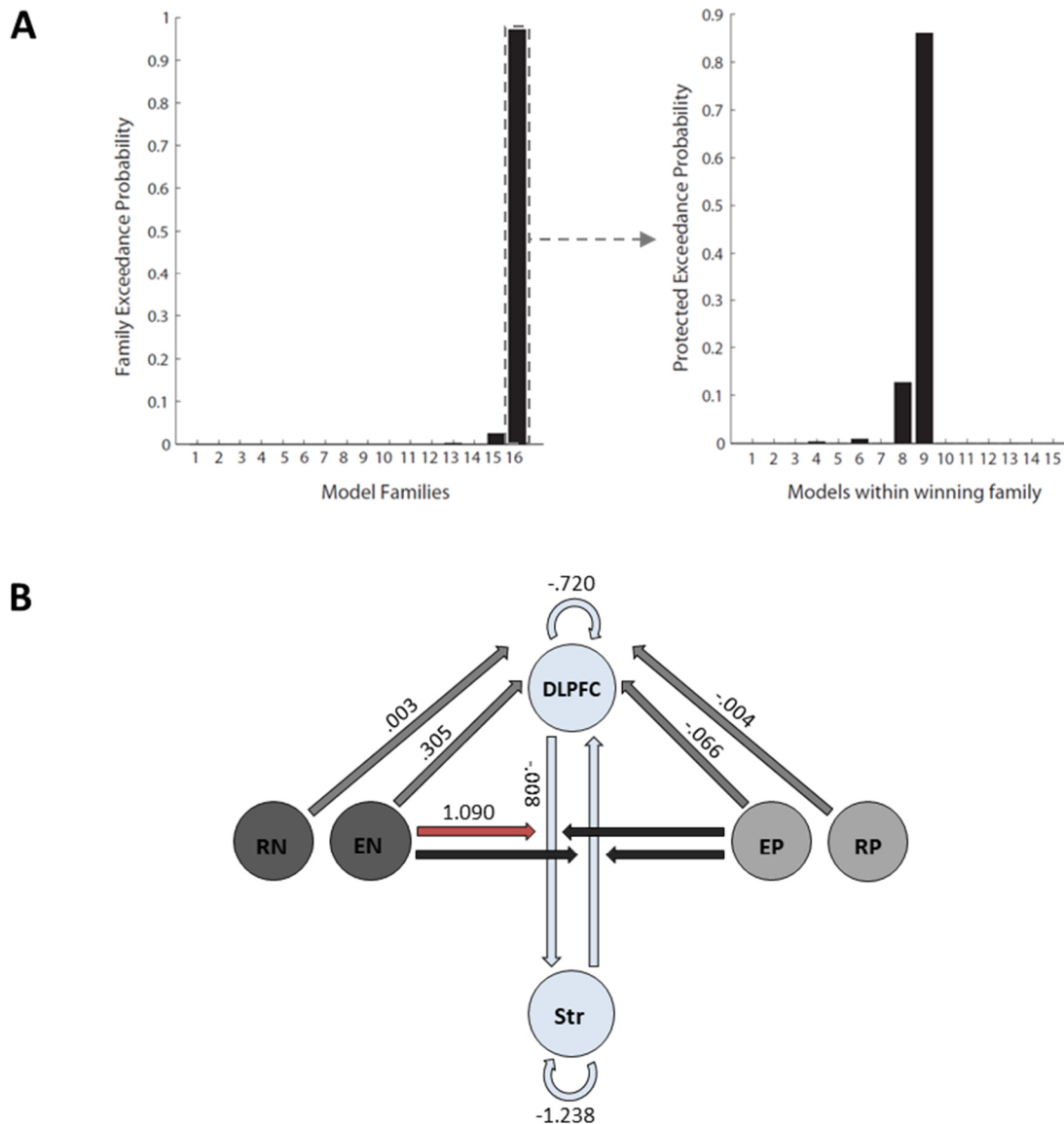


**Figure 9. DCM results with Bayesian model estimation and Bayesian parameter averaging.**

Panel A, left: Bayesian model estimation results for the model families. Winning model family (# 16), with family exceedance probability of  $p = .94$ . Panel A, right: Bayesian parameter averaging results within the winning family. Winning model (# 9) with  $p = .86$ . Panel B: Illustration of the winning model. Driving inputs from all conditions are directed to DLPFC. Red arrow indicates the modulation of the connection from DLPFC to striatum. Abbreviations: EN = encoding novel, EP = encoding practice, RN = retrieval novel, RP = retrieval practiced, DLPFC = dorsolateral prefrontal cortex, Str = striatum.

**TABLE 3: Bayesian parameter averages of the winning model**

<b>Intrinsic connections</b>			
To		From	
		DLPFC	Striatum
	DLPFC	<b>-.720 (1.00)</b>	.018 (.844)
	Striatum	<b>-.008 (.974)</b>	<b>-1.238 (1.00)</b>

<b>Modulation of connectivity</b>			
		Encoding novel	Encoding practice
	DLPFC to Striatum	<b>1.090 (1.00)</b>	.040 (.74)
	Striatum to DLPFC	.043 (.710)	-.146 (.88)

<b>Input</b>			
		Encoding novel	Encoding practice
	DLPFC	<b>.305 (1.00)</b>	<b>-.066 (1.00)</b>
	(Striatum)	-	-
		Retrieval novel	Retrieval practice
	DLPFC	<b>.003 (0.96)</b>	<b>-.004 (0.99)</b>
	(Striatum)	-	-

Note: Significant parameters are in bold print. Posterior probabilities are in parenthesis. Abbreviation: DLPFC = dorsolateral prefrontal cortex.

### 2.1.4 Supplemental analyses

#### Supplemental results – main effect of working memory phase

For the main effect of working memory phase, a significant bilateral activation increase in the putamen ( $t_{\max} = 10.98$ ) and DLPFC ( $t_{\max} = 9.99$ ) during the encoding relative to the retrieval of working memory items (see figure S1) was detected. Other regions surviving whole-brain correction ( $p_{FWE} < 0.05$ ) included the anterior insula, middle temporal gyrus, anterior cingulate cortex, hippocampus, and higher order motor and visual areas (Table S1, page 73 and 74). In the opposite contrast, a single cluster in the left postcentral gyrus was observed (Table S1, page 73 and 74).

## Encoding phase > retrieval phase

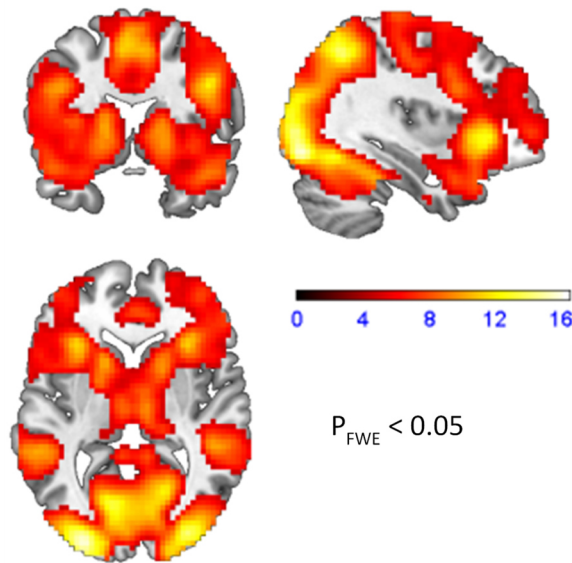


**Figure S1. Activation maps for the main effect of working memory phase (encoding > retrieval).**

Regions were thresholded at  $p < 0.05$ , family-wise error corrected (FWE) for the whole brain. Color bar represents t values. Please note that this contrast's interpretation is limited by the differences in visual stimulation, task demands, and duration between both task phases.

### Supplemental DCM analysis

In order to rule out that the DCM finding was dependent on an unaddressed influence of the thalamus, a supplemental DCM analysis including a VOI for the thalamus was conducted. The subject-specific thalamic VOIs were defined as follows: First, in order to ensure regional specificity, a mask from the group peak activation of the "encoding novel > encoding practiced" contrast by centering a 6-mm sphere around the peak voxel within a structural ROI of the thalamus (AAL atlas) was derived. This empirically defined thalamus mask was used to subsequently localize the individual peak voxel in each subject's contrast image and to extract the first eigenvariate from 6-mm spheres centered around this individual peak. Second, the thalamus was included as an additional region using the same connection and modulation scheme as in the winning model described in the manuscript. Then the location of the input was determined by varying the input to the striatum, DLPFC, and thalamus, respectively, which resulted in three full models. Random effects Bayesian model selection analysis yielded a winning model with the highest protected exceedance probability for the input to the DLPFC ( $p = .83$ ), followed by the striatum ( $p = .122$ ) and the thalamus ( $p = .05$ ). Subsequent Bayesian parameter averaging (BPA) suggests that the modulation of the connection from DLPFC to striatum is robust to the inclusion of the thalamus in the model (see table S2, page 74, all parameters shown have evidence  $> .95$ ).

## 2.2 Study 2: LONGITUDINAL BEHAVIORAL AND BRAIN FUNCTIONAL EFFECTS OF A PLASTICITY-RELATED VARIANT IN BDNF ON VERBAL WORKING MEMORY LEARNING<sup>3</sup>

### 2.2.1 Abstract

Corticostriatal brain circuits play a key role in higher cognitive processes such as working memory function and are important targets for neurotrophin signaling, such as the brain-derived-neurotrophic factor (BDNF). BDNF promotes neural and synaptic growth and has been associated with short-term and long-term memory performance, particularly the polymorphism *BDNF Val66Met*. The effect of this polymorphism on brain function and behavior has been investigated in previous studies suggesting that genetic predispositions related to BDNF contribute to individual differences in learning and memory. However, the longitudinal effects of working memory (WM) learning on the functional plasticity of corticostriatal brain circuits, the behavioral significance of their modifiability, and the relationship to BDNF transmission in humans are not widely understood. A promising approach to investigate plasticity is to characterize learning-induced changes in behavior and brain function by applying exponential learning curves. So far, only a few studies in the field of motor learning have applied learning parameters. To address this gap, a longitudinal neuroimaging study, with a two-week training period and 14-week follow-up assessment, was conducted in healthy carriers and non-carriers of *BDNF Val66Met* polymorphism, performing a modified Sternberg WM task. To characterize learning-induced changes in task performance and corticostriatal function, exponential decay modeling with learning parameters  $\alpha$  (learning speed) and  $\tau$  (learning gain) was applied. Further, voxelwise Linear discriminant analysis (LDA) and brain-behavior correlation methods were used to study the role of *BDNF* genotype. *BDNF*-deficient <sup>66</sup>Met-allele carriers showed a significant WM deficit at the beginning and the 14 week follow up measurement, a delayed prefrontal signal decay, and a lack in an increase in sustained corticostriatal connectivity across the training interval. In addition, a positive association between behavioral learning speed and the speed of signal decay in the striatum and DLPFC was absent in risk allele carriers. Further, a faster and higher increase in functional connectivity resulted in a better follow-up performance, indicating the importance of forming a connectivity “scaffold” for long-term consolidation, which seems to be limited in *BDNF* risk allele carriers. These results extend existing literature by showing that carriers of a functional genetic risk variant linked to inefficient BDNF signaling and impaired neural plasticity show immediate, training-independent deficits in verbal

---

<sup>2</sup> Geiger, L. S., Zang, Z., Melzer, M., Witt, S., Rietschel, M., van Raalten, T. R., Meyer Lindenberg, A., Moessnang, C., Wüstenberg, T. & Tost, H. (2021). Longitudinal behavioral and brain functional effects of a plasticity-related variant in *BDNF* on verbal working memory learning. In Presubmission to *Proc Natl Acad Sci U S A*.

working memory learning that are not fully rescuable by repeated short-term training and persist at long-term follow-up.

## 2.2.2 Methods

### Participants and genotyping procedures

Twenty-three healthy right-handed individuals ( $28 \pm 7.7$  years, 16 females) participated in this longitudinal study, chosen from a larger cohort of research-interested participants based on the *BDNF* genotype. The Val<sup>66</sup>Met single-nucleotide polymorphism (rs6265) in the 5' promoter region of the *BDNF*-Gene was determined using PsychChip arrays (Illumina, San Diego, CA). We used standard methods to extract genomic DNA from lymphoblastoid cell lines and genotype individual single-nucleotide polymorphisms (SNPs) for *BDNF* val66met single-nucleotide polymorphism (rs6265), using the microarrays PsychChip-v1.1-A and PsychChip-v1.0-B (Illumina Inc). Eleven subjects were Val/Val homozygous, ten subjects were Val/Met heterozygous, and two subjects were Met/Met homozygous (see table S6, in section 6, supplemental tables, page 77). One participant with a *BDNF* Val/Met genotype participated in sessions 1-5 but was unable to take part in the 14-week follow-up assessment (session 6). None of the enrolled participants reported a history of severe general medical, neurological or psychiatric illness or substance abuse. All individuals provided written informed consent for a protocol approved by the Ethics Committee of the University of Heidelberg.

### Study protocol, verbal working memory paradigm, and task training

23 Participants underwent five fMRI sessions within 12 days (i.e., on day 1, 2, 5, 9, 12) and an additional session in week 14 after study onset (Mean 90.6 days  $\pm$  10.74 days). In each fMRI session, study participants performed a modified Sternberg working memory task (27-29) consisting of two task phases and four task conditions (Fig. 8). In the encoding phase (3500 ms), individuals were asked to memorize stimulus sets of seven letters. In the following response phase, participants were asked to indicate, by button press, whether or not six consecutively presented single letter probes (presentation time 1400 ms, interstimulus interval 358 ms – 1790 ms, randomly jittered in steps of 358 ms) had been part of the encoding stimulus set.

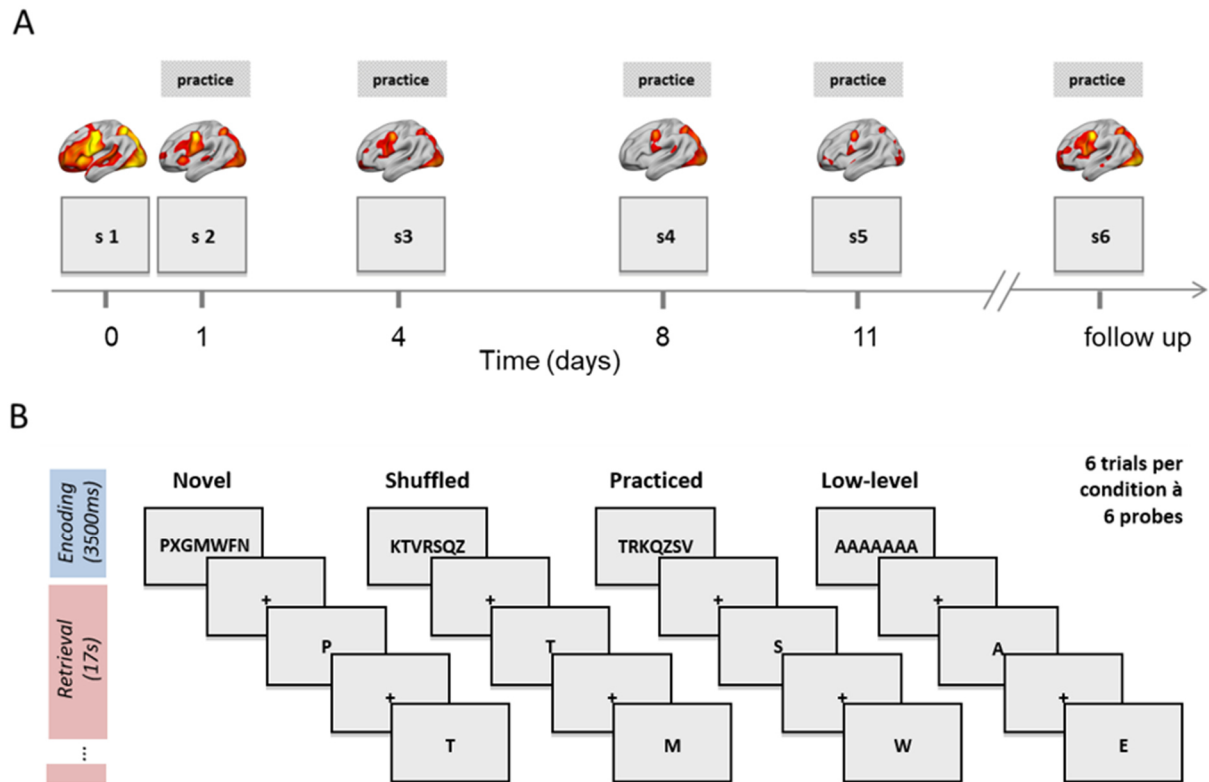


**Figure 10. Study protocol and learning task.**

Panel A: Subjects performed five sessions of a modified Sternberg task (B) within 12 days (day 0, 1, 4, 8, 11) labeled as session 1-5 (S1-S5) and a follow-up session (S6) after 14 weeks. From the second session onwards, fMRI scans were preceded by a practice session where subjects were trained to memorize a fixed target set. Panel B: The longitudinal Sternberg task consisted of two task phases (encoding, retrieval) and four task conditions (novel, shuffled, practiced, and a low-level control condition).

Within the task, the type and familiarity of the encoding sets were systematically varied to match four different task conditions. Each condition was presented six times, and the order of conditions was pseudo-randomized and counterbalanced. Specifically, in the "practiced" condition, a fixed encoding set of seven consonants was presented across the task and in all scanning sessions of an individual (e.g., "TRKQZSV"). In addition, the "practiced" encoding was explicitly trained since, from the second fMRI session onwards, each fMRI scan was preceded by an offline practice session in which the individuals were trained in memorizing their specific "practiced" encoding set (8.8 minute duration, 24 task trials). In the "shuffled" condition, the pre-trained encoding set of individuals was presented in different, randomly shuffled orders (e.g., "KTVRSQZ"). In the "novel" condition, subjects had to memorize entirely novel sets of randomized consonants (e.g., "PXGMWFN"). None of the "novel" consonants were part of any of the "practiced" or "novel" encoding sets. The encoding stimulus set of the low-level control condition consisted of seven identical vowels (e.g., "AAAAAAA").

### **fMRI data acquisition, preprocessing, and first-level analysis**

Functional neuroimaging of the Sternberg task was performed on a 3 Tesla whole body MR Scanner (Siemens, Erlangen, Germany), with a 32-channel head coil (parallel imaging; generalized autocalibrating partially parallel acquisition (GRAPPA); iPAT=2). Functional images were acquired in descending order with a gradient-echo echo-planar imaging (EPI) sequence (TR = 1790 ms, TE = 28 ms, flip angle = 76°, 34 axial slices, 3 mm slice thickness, 1 mm gap, matrix size: 64 × 64, field of view (FoV): 192 × 192 mm; whole brain coverage was ensured by tilting the FoV to -25° from the individual anterior commissure – posterior commissure line).

Data preprocessing was performed using the Statistical Parametric Mapping software (SPM12; <http://www.fil.ion.ucl.ac.uk/spm/software/spm12/>). Briefly, this included a two-pass realignment procedure (i.e., functional images were registered to the mean of the images after a first realignment to the first image), slice time correction, normalization to the Montreal Neurological Institute (MNI) EPI template (using the mean functional image as the source image and the MNI EPI template as the template image), and spatial smoothing with an 8mm full-width at half-maximum (FWHM) Gaussian kernel.

For the first level analysis, a general linear model (GLM) for each subject including the following regressors was defined: four regressors for the encoding phase (novel, shuffled, practiced, low-load cognitive control), one regressor for the cue (indicating a new trial), and four regressors for the retrieval phase. These regressors were modeled using delta (stick) functions for the encoding phases and boxcar functions for the retrieval phases. Based on the results of study 1, demonstrating the sensitivity of task for the encoding process, the second study focused on the encoding phase only. To correct for unspecific effects (e.g. attention, motivation), the low-level control condition was subtracted from the novel, shuffled and practiced condition and defined the following contrasts: [encoding – novel > encoding low-level control], [encoding – shuffled > encoding low-level control], [encoding – practiced > encoding low-level control]

### **Effects of *BDNF* genotype on pre-and post-training behavioral performance**

Mean error rates were calculated for each task condition for the first, fifth, and last session (follow-up) to assess the effect of *BDNF* genotype on working memory performance. The data of the practiced, shuffled, and novel conditions were corrected for non-specific effects such as attention or fatigue by subtracting the respective error rates obtained by the low-level control condition. Analysis of variance (ANOVA; SPSS22 (IBM SPSS Statistics, Chicago, IL)) was used to compare error rates between genotype



groups and task conditions. Significance threshold for report and discussion was set to  $\alpha = 0.05$ . If necessary, degrees of freedom were Greenhouse-Geisser corrected.

The following higher-level analyses were conducted by means of in-house scripts in MatLab (The Mathworks, version 2019a), using routines included in the Matlab statistics toolbox (<https://www.mathworks.com/products/statistics.html>). These scripts are available upon request.

### **Exponential modeling of behavioral and brain data**

Following the law of practice (detailed description in section 1.6), an exponential model of the general form  $Y(t) = \alpha e^{\tau t}$  was fitted to the data time series of the training interval. The model parameter  $\alpha$  reflects mainly the amplitude (i.e. the amount) of change over time in performance, brain response, and functional connectivity (e.g., positive estimates of  $\alpha$  indicating a better performance after learning.) The model parameter  $\tau$  reflects the speed of change over time in performance, brain response, and functional connectivity (e.g., the more negative estimates of  $\tau$  are, the faster the learning process). Models were fitted using in-house Matlab scripts (The Mathworks, version 2019a) using a restricted maximum likelihood parameter estimation. Modeling success was tested as goodness of fit (GoF) for each condition by computing variance explanation  $R^2$ . Only parameter estimates from sufficiently good models (GoF:  $R^2 \geq 0.25$ ) were subjected to post-hoc analyses.

### **Analysis of effects of training and genotype on behavioral performance using exponential modeling**

The model parameters  $\alpha$  and  $\tau$  served (1) as dependent variables in two separate 2x3 repeated measures ANOVA with between-subject predictor genotype (Val/Met-carrier) and within-subject predictor condition (practiced, shuffled, novel); all corrected for control) and (2) two-dimensional linear discriminant analysis (LDA). Statistical analyses were performed in SPSS22 (IBM SPSS Statistics, Chicago, IL). Significance threshold for report and discussion was set to  $\alpha = 0.05$ . If necessary, degrees of freedom were Greenhouse-Geisser corrected.

### **Analysis of effects of training and genotype on brain responses using exponential modeling**

For each training session, beta estimates of brain responses in the encoding phase were calculated. The beta estimates of the practiced condition (which yielded the strongest behavioral effects of genotype) were corrected for unspecific time-variant effects by contrasting them against the respective beta estimates of the low-level control condition. The exponential model was then fitted into the resulting contrast image time series to obtain parameter estimates for  $\alpha$  and  $\tau$  for each brain voxel. GoF maps were used to localize brain regions that were responsive to cross-session learning.

Based on the hypothesis of a key role of the cognitive frontostriatal loop in verbal learning, the further analyses were restricted to learning-responsive voxels within anatomical masks of the left middle frontal gyrus and left striatum (combined mask of putamen, caudatus, and ventral striatum, displayed in figure 11), derived from Harvard Oxford cortical and subcortical structural atlases (Desikan et al., 2006; Frazier et al., 2005; Goldstein et al., 2007; Makris et al., 2006). The resulting mask consisted of 1926 voxels ( $V \approx 52 \text{ cm}^3$ ). In a second step, to avoid spurious effects in subsequent LDA-analyses, all voxels with a worse model fit (GoF:  $R^2 < 0.25$ ) were excluded for the brain response and the functional connectivity map separately. The remaining masks consisted of 849 voxels ( $V \approx 23 \text{ cm}^3$ ) for brain response models and 780 voxels ( $V \approx 19 \text{ cm}^3$ ) for the functional connectivity models.

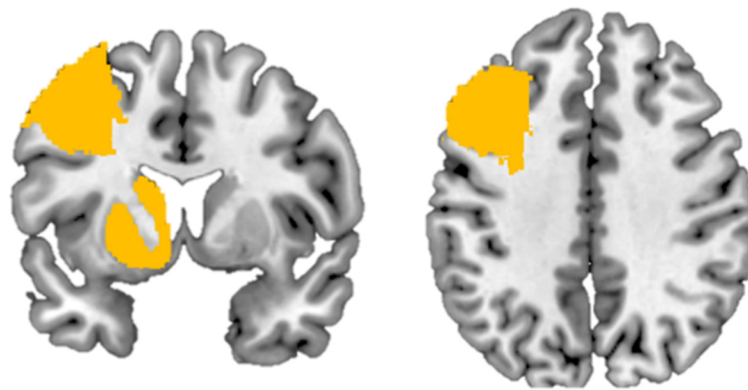


**Figure 11. Illustration of regions of interest for the learning-responsive areas.**

This is a joint mask from the Harvard Oxford Brain Atlas of the middle frontal gyrus, putamen, caudatus, and ventral striatum.

For these ROIs (figure 11), separate voxel-wise two-dimensional LDA-analyses for brain response (BR) and functional connectivity (FC) were conducted, using the model parameter estimates  $\alpha$  and  $\tau$ . The resulting classification maps were subjected to a voxel-wise Chi-square test.

To account for the problem of massive multiple testing, a Monte-Carlo-simulation based approach was applied. This simulation as well as the prior estimation of the smoothness of the Chi-square maps was done by means of AlphaSim as implemented in the software package RESTplus (V1.23, released 20200428, <http://www.restfmri.net/forum/REST>). For each between-group comparison, 1000 simulations were performed within the a-priory masks using the smoothness estimates of the corresponding statistical map for brain response and functional connectivity and a voxel alpha threshold of  $P < .05$ . The size of the first cluster with a probability of occurrence less than 5% was used to threshold the corresponding statistical map. Only clusters with a size equal to or larger than this threshold were considered for report and discussion. This procedure revealed a minimum cluster size

of 15 voxels for brain response maps and 16 voxels for functional connectivity maps (see table S4 in section 6, page 77). These cluster sizes in combination with a statistical threshold of  $p_{\text{Chi}} > .05$  were applied to the Chi-square maps to identify voxels with the genotype-specific pattern of model parameters.

### **Analysis of effects of training on functional connectivity using exponential decay modeling**

To test the effect of genotype on learning-related changes in frontostriatal functional connectivity, a generalized psycho-physiological interaction (gPPI) analysis was used to assess sustained and task-modulated functional connectivity for each session. Seeds were defined as 5-mm spheres centered on the previously defined GoF peak in the left dorsal striatum (MNI  $x = -18, y = 5, z = 6$ ). Seed time courses were extracted as the first eigenvariate and adjusted for effects of interest (i.e., removal of effects of motion). gPPI regressors were generated as the element-by-element product of each encoding condition (i.e., psychological regressors) and the seed time course (physiological regressor), all of which were de-convolved for multiplication and subsequently re-convolved with the hemodynamic response function (HRF). The seed time series and the resulting gPPI regressors were included in a first-level general linear model, along with the task regressors, convolved with the HRF, and the six realignment parameters to account for head motion. During first-level model estimation, data were high-pass filtered with a cutoff of 128 s, and an autoregressive model of the first order was applied. To quantify task-modulated functional connectivity (tmFC), a gPPI contrast that reflected the differential connectivity between the practiced condition and the low-level control condition was computed. Sustained connectivity (sFC) was defined by contrasting the VOI regressor to the implicit baseline. After estimating subject-level gPPI models, the resulting contrast images were analyzed similarly to the brain response data. Voxel-wise signal decay models were fitted to the two connectivity estimates (sFC and tmFC). For each connectivity type, voxels with sufficient model fit (mean GoF:  $r > 0.5$ ) were subjected to a voxel-wise LDA of the model parameter estimates  $\alpha$  and  $\tau$ . Significance was assessed within the predefined DLPFC mask detailed above.

### **Analysis of brain-behavior relationships of learning parameters**

To test for genotype-specific associations between behavior-derived and brain-derived learning parameters ( $\alpha, \tau$ ), voxel-wise parameter maps were subjected to a multiple regression model in SPM, and behavioral learning parameters for each genotype group were entered as covariates of interest. Then, both covariates were compared using an F-contrast [1 -1] to identify the effect of genotype on brain-behavior associations. Results were masked with the previously defined mask of learning-responsive regions (GoF > 0.5).

### Predictive modeling of follow-up behavioral performance

To test whether and how the behavioral performance  $Acc_{PT-CT}^{FU}$  of the remaining 21 participants at the follow-up measurement (14 weeks after training) can be predicted by parameter estimates of the individual exponential models for brain response and functional connectivity, a linear multiple regression model to the performance data was fitted, without distinguishing between genotypes.

In total, three linear fixed-effects models were tested, which resulted from the combination of the brain-derived predictors  $\alpha$  and  $\tau$  extracted for brain responses (DLPFC or striatum) and the sustained functional connectivity (striatum to DLPFC). The three models had the following form:

$$Acc_{PT-CT}^{FU} \sim 1 + \alpha_{FC(Striatum|DLPFC)} + \tau_{FC(Striatum|DLPFC)}$$

$$Acc_{PT-CT}^{FU} \sim 1 + \alpha_{BR(DLPFC)} + \tau_{BR(DLPFC)}$$

$$Acc_{PT-CT}^{FU} \sim 1 + \alpha_{BR(Striatum)} + \tau_{BR(Striatum)}$$

The medians of the parameter estimates ( $\alpha$ ,  $\tau$ ,  $\alpha^*\tau$ ) were computed and z-scaled within the DLPFC-clusters (brain response and functional connectivity) and the striatum-cluster (brain response only). Model generalizability was tested subsequently by means of 999 10-fold model cross-validations. Models were compared using a simulated Likelihood ratio test (LRT) with 1000 simulations. Finally, the best model was selected based on LRT statistics, the median  $R^2$  of the original, and the corrected Akaike information criterion (cAIC).

### Role of head movement and image quality

For fMRI data quality assurance, the individual head motion parameters and the signal-to-noise ratio were computed using SPM12. Using the corresponding parameter estimates, the average translation and rotation across the time series and the frame-wise Euclidean displacement (Power, Barnes, Snyder, Schlaggar, & Petersen, 2012) were calculated, and its average. The displacement time series were then inspected regarding spikes and quantified individual numbers of spikes and average frame-wise displacement (Van Dijk, Sabuncu, & Buckner, 2012). Then, a statistical comparison of the image quality measures between the two genotype groups was conducted with SPSS22 (IBM SPSS Statistics, Chicago, IL) using repeated measures ANOVA (time as within-subject factor and genotype as a between-subject factor).

### 2.2.3 Results

#### Effects of *BDNF* genotype on behavioral performance

*BDNF* Met-allele carriers showed significantly higher error rates compared to the Val/Val homozygotes at session 1 ( $F(1,21) = 11.338, P = 0.003$ ). There were no differences in error rates after repeated training (session 5,  $F(1,21) = 2.41, P = 0.136$ ) but at the 14 week follow-up assessment (session 6,  $F(1,20) = 6.029, P = 0.023$ ). The genotype effect was not modulated by task condition (genotype x condition interaction:  $F(1,42) < .882, P > .406$ ).

#### Effects of *BDNF* genotype on behavioral performance during training

To characterize learning throughout the training interval (sessions 1-5), learning curves (i.e., exponential decay models) were fitted to session-wise error rates with learning gain ( $\alpha$ ) and learning speed ( $\tau$ ) as free parameters (Figure 12A). The goodness of fit (GoF) analyses confirmed a sufficiently good model fit for all task conditions and genotype groups (mean  $r$  values: .62–.84; no significant main effect of interaction: all  $P > .429$ ). For more detail, see Table S3 on page 75. *BDNF* Met-allele carriers showed a higher learning gain compared to Val/Val homozygotes across conditions ( $F(1,21) = 5.10, P = 0.04$ ; post-hoc comparison:  $t(13.4) = 2.74, P = 0.02$ , Table S3, page 75), consistent with their overall lower pre-training performance level in session 1, but displayed similar performance level at the end of the training in session 5 (figure 12 A). Learning speed was not impacted by genotype ( $F(1,21) = 0.53, P = 0.48$ ), and no genotype x condition effects emerged (all  $F < 1.68$ , all  $P > 0.06$ ), see table S3, page 75 for more details.

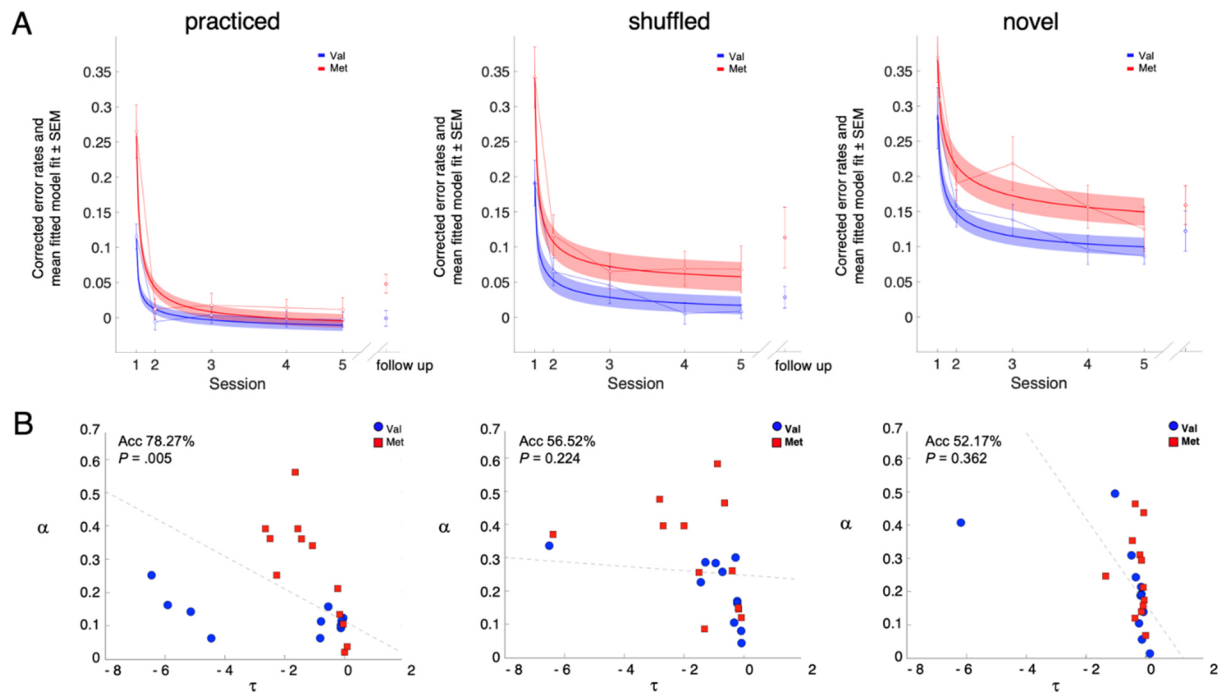


**Figure 12. Behavioral results.**

Panel A: Effect of genotype on learning performance (error rates) for each task condition (practiced, shuffled, novel) across sessions. Displayed are mean error rates and the mean fitted model. Standard error of means are indicated by error bars and shaded areas. Panel B: Results of two-dimensional LDA for each task condition (practiced, shuffled, novel) using  $\alpha$  and  $\tau$  as parameters to distinguish between the genotype groups. Linear discriminant curves are shown as gray dashed lines. Abbreviations: LDA = linear discriminant analysis, Acc = Accuracy, SEM = standard error of mean.

Subsequent two-dimensional linear discriminant analysis (LDA) showed that the consideration of both learning parameters  $\alpha$  and  $\tau$ , allowed for the best discrimination between genotype groups in the practiced condition, the task with the highest learning and automatization demands (accuracy: 0.78,  $P = 0.003$ ; figure 12B, table S3). Taken together, these findings suggest that the consideration of both dimensions of the learning process is a sensitive mean to detect *BDNF*-dependent genotype effects and encouraged the subsequent analysis of learning curves in functional brain space.

### Exponential decay modeling in brain functional space

Signal decay models for the training interval (sessions 1-5) were fitted to each subject's brain responses during verbal working memory performance in the practiced condition. Unspecific psychological effects (e.g., basic attention, motivation) were controlled by accounting for low-level conditions (*control*). Models were fitted for each brain voxel, yielding estimates for the amount ( $\alpha$ ) and speed ( $\tau$ ) of signal decay for the adjusted beta estimates across training sessions. To identify brain voxels that followed the decay model, hereafter referred to as *learning-responsive voxels*, GoF maps across groups

(mean  $r > 0.5$ ; Figure 13 B) were computed. The best model fit was observed in the left dorsal striatum ( $r = 0.68$  Montreal Neurological Institute (MNI) coordinates  $x = -18, y = 5, z = 6$ ) which is displayed in figure 14A. This finding is well in line with the established role of the striatum for verbal working memory learning and automatization (Draganski et al., 2008; Geiger et al., 2018; van Raalten, Ramsey, Duyn, et al., 2008). Based on the hypothesis of *BDNF* genotype effects on frontostriatal brain function, only learning-responsive voxels within the previously defined a-priori mask (figure 11, page 36) were selected for further analyses. More GoF maps, such as group specific maps and GoF maps for functional connectivity are displayed in figure 13.

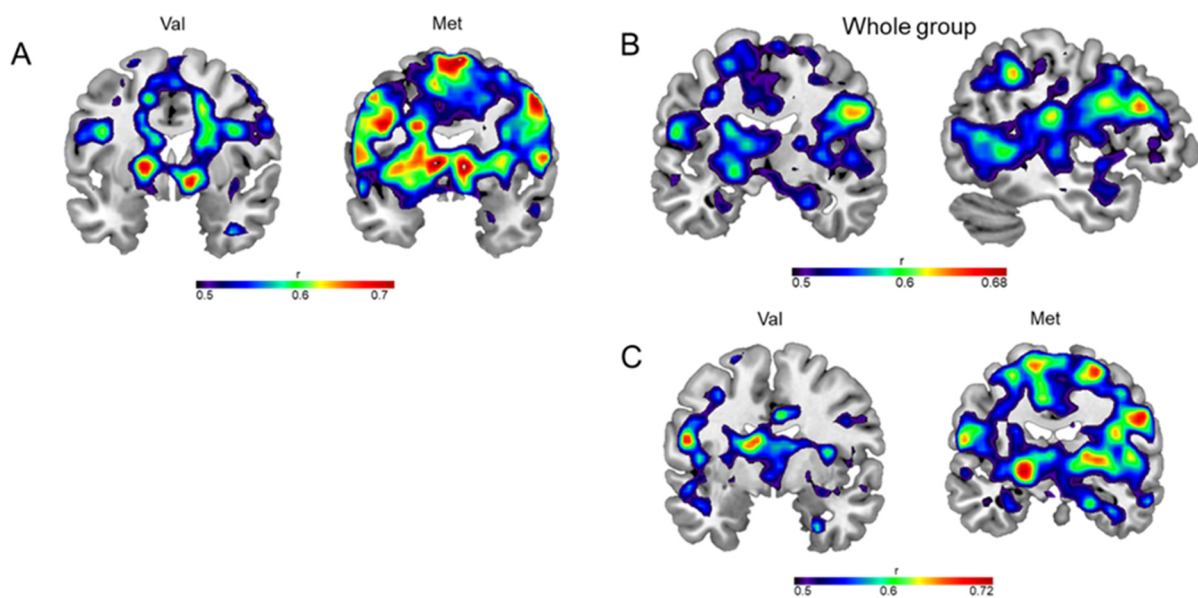


**Figure 13. Illustration of Goodness of Fit maps in the practiced condition.**

Panel A: GoF maps for brain response within each genotype group. Panel B: Combined GoF maps for functional connectivity. Panel C: GoF maps for functional connectivity within each genotype group. All GoF maps are shown for the practiced condition. Higher GoF values indicate brain regions where changes in functional activation follow the postulated signal decay. Abbreviations: GoF = Goodness of Fit, Met = Met allele carrier, Val = Val allele carrier.

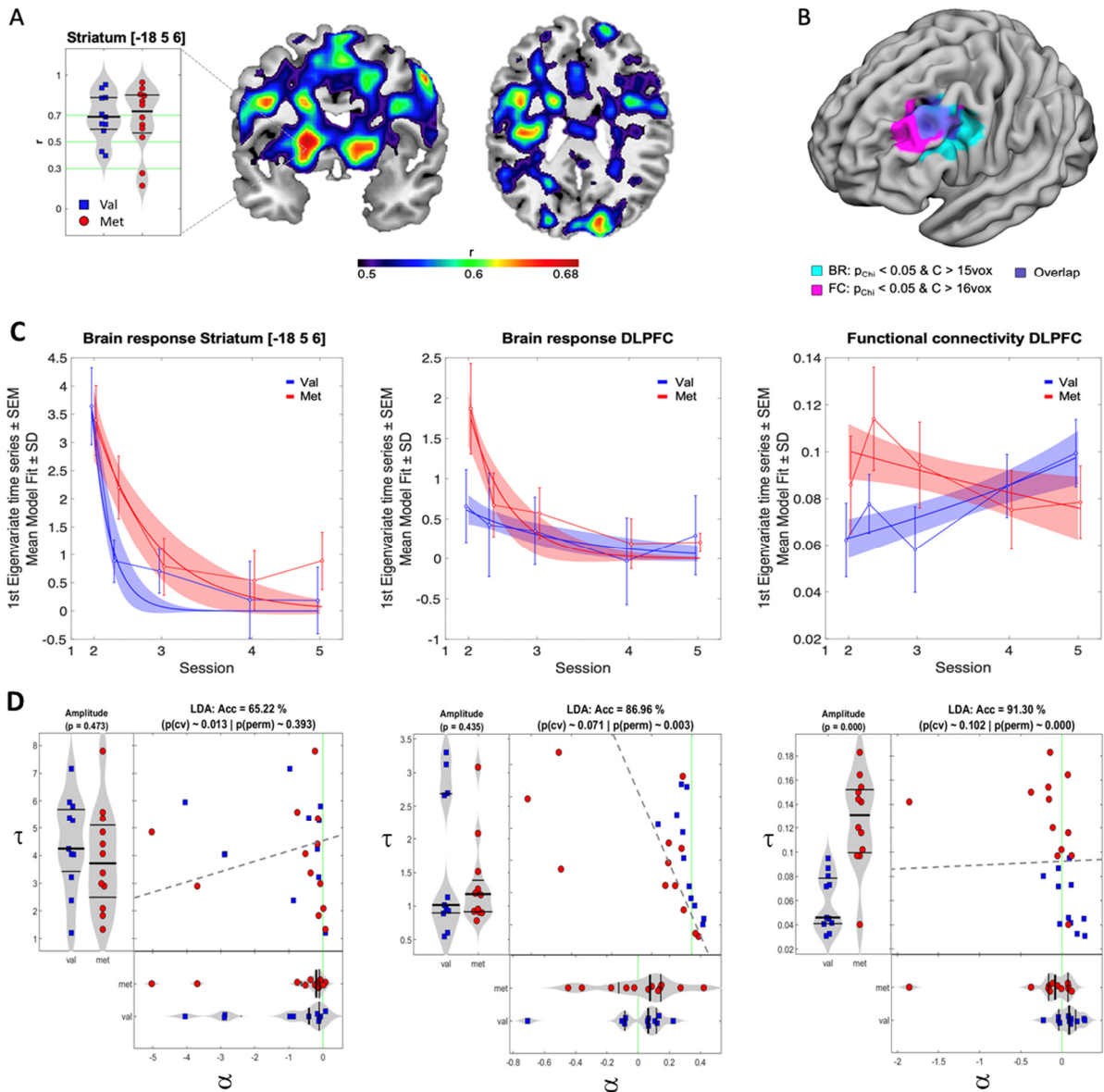


**Figure 14. Results of genotype on brain response and functional connectivity.**

Panel A: Illustration of mean Goodness of fit (GoF) maps for the full sample in the practiced condition (MNI  $y = 5$ ,  $z = 26$ ) and distribution among genotype groups in striatum (left plot). Highest mean GoF was observed in the left dorsal striatum (MNI  $x = -18$ ,  $y = 5$ ,  $z = 6$ ). Panel B: Maps of vwLDA analysis (using  $\alpha$  and  $\tau$  as parameters to distinguish between the genotype groups) within brain response (BR) in striatum (left plot) and DLPFC (middle plot) and functional connectivity (FC) in DLPFC, illustrated within VOI mask for DLPFC. Panel C: Illustration of decay curves extracted from the GoF peak voxel in the left striatum (left plot) and for the accuracy peak voxel within the left DLPFC for brain response and functional connectivity (middle plot, right plot). Shaded areas indicate the 95 % confidence interval of the exponential model fit. Panel D: Results of vwLDA analysis for BR in striatum (left plot) and DLPFC (middle plot) and FC in DLPFC. Linear discriminant curves are shown as gray dashed lines. Abbreviations: MNI = Montreal Neurological Institute, vwLDA = voxelwise linear discriminant analysis, BR = brain response, FC = functional connectivity, VOI = volume of interest, SEM = standard error of mean, DLPFC = dorsolateral prefrontal cortex.



### Effects of genotype on brain signal decay

Consistent with the behavioral analyses, a voxel-wise LDA analysis of the model parameters  $\alpha$  and  $\tau$  was performed to test for *BDNF* genotype-specific differences in learning-responsive voxels within the search regions (see figure 14D). This revealed a cluster within the left DLPFC with good to excellent discrimination between genotype groups (MNI [-39, 11, 30],  $Acc_{Peak} = 0.87$ , cluster size = 47 voxels;  $P < .001$  cluster size corrected for multiple comparisons; Fig. 14B), while there was no significant effect in striatum. For illustration purposes, figure 14C shows decay curves extracted from DLPFC and striatum for each genotype group. The DLPFC decay curves suggest a stronger initial involvement and subsequently delayed decay of activation in the DLPFC in the Met-allele carriers (figure 14C). This pattern is in line with the higher learning gain ( $\alpha$ ) on the behavioral level and suggests that Met-allele carriers initially rely more strongly on prefrontal functional resources during verbal working memory learning.

### Effects of genotype on brain-behavior correlation

To test whether the model parameters for brain response and behavior were correlated, a voxel-wise regression analysis was performed for each of the two learning parameters  $\alpha$  and  $\tau$  in the search regions. Behavioral learning parameters were applied as predictor and genotype as between-subject factor. This revealed a significant effect of genotype on brain-behavior correlations for  $\tau$  in the DLPFC (MNI [-37 17 39],  $F_{(1,20)} = 10.75$ , cluster size = 233 voxels;  $P < .001$  cluster size corrected for multiple comparisons) and striatum (MNI [-12, 11, 9],  $F_{(1,20)} = 13.96$ , cluster size = 82 voxels,  $P = .027$  cluster size corrected for multiple comparisons), see figure 15.

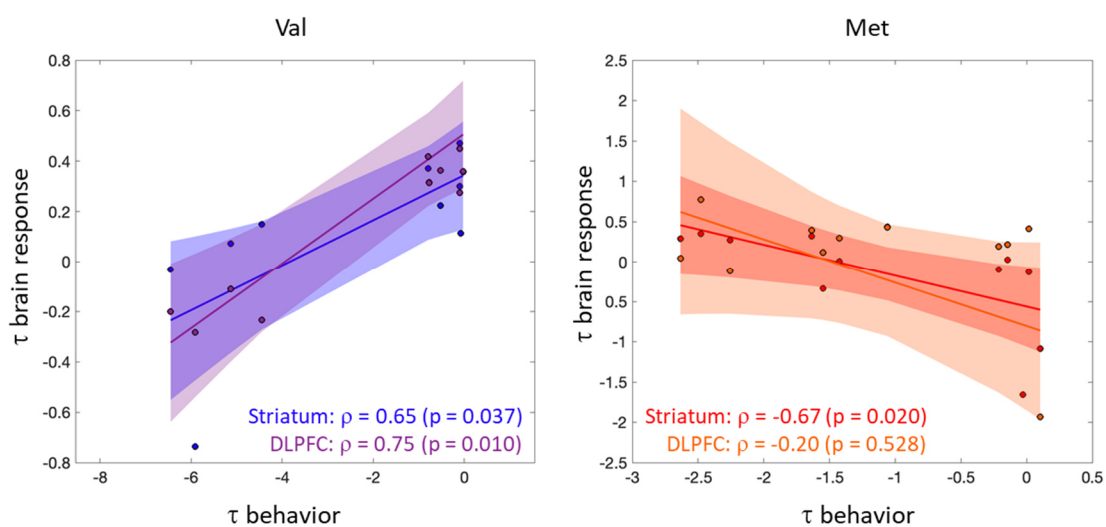


**Figure 15. Effect of genotype on brain-behavior correlations for  $\tau$  in the left striatum and left DLPFC.**

For brain responses, the mean  $\tau$ -values within the respective clusters are shown. Blue and red shades indicate the 95% CI for genotype-specific brain-behavior correlations (Spearman's  $\rho$ ) using 999 bootstrapping operations. Abbreviations: DLPFC = dorsolateral prefrontal cortex.

For post-hoc comparisons between groups, a 95% confidence interval (CI) for genotype-specific brain-behavior correlations (Spearman's  $\rho$ ) was estimated using 999 bootstrapping operations. The comparison of CI-estimates confirmed robust differences in brain-behavior association in both regions (Striatum: Val/Val [0.48, 0.97], Met-carrier [-0.88, -0.36]; DLPFC: Val/Val [0.65, 0.98], Met-carrier [-0.79, 0.31]). Specifically, both groups showed significant and opposite brain-behavior correlations in the striatum (Val/Val:  $\rho = 0.65$ ,  $P = .037$ ; Met:  $\rho = -0.67$ ,  $P = .020$ ). In contrast, in the DLPFC, a significant association was only found for the Val/Val homozygotes (Val/Val:  $\rho = 0.75$ ,  $P = .010$ ; Met:  $\rho = -0.20$ ,  $P = .528$ ).

### Effects of genotype on brain connectivity decay

The observation of a comparable striatal but differential prefrontal activation decay between *BDNF* genotype groups substantiated the hypothesis of an effect of the variant on the functional interaction of frontostriatal networks. Therefore, the effect of genotype on learning-related changes in frontostriatal functional connectivity was tested using generalized context-dependent psychophysiological interaction (gPPI) analysis and voxel-wise linear discriminant analysis (vwLDA). Genotype groups could not be discriminated based on their task-modulated functional connectivity profiles. However, a significant discrimination of genotype groups was observed for sustained functional connectivity (sFC) in a cluster mapping to the left DLPFC (MNI [-35, 36, 35],  $Acc_{Peak} = 0.91$ , cluster size = 49 voxels,  $P < .001$  cluster size corrected for multiple comparisons). Within this cluster, frontostriatal sFC increased in Val/Val homozygotes throughout the training, while it continuously decreased in the Met-allele carries, see right panel of figure 14C and D).

### Predictive value of neural learning parameters ( $\alpha$ and $\tau$ ) on later performance

To answer the question, whether individual decay curves in the striatum and DLPFC were predictive of behavioral performance in the practiced condition at follow-up (i.e., 14 weeks after training), three fixed-effect models were tested (see section 2.2.1, page 38 for more details). The comparison of the models revealed that the follow-up behavioral performance was best predicted by model M1, which is illustrated in figure 16 and has the following form:

$$Acc_{PT-CT}^{FU} \sim 0.024 (0.022|0.025) + 0.175 (0.170|0.180)\alpha_{FC(Striatum|DLPFC)} + 0.175 (0.170|0.180)\tau_{FC(Striatum|DLPFC)}$$

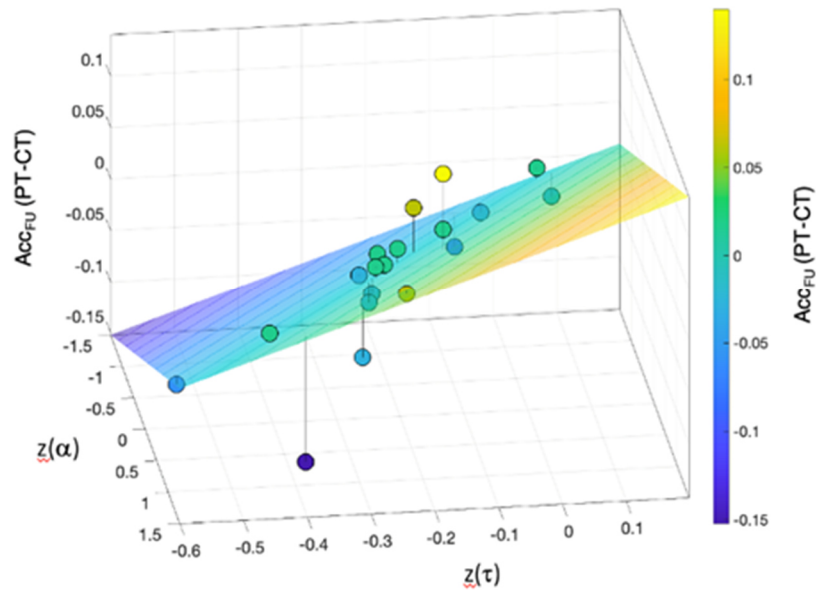


**Figure 16: Plot of the best predictive model M1.**

Prediction of follow-up performance (accuracy PT-CT, y-axis) using exponential model parameters  $\alpha$  (z-axis) and  $\tau$  (y-axis) of the individual exponential models for brain functional connectivity (striatum to DLPFC) for the whole sample. Parameter estimates are z-scaled, indicated at  $z(\tau)$  and  $z(\alpha)$ . Abbreviations: PT = practiced condition, CT = control condition).

The three models and individual goodness parameters are shown in Table 4. The results of model comparisons are shown in Table 5. The median  $R^2$  of and the 95% CI of the cross-validated model M1 was 0.155 (0.055|0.269). The association suggests that more positive  $\tau$  values (i.e., a slower signal decay or even faster increase in connectivity) and more positive  $\alpha$  values (i.e., higher amount of signal change) are related to better performance in the follow-up measurement. In fact, *BDNF* risk-allele carriers showed significantly more negative values of  $\tau$  ( $T_{(19)} = 1.86$ ,  $p = .008$ ), indicating a more prominent decay of frontostriatal connectivity, relating to poorer behavioral performance at the follow-up assessment (table S5, page 77).

**Table 4: Model goodness parameters of all three fixed-effect models**

Model		$R^2_{adj}$	med ( $R^2_{cv}$ )	cAIC	$\ln(L)$
M1	$Acc_{PT-CT}^{FU} \sim 1 + \alpha_{FC(\text{Striatum} DLPFC)} + \tau_{FC(\text{Striatum} DLPFC)}$	0.293	0.155	-79.65	43.83
M2	$Acc_{PT-CT}^{FU} \sim 1 + \alpha_{RR(DLPFC)} + \tau_{BR(DLPFC)}$	0.115	0.041	-74.95	41.48
M3	$Acc_{PT-CT}^{FU} \sim 1 + \alpha_{BR(\text{Striatum})} + \tau_{BR(\text{Striatum})}$	0.075	0.050	-73.94	40.97

Abbreviations: FU = follow-up, PT = practice condition, CT = control condition, FC = functional connectivity; BR = brain response, adj = adjusted; cv = cross-validated; cAIC = corrected Akaike information criterion;  $\ln(L)$  = log-likelihood.

**Table 5:** Model comparison using simulated Likelihood Ratio Test

Model comparison	LRT-Statistics	p-Value (95%CI)
M1 > M2	4.67	0.047* (0.036   0.063)
M1 > M3	5.71	0.030* (0.020   0.043)
M2 > M3	1.01	0.225 (0.199   0.252)

Note: Likelihood ratio test (LRT) with 1000 simulations, \* significant at  $p < .05$ .  
Abbreviations: CI = confidence interval.

### **Role of head movement and image quality**

For fMRI data quality assurance, the individual head motion parameters and the signal-to-noise ratio were computed. As detailed in Table S6 (page 77), both genotype groups were balanced well for all data quality assurance measures (all  $P$  values  $> 0.12$ ). This suggests that the above-reported findings are unlikely influenced by genotype-dependent differences in image quality.

### 3. Discussion

The cognitive loop of the cortical-striatal circuitry is anatomically well-defined (Alexander et al., 1986; Draganski et al., 2004; Lehericy et al., 2005; Seger, 2006) and plays an essential role in higher cognitive processes such as access control into working memory (A. J. Gruber et al., 2006; McNab & Klingberg, 2008; O'Reilly & Frank, 2006). One important aspect of the “gating” mechanism is the relevance of working memory items, such as novelty, a quality that is understudied with respect to its effects on corticostriatal function and connectivity. Study 1 of this thesis was performed as a cross-sectional fMRI study using DCM in a sample of 74 healthy participants performing a Sternberg working memory task, aiming to investigate whether striatal activation during working memory varies across task phase (i.e., encoding and retrieval) and stimulus familiarity (novel vs. practiced) of the presented materials. And further, to explore by which corticostriatal connectivity mechanism the task-phase specific involvement of the striatum is achieved (i.e., top-down or bottom-up control).

There is broad consensus that corticostriatal circuitries are important targets for neurotrophin signaling (Bimonte-Nelson, Hunter, Nelson, & Granholm, 2003; B. Li, Arime, Hall, Uhl, & Sora, 2010). In this context, BDNF is the most widely studied plasticity marker. Unfortunately, most imaging genetic studies with *BDNF Val66Met* have followed either a cross-sectional or a longitudinal design with a simple pre-post approach. A comprehensive longitudinal characterization of *BDNF* effects on cognitive behavior and brain function has not been studied extensively. Furthermore, the effects of a *BDNF* polymorphism (*Val66Met*) have to my knowledge, not been studied by applying exponential decay modeling (i.e., learning curves). Study 2 of this thesis was performed as a longitudinal fMRI study using exponential decay modeling in a sample of 23 healthy participants performing a modified version of the cross-sectional Sternberg task within a two-week training period and a 14-week follow-up measurement. The main goals were to investigate the longitudinal effects of working memory learning on cognitive behavior and brain function (brain activation and connectivity) and examine a possible influence of an established *BDNF* variant (*Val66Met*) on the longitudinal effects of working memory learning.

#### 3.1 Results of the cross-sectional study (study 1)

Firstly, in line with prior reports (Jansma JM, 2001; van Raalten, Ramsey, Duyn, et al., 2008; van Raalten, Ramsey, Jansma, et al., 2008), the behavioral response to novel working memory items was significantly slower and less accurate. This observation is consistent with the theory that previously

practiced stimuli invoke the execution of a well-developed and automatic skill, while novel items demand a more controlled, effortful, and capacity-limited mode of information processing (Shiffrin & Schneider, 1977).

Secondly, the fMRI results showed a highly significant increase in DLPFC and striatal activation during encoding and during the process of cognitively more demanding novel items. This is in line with prior work reporting an increase in activation in working memory-related regions such as the left DLPFC, left anterior insula, superior parietal cortex, anterior cingulate cortex, and the pre-supplementary motor area during the processing of novel relative to practiced Sternberg items, was observed (Jansma JM, 2001; van Raalten, Ramsey, Duyn, et al., 2008). Such activation increases have previously been explained by the inability for a capacity-relieving “chunking” - or binding of separate stimulus-response associations in a higher order representation with fewer information elements - in the context of novel and continuously changing materials (Guida et al., 2012; Jansma JM, 2001; Landau, Schumacher, Garavan, Druzgal, & D'Esposito, 2004). Moreover, as in prior studies with short-term training regimens, the detected activation differences in working memory-related cortical areas were quantitative rather than qualitative in nature. This opinion is supported by the observation that short-term training led to an activation decrease in the very same areas that were engaged during the processing of novel Sternberg items while practice-related activation increases in other regions were not detected (Guida et al. 2012; Landau et al. 2004). A plausible explanation that has been offered for this observation is that short-term acquisition of working memory is restrained to chunk formation within frontal-parietal areas and that the novelty-induced increase in regional activation reflects a decrease in neural efficiency and cognitive capacity (Guida et al. 2012). It should be noted, however, that while our experiment was set out to assess the effects of novelty in the context of working memory processing, we cannot rule out an additional modulation of corticostriatal responses by long-term memory representations in the context of the trained (as compared to the novel) stimulus sets. Despite similar sensory and motor requirements, the comparison of novel to practiced conditions additionally revealed activation in higher-level motor and visual areas. The involvement of these areas is in line with well-known down-stream effects of top-down control mechanisms (e.g., attention) and is reflective of the higher degree of complexity/task difficulty of novel as compared to practiced trials (Gilbert & Li, 2013; Hertrich, Dietrich, & Ackermann, 2016).

These results extend prior knowledge by demonstrating a highly significant engagement of the frontal-striatal circuitry during working memory, which was selective for the encoding relative to the retrieval phase of the task. Here, the effect was mostly explained by an activation increase during the encoding phase of the cognitively more demanding novel stimuli, for which a higher-order representation

through “chunking” was prevented by the continuous changes in stimulus-response relationships and the related requirements for frequent updating. Notably, the detected activation foci in the putamen were dorsal and rostral to the anterior commissure, consistent with recruitment of the associative (i.e., cognitive) territories of the corticostriatal circuitry (Alexander et al. 1986). Although prior working memory studies have mostly focused on effects within frontal-parietal areas (Guida et al. 2012), activation increases in the dorsal anterior putamen have been related to the encoding of stimuli with a higher cognitive load (Chang et al., 2007; Landau et al., 2004), increased level of abstraction (Nee & Brown, 2013), or the requirement for frequent updating (Dahlin, Neely, Larsson, Backman, & Nyberg, 2008). In addition, more ventral (but occasionally also dorsal) responses in the anterior striatum have been associated with the presentation of novel or surprising non-rewarding stimuli (Murty, Ballard, Macduffie, Krebs, & Adcock, 2013; van Schouwenburg et al., 2010; Wittmann, Daw, Seymour, & Dolan, 2008; Zink, Pagnoni, Martin, Dhamala, & Berns, 2003) and related shifts in attention (van Schouwenburg et al., 2010).

Further, these data support a role for the anterior striatum in the stimulus encoding process that goes beyond the traditional roles of the basal ganglia in motor control and reward processing. Computational models propose that the mechanisms of the basal ganglia, by which it supports working memory, are evolved implementations of the same basic machinery supporting the gating of adaptive responses in the “more primitive” striatal motor circuitry (O'Reilly and Frank 2006). Indeed, the increased engagement of the anterior putamen during the encoding of novel Sternberg materials may serve as a critical gating signal for prefrontal working memory buffers. It may indicate, for example, that the presented items are behaviorally relevant and require a more controlled and resourceful neural strategy for their effective handling. Conversely, the relative absence of striatal responses during the encoding of practiced stimuli may signal the availability of “pre-chunked rule sets” or automatized neural representations in the frontal-parietal cortex, allowing for their efficient neural processing.

Next, the conducted DCM analyses extend the activation findings by highlighting a potential mechanism by which the proposed corticostriatal gating function during the processing of novel working memory items might be achieved. The data were best explained by a model assuming significant intrinsic connectivity from DLPFC to anterior striatum, as well as an enhancing significant modulatory effect of the encoding phase of novel items on the connection from the DLPFC to the striatum. In general, this observation is in good agreement with the known excitatory projections from the cortex to the striatum (Alexander et al. 1986) and the role of the DLPFC in the top-down control of subcortical structures. The observed modulation of prefrontal-striatal connectivity reflects a

mechanism by which the DLPFC signals the need for a more resourceful neural strategy (or absence of “pre-chunked cortical rule sets”) for the successful handling of novel items during stimulus encoding. Although such a strategy could plausibly facilitate the enhanced signaling (or gating of relevant stimulus information) in the anterior striatum, further research is needed to substantiate this proposal. Of note, a negative driving input of the practice conditions to the DLPFC was found, an observation that parallels the relative reduction of the activation of the region in these conditions. Similar to prior reports (Jung et al., 2018), we interpret these findings as related, i.e., the reduction of the overall activity in DLPFC during the practice condition as a consequence of the negative driving input, which may be the result of an interaction between excitatory and inhibitory interneurons in the region.

### 3.2 Results of the longitudinal study (study 2)

Study 2 was performed as a longitudinal fMRI study using exponential decay modeling to investigate the longitudinal effects of working memory learning on the behavior as well as on corticostriatal brain activation and connectivity and its modulation by a common *BDNF* polymorphism (*Val66Met*).

Firstly, the behavioral analysis revealed that *BDNF*-deficient <sup>66</sup>Met-allele carriers showed significantly higher error rates at the first and the 14-weeks follow-up measurement (i.e., long after the training interval has been completed). This poorer working memory performance suggests the presence of deficits in both the initial encoding and long-term consolidation of working memory contents in Met allele carriers. This observation in risk allele carriers is in line with previous studies showing deficits in both mnemonic subprocesses (Goldberg et al., 2008; Montag et al., 2014). Notably, no prior fMRI study and only a few behavioral studies (Freundlieb et al., 2015; McHughen et al., 2011) applied a similarly long-lived learning experiment with extended training periods and follow-up assessments covering weeks and months. However, there were no significant differences in behavioral performance directly after the two-week training period. This observation supports the notion that *BDNF* Met allele carriers are able to compensate, at least in parts, for genotype-associated deficits in verbal working memory performance by repeated training. A result that has been reported in a comparable study with consecutive training (Freundlieb et al., 2015; McHughen et al., 2011). The longitudinal study of this thesis extends prior knowledge on the behavioral level in two ways. To date, prior longitudinal studies have mainly used performance measures such as “change” in accuracy, reaction time, or baseline, thus were not able to quantify the evolution of performance (Freundlieb et al., 2015; McHughen et al., 2011; Montag et al., 2014). The application of specific learning parameters ( $\tau$  = learning *speed* and  $\alpha$  = learning *gain*), as used in this thesis, gives an explanation for this outcome. In detail, Met allele



carriers showed a higher learning gain ( $\alpha$ ) compared to Val/Val homozygotes, which directly reflects the behavioral compensatory mechanism. Further, due to the 14-weeks follow-up measurement, this thesis presents evidence that this compensation mechanism is not enduring and the poorer performance level reemerges when the training has stopped.

Besides the poor working memory performance in behavior, this study was able to reflect these deficits on the brain level. Secondly, over the two-week training period, a signal decay in learning-responsive brain regions such as DLPFC and striatum was observed in both genetic groups, but Met allele carrier showed a delayed prefrontal signal decay, which was confirmed by a significant discrimination of these groups in the vwLDA analysis. This is in accordance with the initially observed WM deficits on the behavior level and reflects the increased DLPFC recruitment or protracted deactivation in Met allele carrier, which is in line with prior work suggesting an inefficient activity in this risk allele group (Dennis et al., 2011; Quide, Morris, Shepherd, Rowland, & Green, 2013; Soltesz et al., 2014).

Thirdly, a brain-behavior regression analysis showed a positive association between behavioral learning speed ( $\tau$ ) and speed of signal decay ( $\tau$ ) in striatum and DLPFC in Val/Val homozygotes, indicating that a faster brain signal decay is advantageous for faster learning. The same analysis revealed a negative association in Met allele carriers, which was only significant for the DLPFC, which might indicate that the observed protracted brain signal decay seems to be beneficial for faster learning in the Met allele group. Taken together, these findings suggest that dynamic changes in corticostriatal functional activation are directly linked to behavioral improvement during learning and that this link is only beneficial in the carriers of the plasticity-related protective variant, the *BDNF* Val/Val genotype. Moreover, the lack of an association between behavior and brain response in the DLPFC may signal an inefficient top-down control of learning-related neural responses in the *BDNF* risk allele carriers.

Next, the conducted connectivity analyses showed a frontostriatal increase in sustained functional connectivity (sFC) in Val/Val genotype group during the two-week training period but a continuous decrease in the Met allele carrier. This was confirmed by a vwLDA analysis, which revealed a significant discrimination between the two genetic groups in a cluster within the DLPFC. This observation may suggest that Val homozygotes established a basic frontostriatal “scaffold” supporting tight interactions between striatum and DLPFC. In contrast, Met allele carriers show an inability to increase frontostriatal connectivity and do not seem to strengthen sustained frontostriatal functional interactions as a function of repeated learning. The previously described elongated activation of the DLPFC in Met allele

carriers may indicate a compensatory mechanism for the inability to acquire a basic frontostriatal connectivity “scaffold.”

Further, a significant brain-behavior association between parameter estimates ( $\alpha$  and  $\tau$ ) derived from corticostriatal sFC within a cluster in the DLPFC and behavioral performance at the 14-week follow-up measurement was found. This association suggests that more positive  $\tau$  values (i.e., faster increase in connectivity) together with more positive  $\alpha$  values (i.e., a higher increase in connectivity) are related to a better performance in the follow-up measurement. In other words, the more a subject's functional connectivity between the striatum and DLPFC increased during the learning phase, the better was the performance at the follow-up measurement. Notably, *BDNF* risk-allele carriers showed more negative  $\tau$  values, indicating a more prominent decay of frontostriatal connectivity. These results suggest that the formation of sustainable frontostriatal connectivity is central for long-term consolidation and that this process seems to be limited in *BDNF* risk allele carriers.

The existing literature provides several mechanisms through which BDNF influences higher-order cognitive processes such as learning. BDNF has a high affinity to the tropomyosin receptor kinase B (TrkB), which is essential to synaptic plasticity (Kuipers & Bramham, 2006). TrkB activates three intracellular signaling cascades, namely, mitogen-activated protein kinase (MAPK), phosphoinositide-3kinase (PI3K), and phospholipase C (PLC)-gamma (Numakawa, Odaka, & Adachi, 2018). The *BDNF Val66Met* polymorphism has been linked to deficient activity-dependent (i.e., phasic but not constituent) secretion of *BDNF* in *Met* allele carrier, leading to disrupted intracellular trafficking via TrkB. This results in a lower (protein synthesis-independent) early-phase LTP and with a subsequent decrease synaptic transmission efficacy and short-term memory impairments (Chen et al., 2015; Z. Y. Chen et al., 2004; Chiaruttini et al., 2009; Egan et al., 2003; Notaras et al., 2015; Notaras & van den Buuse, 2019). This mechanism is a plausible explanation of the initially observed *BDNF* encoding deficit in the *Met* allele group. Further, strong evidence points to the role of *BDNF* in late-phase LTP, which requires a de-novo synthesis of proteins and induces structural changes at the synapse via protein kinase (PKA) and MAPK pathways. Moreover, prior work demonstrated that the *BDNF* risk allele variant might alter the encoding of engrams (Notaras & van den Buuse, 2019), which is in line with the observed deficits in working memory maintenance in the longitudinal study of this thesis. Furthermore, accumulating evidence supports a *Val66Met* polymorphism-related signaling effect on the onset of neurological and psychiatric disorders, e.g., Parkinson's disease, schizophrenia, or affective disorders (Lin & Huang, 2020; Numakawa et al., 2018; T. Shen et al., 2018).

### 3.3 Sternberg working memory task and corticostriatal circuitries

The two modified versions of the Sternberg working memory task used in this thesis were found to be highly sensitive in examining the “executive loop” of the corticostriatal circuitries. Both versions of the task differed slightly in the cross-sectional and longitudinal study. See figure 5 (page 19) and figure 10 (page 33) for more detail. In the cross-section study, the task consisted of the following conditions: a novel, practiced, low-cognitive control, and rest condition, which were repeated four times, to investigate the “circumstances” of striatal gating. In line with prior work (Chang et al., 2007; McNab & Klingberg, 2008; Moore et al., 2013; O'Reilly & Frank, 2006; Schroll & Hamker, 2013), this thesis confirmed that striatal gating occurs in the encoding phase of the working memory process. During the course of the first study, behavioral analyses showed a “ceiling” effect in the practice condition, confirming a high practice or automatization effect (due to prior training), which was also reflected in brain signal and can be explained by the “chunking” mechanism. To avoid an immediate “ceiling effect” in the longitudinal study and to capture the effects of recurrent training on different degrees of stimulus familiarity, several adjustments have been made. The initial “encoding set” consisting of five letters was extended to seven letters (in line with the well-established WM capacity of seven items or magical number seven). To increase the task sensitivity for the fMRI analyses, every condition was repeated six times (compared to four). Further, to expand the temporal resolution of learning and examine different degrees of stimulus familiarity, a new task condition, namely “shuffled,” was created, filling the gap between entirely new and highly practiced stimuli. While the practiced condition involved constant letters and a constant configuration, the novel condition contained variable (i.e., entirely new) letters and a variable configuration. The shuffled condition represents an intermediate condition, which includes constant letters (same as in practiced condition) combined with a variable configuration (new shuffled order in every trial). Regarding WM load, the conditions can be defined as novel = high cognitive load/low chunkability, shuffled = intermediate load/intermediate chunkability and practiced = lower cognitive load/high chunkability.

The above-outlined modifications were effective as reflected by a continuous improvement of time, independently of the genetic group, without showing an immediate “ceiling effect”. Further, the behavioral results of the longitudinal study demonstrated a successful modification of the task conditions, showing a significant condition effect for  $\tau$  in the whole-group analyses. In detail, the fastest decay was observed in the practiced condition, followed by the shuffled condition and novel condition, hereby confirming the proposed WM load or chunkability of stimuli. Moreover, this task modification enabled the discrimination of *BDNF Val66Met* groups over a two-week training period. To my knowledge, the original or “unmodified” version of the Sternberg task has, so far, not been

applied to study the effects of *BDNF Val66Met*, and the latest created version was newly conducted within this thesis.

Unfortunately, the analyses of the longitudinal study were limited to the effects of *BDNF Val66Met* on the practiced condition. A detailed analysis of other task conditions, especially of the shuffled condition, in brain activation and connectivity, is beyond the scope of this thesis. Nonetheless, the Sternberg WM task, and its task condition modification, demonstrate that this task facilitates the “chunking mechanism,” especially during the course of repetitive training.

Taken together, the Sternberg WM task is suitable for investigating the “executive loop” of corticostriatal circuitries. Further, the applied modifications into a novel, shuffled, and practiced condition makes it an ideal candidate to investigate WM load, different degrees of stimulus familiarity, and the chunking mechanism, be it in a cross-sectional or longitudinal design.

### **3.4 Limitations and further directions**

First, the Sternberg WM task and its modifications are highly suitable to investigate corticostriatal circuitry function and plasticity processes. Unfortunately, the repetition of each task condition was restricted to four or six repetitions, which may not be ideal. A higher repetition of task trials (e.g., eight or ten repetitions) might have led to more accurate results, especially for connectivity analyses such as DCM, and should be considered in further studies.

Furthermore, the sample size in the longitudinal study was relatively small ( $n = 23$ ), especially after allocating them into two genotype groups. Further, the *BDNF Val66Met* subgroup of Met homozygotes (Met/Met) was underrepresented (only two subjects). This specific allele is very rare (ca. 5% in a Caucasian population; T. Shen et al. (2018)) and thus difficult to recruit. As a consequence, all Met allele carriers (Val/Met and Met/Met) were summarized into a single group, and a potential “additive” or “dosage” *BDNF* effect could not be investigated. A source of concern in longitudinal studies are high dropout rates, especially in designs with multiple measurements and follow-up assessments. Fortunately, dropout rates in the presented longitudinal study were very low ( $n = 1$ ). Furthermore, longitudinal studies are time-intensive, need a high amount of staff members, and cost implications are high. Future studies with much higher sample sizes on this topic are therefore needed, e.g., to replicate the presented behavioral and brain function results.

Another limitation closely related to imaging genetic studies is the focus on a single genetic polymorphism. As outlined in the introduction, *BDNF* interacts with several other polymorphisms such as *COMT Val66Met*. Further studies should investigate corticostriatal circuitry functioning and plasticity processes in polymorphisms, e.g., in *COMT*, ideally multiple polymorphisms (divided into separate groups) in one longitudinal study. Further, the effects of NMDA-Receptor antagonists such as Ketamine or other drug challenges should be considered. One of the major advantages of the longitudinal study presented in this thesis, is the “consecutive” training protocol, nonetheless, training was not conducted daily. To ensure the maximal evolution of training and learning processes, further studies should consider daily training. Besides, an additional “late-follow-up” measurement, e.g., after 6 or 12 months, would have been advantageous to explore a “potential end” of a learning effect. The partly diverging results of a *BDNF* effect or the present longitudinal study and previously reported studies, such as the compensation mechanism in Met allele carrier, could be explained by different task and study protocols, e.g., consecutive training, pre-post-measurement. This should be addressed in further studies by combining two learning tasks, e.g., motor and cognitive tasks, or by comparing subgroups of different tasks and genetic groups in a single longitudinal study.

Both studies presented in this thesis investigated solely healthy participants. However, dysfunctions in corticostriatal circuitries are linked to several neurological diseases and psychiatric disorders. Unfortunately, the results of this thesis are not immediately applicable to clinical populations. Future studies should target corticostriatal functioning and plasticity processes in patients, e.g., suffering from schizophrenia, depression, or Parkinson’s disease, especially in a longitudinal study approach. Further, an examination of post-stroke patients would be of great interest.

Finally, the here newly created version of the Sternberg WM task proved to be highly sensitive to study learning and WM, especially the different degrees of stimulus familiarity as well as the “chunking” mechanism. Moreover, it is suitable to investigate short-term and long-term plasticity effects related to genetic polymorphism, e.g., *BDNF Val66Met*, in brain function and behavior. I am confident that this task will serve as a base for future studies. Ideally, this Sternberg WM task should be applied in a longitudinal approach, over a two-week training protocol with daily training and multiple follow-up sessions (e.g., 3, 6, 9, 12, 24 months) considering several genetic polymorphisms and/or multiple patient groups.

## 4. Summary

Corticostriatal brain circuitries play an essential role in basic and high-level functions of the human brain, such as motor control, goal-director behavior, cognition, as well as learning and memory. Growing evidence supports a “gating” function of basal ganglia, particularly the striatum, within the motor and cognitive domains. Study 1 of this thesis was conducted as a cross-sectional functional magnetic resonance imaging (fMRI) study in a sample of 74 healthy participants performing a Sternberg working memory (WM) task to investigate whether striatal activation during working memory varies across task phase (i.e., encoding and retrieval) and stimulus familiarity (novel vs. practiced items). Further connectivity analyses (using dynamic causal modeling) were applied to explore by which corticostriatal connectivity mechanism the task-phase specific involvement of the striatum is achieved (i.e., top-down or bottom-up control). Activation analyses demonstrated a highly significant engagement of the anterior striatum, particularly during the encoding of novel WM items. Dynamic causal modeling (DCM) of corticostriatal circuit connectivity identified a selective positive modulatory influence of novelty encoding on the connection from the dorsolateral prefrontal cortex (DLPFC) to the anterior striatum. These data extend prior research by further underscoring the relevance of the basal ganglia for human cognitive function and provide a mechanistic account of the DLPFC as a plausible top-down regulatory element of striatal function that may facilitate the “input-gating” of novel working memory materials.

The brain derived neurotrophic factor (BDNF) promotes neural synaptic growth and has become the most widely studied neurotrophin. Growing evidence demonstrates that a specific *BDNF* polymorphism, *Val66Met*, impacts memory performance and brain function, resulting in poor performance and abnormal brain activity or connectivity in risk-allele carriers (Met allele carrier). Study 2 of this thesis was conducted in a longitudinal approach, over a two-week learning period with regular fMRI acquisition and additional 14-week follow-up measurement. The aim was to characterize learning-induced changes in cognitive behavior and brain function and its modulation by effects of the *BDNF Val66Met* genotype. Therefore, a sample of 23 healthy subjects performing a modified Sternberg WM task was examined, and exponential decay modeling (i.e., learning curves) was applied using the parameters  $\tau$  (learning speed) and  $\alpha$  (learning gain) to examine learning-induced effects. Behavioral analyses demonstrated that *BDNF* risk allele carriers (Met allele carriers) showed significant WM deficits at the beginning and at the 14-week follow-up measurement (i.e., long after the training interval). Interestingly, Met allele carriers were able to compensate for the initially disadvantageous effect by repetitive training. The behavioral WM deficits could be directly linked to a delayed signal decay in the DLPFC and a lack in the increase in frontostriatal connectivity in Met allele carrier. Further, a faster and higher increase in functional connectivity resulted in a higher follow-up performance,

indicating the importance of forming a connectivity “scaffold” for long-term consolidation, which seems to be limited in *BDNF* risk allele carriers. These results extend prior knowledge by demonstrating immediate and long-term WM learning deficits and impaired neural plasticity in *BDNF* risk allele carriers. Taken together, this thesis highlights the role of corticostriatal circuits for WM learning and may provide new insights into the relationship between regulated BDNF signaling on short-term and long-term plasticity.

## 5. References

- Albin, R. L., Young, A. B., & Penney, J. B. (1989). The functional anatomy of basal ganglia disorders. *Trends Neurosci*, *12*(10), 366-375.
- Alexander, G. E., DeLong, M. R., & Strick, P. L. (1986). Parallel organization of functionally segregated circuits linking basal ganglia and cortex. *Annu Rev Neurosci*, *9*, 357-381. doi:10.1146/annurev.ne.09.030186.002041
- Allman, W. F. (1989). *Apprentices of Wonder: Inside the Neural Network Revolution*: Bantam Books.
- Atkinson, R. C., & Shiffrin, R. M. (1968). Human memory: a proposed system and its control processes. In *The psychology of learning and motivation: Advances in research and theory*. (Vol. 2) (K.W. Spence & J.T. Spence ed., pp. 89-195). New York: Academic Press.
- Baddeley, A. (2000). The episodic buffer: a new component of working memory? *Trends Cogn Sci*, *4*(11), 417-423.
- Baddeley, A. (2003). Working memory: looking back and looking forward. *Nat Rev Neurosci*, *4*(10), 829-839. doi:10.1038/nrn1201
- Baddeley, A. (2010). Working memory. *Curr Biol*, *20*(4), R136-140. doi:10.1016/j.cub.2009.12.014
- Baddeley, A., & Hitch, G. (1974). Working Memory. *Psychology of Learning and Memory*, *8*, 47-89. doi:https://doi.org/10.1016/S0079-7421(08)60452-1
- Baig, B. J., Whalley, H. C., Hall, J., McIntosh, A. M., Job, D. E., Cunningham-Owens, D. G., Johnstone, E. C., & Lawrie, S. M. (2010). Functional magnetic resonance imaging of BDNF val66met polymorphism in unmedicated subjects at high genetic risk of schizophrenia performing a verbal memory task. *Psychiatry Res*, *183*(3), 195-201. doi:10.1016/j.psychres.2010.06.009
- Bassett, D. S., Yang, M., Wymbs, N. F., & Grafton, S. T. (2015). Learning-induced autonomy of sensorimotor systems. *Nat Neurosci*, *18*(5), 744-751. doi:10.1038/nn.3993
- Bimonte-Nelson, H. A., Hunter, C. L., Nelson, M. E., & Granholm, A. C. (2003). Frontal cortex BDNF levels correlate with working memory in an animal model of Down syndrome. *Behav Brain Res*, *139*(1-2), 47-57. doi:10.1016/s0166-4328(02)00082-7
- Bliss, T. V., & Collingridge, G. L. (1993). A synaptic model of memory: long-term potentiation in the hippocampus. *Nature*, *361*(6407), 31-39. doi:10.1038/361031a0
- Bliss, T. V., & Lomo, T. (1973). Long-lasting potentiation of synaptic transmission in the dentate area of the anaesthetized rabbit following stimulation of the perforant path. *J Physiol*, *232*(2), 331-356. doi:10.1113/jphysiol.1973.sp010273
- Bohlin, G., & Janols, L. O. (2004). Behavioural problems and psychiatric symptoms in 5-13 year-old Swedish children-a comparison of parent ratings on the FTF (Five to Fifteen) with the ratings



- on CBCL (Child Behavior Checklist). *Eur Child Adolesc Psychiatry*, 13 Suppl 3, 14-22. doi:10.1007/s00787-004-3003-1
- Bor, D., Cumming, N., Scott, C. E., & Owen, A. M. (2004). Prefrontal cortical involvement in verbal encoding strategies. *Eur J Neurosci*, 19(12), 3365-3370. doi:10.1111/j.1460-9568.2004.03438.x
- Bor, D., Duncan, J., Wiseman, R. J., & Owen, A. M. (2003). Encoding strategies dissociate prefrontal activity from working memory demand. *Neuron*, 37(2), 361-367. doi:10.1016/s0896-6273(02)01171-6
- Braver, T. S., Cohen, J. D., Nystrom, L. E., Jonides, J., Smith, E. E., & Noll, D. C. (1997). A parametric study of prefrontal cortex involvement in human working memory. *Neuroimage*, 5(1), 49-62. doi:10.1006/nimg.1996.0247
- Brehmer, Y., Westerberg, H., Bellander, M., Furth, D., Karlsson, S., & Backman, L. (2009). Working memory plasticity modulated by dopamine transporter genotype. *Neurosci Lett*, 467(2), 117-120. doi:10.1016/j.neulet.2009.10.018
- Bruder, G. E., Keilp, J. G., Xu, H., Shikhman, M., Schori, E., Gorman, J. M., & Gilliam, T. C. (2005). Catechol-O-methyltransferase (COMT) genotypes and working memory: associations with differing cognitive operations. *Biol Psychiatry*, 58(11), 901-907. doi:10.1016/j.biopsych.2005.05.010
- Bryan, W. L., & Harter, N. (1899). Studies on the telegraphic language: The acquisition of a hierarchy of habits. *Psychological Review*, 6(4), 345-375. doi:10.1037/h0073117
- Bunzeck, N., & Thiel, C. (2016). Neurochemical modulation of repetition suppression and novelty signals in the human brain. *Cortex*, 80, 161-173. doi:10.1016/j.cortex.2015.10.013
- Cairo, T. A., Liddle, P. F., Woodward, T. S., & Ngan, E. T. (2004). The influence of working memory load on phase specific patterns of cortical activity. *Brain Res Cogn Brain Res*, 21(3), 377-387. doi:10.1016/j.cogbrainres.2004.06.014
- Chang, C., Crottaz-Herbette, S., & Menon, V. (2007). Temporal dynamics of basal ganglia response and connectivity during verbal working memory. *Neuroimage*, 34(3), 1253-1269. doi:10.1016/j.neuroimage.2006.08.056
- Chase, W. G., & Simon, H. A. (1973). Perception in chess. *Cognitive Psychology*, 4(1), 55-81. doi:10.1016/0010-0285(73)90004-2
- Chatham, C. H., & Badre, D. (2015). Multiple gates on working memory. *Current Opinion in Behavioral Sciences*, 1, 23-31. doi:10.1016/j.cobeha.2014.08.001
- Chen, C. C., Chen, C. J., Wu, D., Chi, N. F., Chen, P. C., Liao, Y. P., Chiu, H. W., & Hu, C. J. (2015). BDNF Val66Met Polymorphism on Functional MRI During n-Back Working Memory Tasks. *Medicine (Baltimore)*, 94(42), e1586. doi:10.1097/md.0000000000001586

- Chen, J., Lipska, B. K., Halim, N., Ma, Q. D., Matsumoto, M., Melhem, S., Kolachana, B. S., Hyde, T. M., Herman, M. M., Apud, J., Egan, M. F., Kleinman, J. E., & Weinberger, D. R. (2004). Functional analysis of genetic variation in catechol-O-methyltransferase (COMT): effects on mRNA, protein, and enzyme activity in postmortem human brain. *Am J Hum Genet*, *75*(5), 807-821. doi:10.1086/425589
- Chen, Z. Y., Patel, P. D., Sant, G., Meng, C. X., Teng, K. K., Hempstead, B. L., & Lee, F. S. (2004). Variant brain-derived neurotrophic factor (BDNF) (Met66) alters the intracellular trafficking and activity-dependent secretion of wild-type BDNF in neurosecretory cells and cortical neurons. *J Neurosci*, *24*(18), 4401-4411. doi:10.1523/jneurosci.0348-04.2004
- Chevalier, G., & Deniau, J. M. (1990). Disinhibition as a basic process in the expression of striatal functions. *Trends Neurosci*, *13*(7), 277-280.
- Chiaruttini, C., Vicario, A., Li, Z., Baj, G., Braiuca, P., Wu, Y., Lee, F. S., Gardossi, L., Baraban, J. M., & Tongiorgi, E. (2009). Dendritic trafficking of BDNF mRNA is mediated by translin and blocked by the G196A (Val66Met) mutation. *Proc Natl Acad Sci U S A*, *106*(38), 16481-16486. doi:10.1073/pnas.0902833106
- Chudasama, Y., & Robbins, T. W. (2006). Functions of frontostriatal systems in cognition: comparative neuropsychopharmacological studies in rats, monkeys and humans. *Biol Psychol*, *73*(1), 19-38. doi:10.1016/j.biopsycho.2006.01.005
- Chuhma, N., Mingote, S., Moore, H., & Rayport, S. (2014). Dopamine neurons control striatal cholinergic neurons via regionally heterogeneous dopamine and glutamate signaling. *Neuron*, *81*(4), 901-912. doi:10.1016/j.neuron.2013.12.027
- Cohen, J. D., Perlstein, W. M., Braver, T. S., Nystrom, L. E., Noll, D. C., Jonides, J., & Smith, E. E. (1997). Temporal dynamics of brain activation during a working memory task. *Nature*, *386*(6625), 604-608. doi:10.1038/386604a0
- Creese, I., Burt, D. R., & Snyder, S. H. (1976). Dopamine receptor binding predicts clinical and pharmacological potencies of antischizophrenic drugs. *Science*, *192*(4238), 481-483. doi:10.1126/science.3854
- Dahlin, E., Neely, A. S., Larsson, A., Backman, L., & Nyberg, L. (2008). Transfer of learning after updating training mediated by the striatum. *Science*, *320*(5882), 1510-1512. doi:10.1126/science.1155466
- Davis, K. L., Kahn, R. S., Ko, G., & Davidson, M. (1991). Dopamine in schizophrenia: a review and reconceptualization. *Am J Psychiatry*, *148*(11), 1474-1486. doi:10.1176/ajp.148.11.1474
- DeLong, M. R. (1990). Primate models of movement disorders of basal ganglia origin. *Trends Neurosci*, *13*(7), 281-285.
- Deniau, J. M., & Chevalier, G. (1985). Disinhibition as a basic process in the expression of striatal functions. II. The striato-nigral influence on thalamocortical cells of the ventromedial thalamic nucleus. *Brain Res*, *334*(2), 227-233.

- Dennis, N. A., Cabeza, R., Need, A. C., Waters-Metenier, S., Goldstein, D. B., & LaBar, K. S. (2011). Brain-derived neurotrophic factor val66met polymorphism and hippocampal activation during episodic encoding and retrieval tasks. *Hippocampus*, *21*(9), 980-989. doi:10.1002/hipo.20809
- Desikan, R. S., Ségonne, F., Fischl, B., Quinn, B. T., Dickerson, B. C., Blacker, D., Buckner, R. L., Dale, A. M., Maguire, R. P., Hyman, B. T., Albert, M. S., & Killiany, R. J. (2006). An automated labeling system for subdividing the human cerebral cortex on MRI scans into gyral based regions of interest. *Neuroimage*, *31*(3), 968-980. doi:10.1016/j.neuroimage.2006.01.021
- Draganski, B., Gaser, C., Busch, V., Schuierer, G., Bogdahn, U., & May, A. (2004). Neuroplasticity: changes in grey matter induced by training. *Nature*, *427*(6972), 311-312. doi:10.1038/427311a
- Draganski, B., Kherif, F., Klöppel, S., Cook, P. A., Alexander, D. C., Parker, G. J., Deichmann, R., Ashburner, J., & Frackowiak, R. S. (2008). Evidence for segregated and integrative connectivity patterns in the human Basal Ganglia. *J Neurosci*, *28*(28), 7143-7152. doi:10.1523/jneurosci.1486-08.2008
- Driesen, N. R., McCarthy, G., Bhagwagar, Z., Bloch, M. H., Calhoun, V. D., D'Souza, D. C., Gueorguieva, R., He, G., Leung, H. C., Ramani, R., Anticevic, A., Suckow, R. F., Morgan, P. T., & Krystal, J. H. (2013). The impact of NMDA receptor blockade on human working memory-related prefrontal function and connectivity. *Neuropsychopharmacology*, *38*(13), 2613-2622. doi:10.1038/npp.2013.170
- Egan, M. F., Goldberg, T. E., Kolachana, B. S., Callicott, J. H., Mazzanti, C. M., Straub, R. E., Goldman, D., & Weinberger, D. R. (2001). Effect of COMT Val108/158 Met genotype on frontal lobe function and risk for schizophrenia. *Proc Natl Acad Sci U S A*, *98*(12), 6917-6922. doi:10.1073/pnas.111134598
- Egan, M. F., Kojima, M., Callicott, J. H., Goldberg, T. E., Kolachana, B. S., Bertolino, A., Zaitsev, E., Gold, B., Goldman, D., Dean, M., Lu, B., & Weinberger, D. R. (2003). The BDNF val66met polymorphism affects activity-dependent secretion of BDNF and human memory and hippocampal function. *Cell*, *112*(2), 257-269.
- Eichenbaum, H. (2004). Hippocampus: cognitive processes and neural representations that underlie declarative memory. *Neuron*, *44*(1), 109-120. doi:10.1016/j.neuron.2004.08.028
- Ericsson, K. A., Chase, W. G., & Faloon, S. (1980). Acquisition of a memory skill. *Science*, *208*(4448), 1181-1182. doi:10.1126/science.7375930
- Evans, N. J., Brown, S. D., Mewhort, D. J. K., & Heathcote, A. (2018). Refining the law of practice. *Psychol Rev*, *125*(4), 592-605. doi:10.1037/rev0000105
- Figurov, A., Pozzo-Miller, L. D., Olafsson, P., Wang, T., & Lu, B. (1996). Regulation of synaptic responses to high-frequency stimulation and LTP by neurotrophins in the hippocampus. *Nature*, *381*(6584), 706-709. doi:10.1038/381706a0

- Floyer-Lea, A., & Matthews, P. M. (2005). Distinguishable brain activation networks for short- and long-term motor skill learning. *J Neurophysiol*, *94*(1), 512-518. doi:10.1152/jn.00717.2004
- Francois, J., Grimm, O., Schwarz, A. J., Schweiger, J., Haller, L., Risterucci, C., Bohringer, A., Zang, Z., Tost, H., Gilmour, G., & Meyer-Lindenberg, A. (2016). Ketamine Suppresses the Ventral Striatal Response to Reward Anticipation: A Cross-Species Translational Neuroimaging Study. *Neuropsychopharmacology*, *41*(5), 1386-1394. doi:10.1038/npp.2015.291
- Frank, M. J., & Fossella, J. A. (2011). Neurogenetics and pharmacology of learning, motivation, and cognition. *Neuropsychopharmacology*, *36*(1), 133-152. doi:10.1038/npp.2010.96
- Frank, M. J., Loughry, B., & O'Reilly, R. C. (2001a). Interactions between frontal cortex and basal ganglia in working memory: A computational model. *Cognitive, Affective, & Behavioral Neuroscience*, *1*(2), 137-160.
- Frank, M. J., Loughry, B., & O'Reilly, R. C. (2001b). Interactions between frontal cortex and basal ganglia in working memory: a computational model. *Cogn Affect Behav Neurosci*, *1*(2), 137-160.
- Frazier, J. A., Chiu, S., Breeze, J. L., Makris, N., Lange, N., Kennedy, D. N., Herbert, M. R., Bent, E. K., Koneru, V. K., Dieterich, M. E., Hodge, S. M., Rauch, S. L., Grant, P. E., Cohen, B. M., Seidman, L. J., Caviness, V. S., & Biederman, J. (2005). Structural brain magnetic resonance imaging of limbic and thalamic volumes in pediatric bipolar disorder. *Am J Psychiatry*, *162*(7), 1256-1265. doi:10.1176/appi.ajp.162.7.1256
- Freundlieb, N., Backhaus, W., Bruggemann, N., Gerloff, C., Klein, C., Pinnschmidt, H. O., & Hummel, F. C. (2015). Differential effects of BDNF val(66)met in repetitive associative learning paradigms. *Neurobiol Learn Mem*, *123*, 11-17. doi:10.1016/j.nlm.2015.04.010
- Friston, K. J., Harrison, L., & Penny, W. (2003). Dynamic causal modelling. *Neuroimage*, *19*(4), 1273-1302.
- Fusar-Poli, P., Howes, O. D., Allen, P., Broome, M., Valli, I., Asselin, M. C., Grasby, P. M., & McGuire, P. K. (2010). Abnormal frontostriatal interactions in people with prodromal signs of psychosis: a multimodal imaging study. *Arch Gen Psychiatry*, *67*(7), 683-691. doi:10.1001/archgenpsychiatry.2010.77
- Gaebel, W., & Zielasek, J. (2015). Schizophrenia in 2020: Trends in diagnosis and therapy. *Psychiatry Clin Neurosci*, *69*(11), 661-673. doi:10.1111/pcn.12322
- Garavan, H., Kelley, D., Rosen, A., Rao, S. M., & Stein, E. A. (2000). Practice-related functional activation changes in a working memory task. *Microsc Res Tech*, *51*(1), 54-63. doi:10.1002/1097-0029(20001001)51:1<54::aid-jemt6>3.0.co;2-j
- Geiger, L. S., Moessnang, C., Schafer, A., Zang, Z., Zangl, M., Cao, H., van Raalten, T. R., Meyer-Lindenberg, A., & Tost, H. (2018). Novelty modulates human striatal activation and prefrontal-striatal effective connectivity during working memory encoding. *Brain Struct Funct*. doi:10.1007/s00429-018-1679-0

- Gerfen, C. R. (2000). Molecular effects of dopamine on striatal-projection pathways. *Trends Neurosci*, 23(10 Suppl), S64-70.
- Gerfen, C. R., Engber, T. M., Mahan, L. C., Susel, Z., Chase, T. N., Monsma, F. J., Jr., & Sibley, D. R. (1990). D1 and D2 dopamine receptor-regulated gene expression of striatonigral and striatopallidal neurons. *Science*, 250(4986), 1429-1432. doi:10.1126/science.2147780
- Gerfen, C. R., & Surmeier, D. J. (2011). Modulation of striatal projection systems by dopamine. *Annu Rev Neurosci*, 34, 441-466. doi:10.1146/annurev-neuro-061010-113641
- Gibon, J., & Barker, P. A. (2017). Neurotrophins and Proneurotrophins: Focus on Synaptic Activity and Plasticity in the Brain. *Neuroscientist*, 23(6), 587-604. doi:10.1177/1073858417697037
- Gilbert, C. D., & Li, W. (2013). Top-down influences on visual processing. *Nat Rev Neurosci*, 14(5), 350-363. doi:10.1038/nrn3476
- Girasole, A. E., & Nelson, A. B. (2015). Probing striatal microcircuitry to understand the functional role of cholinergic interneurons. *Mov Disord*, 30(10), 1306-1318. doi:10.1002/mds.26340
- Girdler, S. J., Confino, J. E., & Woesner, M. E. (2019). Exercise as a Treatment for Schizophrenia: A Review. *Psychopharmacol Bull*, 49(1), 56-69.
- Goh, J. O., An, Y., & Resnick, S. M. (2012). Differential trajectories of age-related changes in components of executive and memory processes. *Psychol Aging*, 27(3), 707-719. doi:10.1037/a0026715
- Goh, J. O., Beason-Held, L. L., An, Y., Kraut, M. A., & Resnick, S. M. (2013). Frontal function and executive processing in older adults: process and region specific age-related longitudinal functional changes. *Neuroimage*, 69, 43-50. doi:10.1016/j.neuroimage.2012.12.026
- Goldberg, T. E., Iudicello, J., Russo, C., Elvevag, B., Straub, R., Egan, M. F., & Weinberger, D. R. (2008). BDNF Val66Met polymorphism significantly affects d' in verbal recognition memory at short and long delays. *Biol Psychol*, 77(1), 20-24. doi:10.1016/j.biopsycho.2007.08.009
- Goldberg, T. E., & Weinberger, D. R. (2004). Genes and the parsing of cognitive processes. *Trends Cogn Sci*, 8(7), 325-335. doi:10.1016/j.tics.2004.05.011
- Goldstein, J. M., Seidman, L. J., Makris, N., Ahern, T., O'Brien, L. M., Caviness, V. S., Jr., Kennedy, D. N., Faraone, S. V., & Tsuang, M. T. (2007). Hypothalamic abnormalities in schizophrenia: sex effects and genetic vulnerability. *Biol Psychiatry*, 61(8), 935-945. doi:10.1016/j.biopsycho.2006.06.027
- Goode, T. D., Tanaka, K. Z., Sahay, A., & McHugh, T. J. (2020). An Integrated Index: Engrams, Place Cells, and Hippocampal Memory. *Neuron*, 107(5), 805-820. doi:10.1016/j.neuron.2020.07.011

- Gruber, A. J., Dayan, P., Gutkin, B. S., & Solla, S. A. (2006). Dopamine modulation in the basal ganglia locks the gate to working memory. *J Comput Neurosci*, *20*(2), 153-166. doi:10.1007/s10827-005-5705-x
- Gruber, O., Hasan, A., Scherk, H., Wobrock, T., Schneider-Axmann, T., Ekawardhani, S., Schmitt, A., Backens, M., Reith, W., Meyer, J., & Falkai, P. (2012). Association of the brain-derived neurotrophic factor val66met polymorphism with magnetic resonance spectroscopic markers in the human hippocampus: in vivo evidence for effects on the glutamate system. *Eur Arch Psychiatry Clin Neurosci*, *262*(1), 23-31. doi:10.1007/s00406-011-0214-6
- Guida, A., Gobet, F., Tardieu, H., & Nicolas, S. (2012). How chunks, long-term working memory and templates offer a cognitive explanation for neuroimaging data on expertise acquisition: a two-stage framework. *Brain Cogn*, *79*(3), 221-244. doi:10.1016/j.bandc.2012.01.010
- Gulliksen, H. (1934). A Rational Equation of the Learning Curve Based on Thorndike's Law of Effect. *The Journal of General Psychology*, *11*(2), 395-434. doi:10.1080/00221309.1934.9917847
- Haber, S. N. (2003). The primate basal ganglia: parallel and integrative networks. *J Chem Neuroanat*, *26*(4), 317-330. doi:10.1016/j.jchemneu.2003.10.003
- Hainmueller, T., & Bartos, M. (2020). Dentate gyrus circuits for encoding, retrieval and discrimination of episodic memories. *Nat Rev Neurosci*, *21*(3), 153-168. doi:10.1038/s41583-019-0260-z
- Hariri, A. R., Goldberg, T. E., Mattay, V. S., Kolachana, B. S., Callicott, J. H., Egan, M. F., & Weinberger, D. R. (2003). Brain-derived neurotrophic factor val66met polymorphism affects human memory-related hippocampal activity and predicts memory performance. *J Neurosci*, *23*(17), 6690-6694.
- Harris, S. E., Fox, H., Wright, A. F., Hayward, C., Starr, J. M., Whalley, L. J., & Deary, I. J. (2006). The brain-derived neurotrophic factor Val66Met polymorphism is associated with age-related change in reasoning skills. *Mol Psychiatry*, *11*(5), 505-513. doi:10.1038/sj.mp.4001799
- Hashimoto, R., Moriguchi, Y., Yamashita, F., Mori, T., Nemoto, K., Okada, T., Hori, H., Noguchi, H., Kunugi, H., & Ohnishi, T. (2008). Dose-dependent effect of the Val66Met polymorphism of the brain-derived neurotrophic factor gene on memory-related hippocampal activity. *Neurosci Res*, *61*(4), 360-367. doi:10.1016/j.neures.2008.04.003
- Hebb, D. O. (1949). *The Organization of Behavior: A Neuropsychological Theory*. New York: Wiley.
- Hertrich, I., Dietrich, S., & Ackermann, H. (2016). The role of the supplementary motor area for speech and language processing. *Neurosci Biobehav Rev*, *68*, 602-610. doi:10.1016/j.neubiorev.2016.06.030
- Hikosaka, O., Takikawa, Y., & Kawagoe, R. (2000). Role of the basal ganglia in the control of purposive saccadic eye movements. *Physiol Rev*, *80*(3), 953-978.
- Howes, O., McCutcheon, R., & Stone, J. (2015). Glutamate and dopamine in schizophrenia: an update for the 21st century. *J Psychopharmacol*, *29*(2), 97-115. doi:10.1177/0269881114563634

- Howes, O. D., McCutcheon, R., Owen, M. J., & Murray, R. M. (2017). The Role of Genes, Stress, and Dopamine in the Development of Schizophrenia. *Biol Psychiatry*, *81*(1), 9-20. doi:10.1016/j.biopsych.2016.07.014
- Jabbi, M., Cropp, B., Nash, T., Kohn, P., Kippenhan, J. S., Masdeu, J. C., Mattay, R., Kolachana, B., & Berman, K. F. (2017). BDNF Val(66)Met polymorphism tunes frontolimbic circuitry during affective contextual learning. *Neuroimage*, *162*, 373-383. doi:10.1016/j.neuroimage.2017.08.080
- Jansma JM, R. N., Slagter HA, Kahn RS (2001). Functional anatomical correlates of controlled and automatic processing. *Journal of Cognitive Neuroscience* *13*:730-743. doi:doi:10.1162/08989290152541403
- Jenkinson, M., Bannister, P., Brady, M., & Smith, S. (2002). Improved optimization for the robust and accurate linear registration and motion correction of brain images. *Neuroimage*, *17*(2), 825-841.
- Jovanovic, J. N., Czernik, A. J., Fienberg, A. A., Greengard, P., & Sihra, T. S. (2000). Synapsins as mediators of BDNF-enhanced neurotransmitter release. *Nat Neurosci*, *3*(4), 323-329. doi:10.1038/73888
- Jung, K., Friston, K. J., Pae, C., Choi, H. H., Tak, S., Choi, Y. K., Park, B., Park, C. A., Cheong, C., & Park, H. J. (2018). Effective connectivity during working memory and resting states: A DCM study. *Neuroimage*, *169*, 485-495. doi:10.1016/j.neuroimage.2017.12.067
- Kambeitz, J. P., Bhattacharyya, S., Kambeitz-Ilankovic, L. M., Valli, I., Collier, D. A., & McGuire, P. (2012). Effect of BDNF val(66)met polymorphism on declarative memory and its neural substrate: a meta-analysis. *Neurosci Biobehav Rev*, *36*(9), 2165-2177. doi:10.1016/j.neubiorev.2012.07.002
- Karnik, M. S., Wang, L., Barch, D. M., Morris, J. C., & Csernansky, J. G. (2010). BDNF polymorphism rs6265 and hippocampal structure and memory performance in healthy control subjects. *Psychiatry Res*, *178*(2), 425-429. doi:10.1016/j.psychres.2009.09.008
- Kemp, J. M., & Powell, T. P. (1970). The cortico-striate projection in the monkey. *Brain*, *93*(3), 525-546. doi:10.1093/brain/93.3.525
- Kim, D. J., Park, B., & Park, H. J. (2013). Functional connectivity-based identification of subdivisions of the basal ganglia and thalamus using multilevel independent component analysis of resting state fMRI. *Hum Brain Mapp*, *34*(6), 1371-1385. doi:10.1002/hbm.21517
- Kodama, M., Ono, T., Yamashita, F., Ebata, H., Liu, M., Kasuga, S., & Ushiba, J. (2018). Structural Gray Matter Changes in the Hippocampus and the Primary Motor Cortex on An-Hour-to-One- Day Scale Can Predict Arm-Reaching Performance Improvement. *Front Hum Neurosci*, *12*, 209. doi:10.3389/fnhum.2018.00209
- Koob, G. F., & Volkow, N. D. (2010). Neurocircuitry of addiction. *Neuropsychopharmacology*, *35*(1), 217-238. doi:10.1038/npp.2009.110

- Kreitzer, A. C., & Malenka, R. C. (2008). Striatal plasticity and basal ganglia circuit function. *Neuron*, *60*(4), 543-554. doi:10.1016/j.neuron.2008.11.005
- Kuipers, S. D., & Bramham, C. R. (2006). Brain-derived neurotrophic factor mechanisms and function in adult synaptic plasticity: new insights and implications for therapy. *Curr Opin Drug Discov Devel*, *9*(5), 580-586.
- Landau, S. M., Schumacher, E. H., Garavan, H., Druzgal, T. J., & D'Esposito, M. (2004). A functional MRI study of the influence of practice on component processes of working memory. *Neuroimage*, *22*(1), 211-221. doi:10.1016/j.neuroimage.2004.01.003
- Lazarov, O., & Hollands, C. (2016). Hippocampal neurogenesis: Learning to remember. *Prog Neurobiol*, *138-140*, 1-18. doi:10.1016/j.pneurobio.2015.12.006
- Lehericy, S., Benali, H., Van de Moortele, P. F., Pelegrini-Issac, M., Waechter, T., Ugurbil, K., & Doyon, J. (2005). Distinct basal ganglia territories are engaged in early and advanced motor sequence learning. *Proc Natl Acad Sci U S A*, *102*(35), 12566-12571. doi:10.1073/pnas.0502762102
- LeMoult, J., Carver, C. S., Johnson, S. L., & Joormann, J. (2015). Predicting change in symptoms of depression during the transition to university: the roles of BDNF and working memory capacity. *Cogn Affect Behav Neurosci*, *15*(1), 95-103. doi:10.3758/s13415-014-0305-8
- Li, B., Arime, Y., Hall, F. S., Uhl, G. R., & Sora, I. (2010). Impaired spatial working memory and decreased frontal cortex BDNF protein level in dopamine transporter knockout mice. *Eur J Pharmacol*, *628*(1-3), 104-107. doi:10.1016/j.ejphar.2009.11.036
- Li, Y. X., Zhang, Y., Lester, H. A., Schuman, E. M., & Davidson, N. (1998). Enhancement of neurotransmitter release induced by brain-derived neurotrophic factor in cultured hippocampal neurons. *J Neurosci*, *18*(24), 10231-10240. doi:10.1523/jneurosci.18-24-10231.1998
- Lin, C.-C., & Huang, T.-L. (2020). Brain-derived neurotrophic factor and mental disorders. *Biomedical Journal*, *43*(2), 134-142. doi:https://doi.org/10.1016/j.bj.2020.01.001
- Makris, N., Goldstein, J. M., Kennedy, D., Hodge, S. M., Caviness, V. S., Faraone, S. V., Tsuang, M. T., & Seidman, L. J. (2006). Decreased volume of left and total anterior insular lobule in schizophrenia. *Schizophr Res*, *83*(2-3), 155-171. doi:10.1016/j.schres.2005.11.020
- Marreiros, A. C., Cagnan, H., Moran, R. J., Friston, K. J., & Brown, P. (2013). Basal ganglia-cortical interactions in Parkinsonian patients. *Neuroimage*, *66*, 301-310. doi:10.1016/j.neuroimage.2012.10.088
- Mazur, J. E., & Hastie, R. (1978). Learning as accumulation: a reexamination of the learning curve. *Psychol Bull*, *85*(6), 1256-1274.
- McClelland, J. L., McNaughton, B. L., & O'Reilly, R. C. (1995). Why there are complementary learning systems in the hippocampus and neocortex: insights from the successes and failures of



- connectionist models of learning and memory. *Psychol Rev*, 102(3), 419-457.  
doi:10.1037/0033-295x.102.3.419
- McCutcheon, R. A., Abi-Dargham, A., & Howes, O. D. (2019). Schizophrenia, Dopamine and the Striatum: From Biology to Symptoms. *Trends Neurosci*, 42(3), 205-220.  
doi:10.1016/j.tins.2018.12.004
- McHughen, S. A., Pearson-Fuhrhop, K., Ngo, V. K., & Cramer, S. C. (2011). Intense training overcomes effects of the val66met BDNF polymorphism on short-term plasticity. *Experimental Brain Research*, 213(4), 415. doi:10.1007/s00221-011-2791-z
- McNab, F., & Klingberg, T. (2008). Prefrontal cortex and basal ganglia control access to working memory. *Nat Neurosci*, 11(1), 103-107. doi:10.1038/nn2024
- Menegas, W., Akiti, K., Amo, R., Uchida, N., & Watabe-Uchida, M. (2018). Dopamine neurons projecting to the posterior striatum reinforce avoidance of threatening stimuli. *Nat Neurosci*, 21(10), 1421-1430. doi:10.1038/s41593-018-0222-1
- Menegas, W., Babayan, B. M., Uchida, N., & Watabe-Uchida, M. (2017). Opposite initialization to novel cues in dopamine signaling in ventral and posterior striatum in mice. *Elife*, 6.  
doi:10.7554/eLife.21886
- Menon, V. (2011). Large-scale brain networks and psychopathology: a unifying triple network model. *Trends Cogn Sci*, 15(10), 483-506. doi:10.1016/j.tics.2011.08.003
- Meyer-Lindenberg, A. (2010). From maps to mechanisms through neuroimaging of schizophrenia. *Nature*, 468(7321), 194-202. doi:10.1038/nature09569
- Meyer-Lindenberg, A., Kohn, P. D., Kolachana, B., Kippenhan, S., McInerney-Leo, A., Nussbaum, R., Weinberger, D. R., & Berman, K. F. (2005). Midbrain dopamine and prefrontal function in humans: interaction and modulation by COMT genotype. *Nat Neurosci*, 8(5), 594-596.  
doi:10.1038/nn1438
- Meyer-Lindenberg, A., Nichols, T., Callicott, J. H., Ding, J., Kolachana, B., Buckholtz, J., Mattay, V. S., Egan, M., & Weinberger, D. R. (2006). Impact of complex genetic variation in COMT on human brain function. *Molecular Psychiatry*, 11(9), 867-877. doi:10.1038/sj.mp.4001860
- Meyer-Lindenberg, A., & Weinberger, D. R. (2006). Intermediate phenotypes and genetic mechanisms of psychiatric disorders. *Nat Rev Neurosci*, 7(10), 818-827. doi:10.1038/nrn1993
- Miller, G. A. (1956). The magical number seven plus or minus two: some limits on our capacity for processing information. *Psychol Rev*, 63(2), 81-97.
- Mink, J. W. (1996). The basal ganglia: focused selection and inhibition of competing motor programs. *Prog Neurobiol*, 50(4), 381-425.

- Montag, C., Felten, A., Markett, S., Fischer, L., Winkel, K., Cooper, A., & Reuter, M. (2014). The role of the BDNF Val66Met polymorphism in individual differences in long-term memory capacity. *J Mol Neurosci*, *54*(4), 796-802. doi:10.1007/s12031-014-0417-1
- Moore, A. B., Li, Z., Tyner, C. E., Hu, X., & Crosson, B. (2013). Bilateral basal ganglia activity in verbal working memory. *Brain Lang*, *125*(3), 316-323. doi:10.1016/j.bandl.2012.05.003
- Muller, N. G., & Knight, R. T. (2006). The functional neuroanatomy of working memory: contributions of human brain lesion studies. *Neuroscience*, *139*(1), 51-58. doi:10.1016/j.neuroscience.2005.09.018
- Murty, V. P., Ballard, I. C., Macduffie, K. E., Krebs, R. M., & Adcock, R. A. (2013). Hippocampal networks habituate as novelty accumulates. *Learn Mem*, *20*(4), 229-235. doi:10.1101/lm.029728.112
- Nagel, B. J., Herting, M. M., Maxwell, E. C., Bruno, R., & Fair, D. (2013). Hemispheric lateralization of verbal and spatial working memory during adolescence. *Brain Cogn*, *82*(1), 58-68. doi:10.1016/j.bandc.2013.02.007
- Nee, D. E., & Brown, J. W. (2013). Dissociable frontal-striatal and frontal-parietal networks involved in updating hierarchical contexts in working memory. *Cereb Cortex*, *23*(9), 2146-2158. doi:10.1093/cercor/bhs194
- Nelson, A. B., & Kreitzer, A. C. (2014). Reassessing models of basal ganglia function and dysfunction. *Annu Rev Neurosci*, *37*, 117-135. doi:10.1146/annurev-neuro-071013-013916
- Newell, A., & Rosenbloom, P. S. (1980). *Mechanisms of Skill Acquisition and the Law of Practice*: Carnegie-Mellon University, Department of Computer Science.
- Nicoll, R. A. (2017). A Brief History of Long-Term Potentiation. *Neuron*, *93*(2), 281-290. doi:10.1016/j.neuron.2016.12.015
- Notaras, M., Hill, R., & van den Buuse, M. (2015). The BDNF gene Val66Met polymorphism as a modifier of psychiatric disorder susceptibility: progress and controversy. *Mol Psychiatry*, *20*(8), 916-930. doi:10.1038/mp.2015.27
- Notaras, M., & van den Buuse, M. (2019). Brain-Derived Neurotrophic Factor (BDNF): Novel Insights into Regulation and Genetic Variation. *Neuroscientist*, *25*(5), 434-454. doi:10.1177/1073858418810142
- Numakawa, T., Odaka, H., & Adachi, N. (2018). Actions of Brain-Derived Neurotrophin Factor in the Neurogenesis and Neuronal Function, and Its Involvement in the Pathophysiology of Brain Diseases. *Int J Mol Sci*, *19*(11). doi:10.3390/ijms19113650
- O'Reilly, R. C., & Frank, M. J. (2006). Making working memory work: a computational model of learning in the prefrontal cortex and basal ganglia. *Neural Comput*, *18*(2), 283-328. doi:10.1162/089976606775093909

- O'Reilly, R. C., & Rudy, J. W. (2001). Conjunctive representations in learning and memory: principles of cortical and hippocampal function. *Psychol Rev*, *108*(2), 311-345. doi:10.1037/0033-295x.108.2.311
- Oldfield, R. C. (1971). The assessment and analysis of handedness: the Edinburgh inventory. *Neuropsychologia*, *9*(1), 97-113.
- Parent, A. (1990). Extrinsic connections of the basal ganglia. *Trends Neurosci*, *13*(7), 254-258.
- Parent, A., & Hazrati, L. N. (1995). Functional anatomy of the basal ganglia. I. The cortico-basal ganglia-thalamo-cortical loop. *Brain Res Brain Res Rev*, *20*(1), 91-127.
- Park, H., Popescu, A., & Poo, M. M. (2014). Essential role of presynaptic NMDA receptors in activity-dependent BDNF secretion and corticostriatal LTP. *Neuron*, *84*(5), 1009-1022. doi:10.1016/j.neuron.2014.10.045
- Penny, W. D., Stephan, K. E., Daunizeau, J., Rosa, M. J., Friston, K. J., Schofield, T. M., & Leff, A. P. (2010). Comparing families of dynamic causal models. *PLoS Comput Biol*, *6*(3), e1000709. doi:10.1371/journal.pcbi.1000709
- Perakyla, J., Sun, L., Lehtimaki, K., Peltola, J., Ohman, J., Mottonen, T., Ogawa, K. H., & Hartikainen, K. M. (2017). Causal Evidence from Humans for the Role of Mediodorsal Nucleus of the Thalamus in Working Memory. *J Cogn Neurosci*, *29*(12), 2090-2102. doi:10.1162/jocn\_a\_01176
- Peters, S. K., Dunlop, K., & Downar, J. (2016). Cortico-Striatal-Thalamic Loop Circuits of the Salience Network: A Central Pathway in Psychiatric Disease and Treatment. *Front Syst Neurosci*, *10*, 104. doi:10.3389/fnsys.2016.00104
- Power, J. D., Barnes, K. A., Snyder, A. Z., Schlaggar, B. L., & Petersen, S. E. (2012). Spurious but systematic correlations in functional connectivity MRI networks arise from subject motion. *Neuroimage*, *59*(3), 2142-2154. doi:10.1016/j.neuroimage.2011.10.018
- Quide, Y., Morris, R. W., Shepherd, A. M., Rowland, J. E., & Green, M. J. (2013). Task-related fronto-striatal functional connectivity during working memory performance in schizophrenia. *Schizophr Res*, *150*(2-3), 468-475. doi:10.1016/j.schres.2013.08.009
- Rebola, N., Carta, M., & Mulle, C. (2017). Operation and plasticity of hippocampal CA3 circuits: implications for memory encoding. *Nat Rev Neurosci*, *18*(4), 208-220. doi:10.1038/nrn.2017.10
- Reiner, A., Dragatsis, I., & Dietrich, P. (2011). Genetics and neuropathology of Huntington's disease. *Int Rev Neurobiol*, *98*, 325-372. doi:10.1016/b978-0-12-381328-2.00014-6
- Restle, F., & Greeno, J. G. (1970). *Introduction to mathematical psychology*. Oxford, England: Addison-Wesley.

- Rigoux, L., Stephan, K. E., Friston, K. J., & Daunizeau, J. (2014). Bayesian model selection for group studies - revisited. *Neuroimage*, *84*, 971-985. doi:10.1016/j.neuroimage.2013.08.065
- Robertson, L. T. (2002). Memory and the brain. *J Dent Educ*, *66*(1), 30-42.
- Sankar, A., Adams, T. M., Costafreda, S. G., Marangell, L. B., & Fu, C. H. (2017). Effects of antidepressant therapy on neural components of verbal working memory in depression. *J Psychopharmacol*, *31*(9), 1176-1183. doi:10.1177/0269881117724594
- Schofield, P. R., Williams, L. M., Paul, R. H., Gatt, J. M., Brown, K., Luty, A., Cooper, N., Grieve, S., Dobson-Stone, C., Morris, C., Kuan, S. A., & Gordon, E. (2009). Disturbances in selective information processing associated with the BDNF Val66Met polymorphism: evidence from cognition, the P300 and fronto-hippocampal systems. *Biol Psychol*, *80*(2), 176-188. doi:10.1016/j.biopsycho.2008.09.001
- Schroll, H., & Hamker, F. H. (2013). Computational models of basal-ganglia pathway functions: focus on functional neuroanatomy. *Front Syst Neurosci*, *7*, 122. doi:10.3389/fnsys.2013.00122
- Schweiger, J. I., Bilek, E., Schäfer, A., Braun, U., Moessnang, C., Harneit, A., Post, P., Otto, K., Romanczuk-Seiferth, N., Erk, S., et al. (2019). Effects of BDNF Val(66)Met genotype and schizophrenia familial risk on a neural functional network for cognitive control in humans. *Neuropsychopharmacology*, *44*(3), 590-597. doi:10.1038/s41386-018-0248-9
- Seeman, P., & Lee, T. (1975). Antipsychotic drugs: direct correlation between clinical potency and presynaptic action on dopamine neurons. *Science*, *188*(4194), 1217-1219. doi:10.1126/science.1145194
- Seeman, P., Lee, T., Chau-Wong, M., & Wong, K. (1976). Antipsychotic drug doses and neuroleptic/dopamine receptors. *Nature*, *261*(5562), 717-719. doi:10.1038/261717a0
- Seger, C. A. (2006). The basal ganglia in human learning. *Neuroscientist*, *12*(4), 285-290. doi:10.1177/1073858405285632
- Shastri, L. (2002). Episodic memory and cortico-hippocampal interactions. *Trends Cogn Sci*, *6*(4), 162-168. doi:10.1016/s1364-6613(02)01868-5
- Shen, T., You, Y., Joseph, C., Mirzaei, M., Klistorner, A., Graham, S. L., & Gupta, V. (2018). BDNF Polymorphism: A Review of Its Diagnostic and Clinical Relevance in Neurodegenerative Disorders. *Aging Dis*, *9*(3), 523-536. doi:10.14336/ad.2017.0717
- Shen, W., Flajolet, M., Greengard, P., & Surmeier, D. J. (2008). Dichotomous dopaminergic control of striatal synaptic plasticity. *Science*, *321*(5890), 848-851. doi:10.1126/science.1160575
- Shepherd, G. M. (2013). Corticostriatal connectivity and its role in disease. *Nat Rev Neurosci*, *14*(4), 278-291. doi:10.1038/nrn3469
- Shiffrin, R., & Schneider, W. (1977). Controlled and automatic human information processing: II. Perceptual learning, automatic attending, and a general theory. *Psychol Rev* (84), 127-190.

- Snyder, S. H. (1976). The dopamine hypothesis of schizophrenia: focus on the dopamine receptor. *Am J Psychiatry*, *133*(2), 197-202. doi:10.1176/ajp.133.2.197
- Soltész, F., Suckling, J., Lawrence, P., Tait, R., Ooi, C., Bentley, G., Dodds, C. M., Miller, S. R., Wille, D. R., Byrne, M., McHugh, S. M., Bellgrove, M. A., Croft, R. J., Lu, B., Bullmore, E. T., & Nathan, P. J. (2014). Identification of BDNF sensitive electrophysiological markers of synaptic activity and their structural correlates in healthy subjects using a genetic approach utilizing the functional BDNF Val66Met polymorphism. *PLoS One*, *9*(4), e95558. doi:10.1371/journal.pone.0095558
- Sorg, C., Manoliu, A., Neufang, S., Myers, N., Peters, H., Schwerthöffer, D., Scherr, M., Mühlau, M., Zimmer, C., Drzezga, A., Förstl, H., Bäuml, J., Eichele, T., Wohlschläger, A. M., & Riedl, V. (2013). Increased intrinsic brain activity in the striatum reflects symptom dimensions in schizophrenia. *Schizophr Bull*, *39*(2), 387-395. doi:10.1093/schbul/sbr184
- Staresina, B. P., Cooper, E., & Henson, R. N. (2013). Reversible information flow across the medial temporal lobe: the hippocampus links cortical modules during memory retrieval. *J Neurosci*, *33*(35), 14184-14192. doi:10.1523/JNEUROSCI.1987-13.2013
- Stephan, K. E., Penny, W. D., Daunizeau, J., Moran, R. J., & Friston, K. J. (2009). Bayesian model selection for group studies. *Neuroimage*, *46*(4), 1004-1017. doi:10.1016/j.neuroimage.2009.03.025
- Stephan, K. E., Penny, W. D., Moran, R. J., den Ouden, H. E., Daunizeau, J., & Friston, K. J. (2010). Ten simple rules for dynamic causal modeling. *Neuroimage*, *49*(4), 3099-3109. doi:10.1016/j.neuroimage.2009.11.015
- Stephan, K. E., Weiskopf, N., Drysdale, P. M., Robinson, P. A., & Friston, K. J. (2007). Comparing hemodynamic models with DCM. *Neuroimage*, *38*(3), 387-401. doi:10.1016/j.neuroimage.2007.07.040
- Thurstone, L. L. (1919). The learning curve equation. *Psychological Monographs*, *26*(3), i-51. doi:10.1037/h0093187
- Tost, H., Alam, T., & Meyer-Lindenberg, A. (2010). Dopamine and psychosis: theory, pathomechanisms and intermediate phenotypes. *Neurosci Biobehav Rev*, *34*(5), 689-700. doi:10.1016/j.neubiorev.2009.06.005
- Trapp, S., Schroll, H., & Hamker, F. H. (2012). Open and closed loops: A computational approach to attention and consciousness. *Adv Cogn Psychol*, *8*(1), 1-8. doi:10.2478/v10053-008-0096-y
- Tyler, W. J., & Pozzo-Miller, L. D. (2001). BDNF enhances quantal neurotransmitter release and increases the number of docked vesicles at the active zones of hippocampal excitatory synapses. *J Neurosci*, *21*(12), 4249-4258. doi:10.1523/jneurosci.21-12-04249.2001
- Tzourio-Mazoyer, N., Landeau, B., Papathanassiou, D., Crivello, F., Etard, O., Delcroix, N., Mazoyer, B., & Joliot, M. (2002). Automated anatomical labeling of activations in SPM using a macroscopic anatomical parcellation of the MNI MRI single-subject brain. *Neuroimage*, *15*(1), 273-289. doi:10.1006/nimg.2001.0978

- Vallar, G., Di Betta, A. M., & Silveri, M. C. (1997). The phonological short-term store-rehearsal system: patterns of impairment and neural correlates. *Neuropsychologia*, *35*(6), 795-812.
- Vallar, G. P., C. (2002). *Handbook of Memory Disorders* A. D. Baddeley, Kopelman, M. D. & Wilson, B. A. Ed. Wiley, Chichester.
- Van Dijk, K. R., Sabuncu, M. R., & Buckner, R. L. (2012). The influence of head motion on intrinsic functional connectivity MRI. *Neuroimage*, *59*(1), 431-438. doi:10.1016/j.neuroimage.2011.07.044
- van Raalten, T. R., Ramsey, N. F., Duyn, J., & Jansma, J. M. (2008). Practice induces function-specific changes in brain activity. *PLoS ONE*, *3*(10), e3270. doi:10.1371/journal.pone.0003270
- van Raalten, T. R., Ramsey, N. F., Jansma, J. M., Jager, G., & Kahn, R. S. (2008). Automatization and working memory capacity in schizophrenia. *Schizophr Res*, *100*(1-3), 161-171. doi:10.1016
- van Schouwenburg, M. R., den Ouden, H. E., & Cools, R. (2010). The human basal ganglia modulate frontal-posterior connectivity during attention shifting. *J Neurosci*, *30*(29), 9910-9918. doi:10.1523/JNEUROSCI.1111-10.2010
- von Bastian, C. C., & Oberauer, K. (2014). Effects and mechanisms of working memory training: a review. *Psychol Res*, *78*(6), 803-820. doi:10.1007/s00426-013-0524-6
- Wang, C., Liu, B., Long, H., Fan, L., Li, J., Zhang, X., Qiu, C., Yu, C., & Jiang, T. (2015). Epistatic interaction of BDNF and COMT on the frontostriatal system. *Neuroscience*, *298*, 380-388. doi:10.1016/j.neuroscience.2015.04.014
- Wang, C., Zhang, Y., Liu, B., Long, H., Yu, C., & Jiang, T. (2014). Dosage effects of BDNF Val66Met polymorphism on cortical surface area and functional connectivity. *J Neurosci*, *34*(7), 2645-2651. doi:10.1523/JNEUROSCI.3501-13.2014
- Wittmann, B. C., Daw, N. D., Seymour, B., & Dolan, R. J. (2008). Striatal activity underlies novelty-based choice in humans. *Neuron*, *58*(6), 967-973. doi:10.1016/j.neuron.2008.04.027
- Zang, Z., Geiger, L. S., Braun, U., Cao, H., Zangl, M., Schafer, A., Moessnang, C., Ruf, M., Reis, J., Schweiger, J. I., Dixon, L., Moscicki, A., Schwarz, E., Meyer-Lindenberg, A., & Tost, H. (2018). Resting-state brain network features associated with short-term skill learning ability in humans and the influence of N-methyl-d-aspartate receptor antagonism. *Netw Neurosci*, *2*(4), 464-480. doi:10.1162/netn\_a\_00045
- Zink, C. F., Pagnoni, G., Martin, M. E., Dhamala, M., & Berns, G. S. (2003). Human striatal response to salient nonrewarding stimuli. *J Neurosci*, *23*(22), 8092-8097.

## 6. Supplemental Tables

**TABLE S1:** Brain activations for the main effect of memory phase and their respective coordinates in MNI space from AAL atlas.

Region (Brodmann area)	Cluster size	t value	Peak MNI coordinates		
			x	y	z
<i>Encoding &gt; retrieval</i>					
Middle occipital gyrus (BA 18)	30.559	17.04	-30	-94	9
Inferior occipital gyrus (BA 19)		16.39	33	-85	-9
Inferior occipital gyrus (BA 19)		16.14	-39	-82	-9
Fusiform gyrus (BA 19/37)		15.84	42	-64	-12
Fusiform gyrus (BA 19/37)		15.68	-39	-70	-12
Middle Cingulum (BA 23)		15.42	-3	-31	33
Precuneus (BA 7)		15.38	27	-64	45
Middle occipital gyrus (BA 18)		14.51	30	-88	-12
Middle Cingulum (BA 23)		14.16	3	-31	33
Precuneus (BA 7)		13.98	-27	-61	51
Insula (BA 13)		13.72	-33	23	0
Precentral gyrus (BA 4)		13.36	-48	-7	42
Insula (BA 13)		13.22	36	26	-3
Middle temporal gyrus (BA 22)		13.1	-54	-34	0
Anterior Cingulum (BA 32)		13.1	12	26	27
Superior temporal gyrus (BA 39/40)		13.1	-54	-34	0
Middle temporal gyrus (BA 22)		12.98	48	-28	-3
Superior temporal gyrus (BA 39/40)		12.98	48	-28	-3
SMA (BA 6)		12.71	-3	5	63
Hippocampus		12.35	-21	-31	-6
Anterior Cingulum (BA 24/32)		12.34	-9	32	24
Precentral Gyrus (BA 4)		11.67	51	-1	42
Hippocampus		11.2	21	-31	-6
Thalamus		11.01	6	-10	0
Anterior Putamen		10.98	-18	14	3
SMA (BA 6)		10.81	3	5	63
Anterior Putamen		10.64	18	14	0
Thalamus		10.35	-6	-13	0
DLPFC (BA 10/46)		9.99	51	35	15
Parietal inferior gyrus (40)		9.81	42	-58	48
Cerebellum/Vermis		9.11	-3	-73	-27
DLPFC (10/46)		8.27	-48	35	15
Cerebellum		7.92	-27	-64	-30
Parietal inferior gyrus (BA 40)		7.55	-42	-43	45
Inferior frontal gyrus (BA 44/45)		7.05	-54	17	6
Cerebellum		6.52	33	-61	-33
Inferior frontal gyrus (BA 44/45)		6.22	51	23	3

Region (Brodmann area)	Cluster size	t value	Peak MNI coordinates		
			x	y	z
<i>Retrieval &gt; novel</i>					
Postcentral gyrus (BA3)	24	5.69	-39	-28	57

Note: Regions are  $p < 0.05$  family-wise error corrected for the whole brain and classified according to the AAL Atlas (Tzourio-Mazoyer et al., 2002). Coordinates (MNI space) and statistical information refer to the peak voxel in the corresponding area. Abbreviations: Automated Anatomical Labeling (AAL), Montreal Neuroimaging (MNI), supplementary motor areas (SMA), dorsal premotor cortex (dPMC), dorsolateral prefrontal cortex (DLPFC).

**TABLE S2:** Bayesian parameter averages of the winning model.

Intrinsic connections		From		
		DLPFC	Striatum	Thalamus
To	DLPFC	-.74	-.03	-.02
	Striatum	-.04	-1.30	-.14
	Thalamus	.03	-.03	-1.54
<b>Modulation of connectivity</b>		Encoding novel		
		From		
		DLPFC	Striatum	Thalamus
To	DLPFC	-	0.87	-1.28
	Striatum	1.33	-	.64
	Thalamus	.29	.47	-
		Encoding practiced		
		From		
		DLPFC	Striatum	Thalamus
To	DLPFC	-	not significant	-.85
	Striatum	.14	-	1.46
	Thalamus	not significant	.49	-
<b>Input</b>		Encoding novel		Encoding practiced
To	DLPFC	.24		-.09



**Table S3: Behavioral analysis of short-term effects (learning curves)**

Descriptive statistics			Inference statistics			
Mean (SD)				2x3 rmANOVA		Post-hoc
Val/Val (N = 11)	Met-carrier (N = 12)	Effect	F-statistics	$\eta^2$	T-statistics	
<b>LEARNING CURVE</b>						
<b><math>\rho</math> - GoF<sup>3)</sup></b>						
P	0.76 (0.29)	0.72 (0.35)	Genotype: $F_{(1,21)} = 0.09$ , $p = .761$	.005		
S	0.75 (0.34)	0.84 (0.29)	Condition: $F_{(1.73,36.4)} = 0.83$ , $p = .429$	.038		
N	0.74 (0.25)	0.62 (0.33)	Interaction: $F_{(1.73,36.4)} = 0.77$ , $p = .454$	.035		
<b><math>\alpha</math> - learning gain</b>						
P	0.12 (0.05)	0.26 (0.17)	Genotype: $F_{(1,21)} = 5.10$ , $p = .035^*$	.195	Met>Val: <sup>a</sup> $T_{(13.4)} = 2.74$ , $p = .016^*$	
S	0.20 (0.10)	0.30 (0.16)	Condition: $F_{(2.0,41.3)} = 1.68$ , $p = .200$	.074		
N	0.22 (0.14)	0.25 (0.13)	Interaction: $F_{(2.0,41.3)} = 1.68$ , $p = .266$	.061		
<b><math>\tau</math> - learning speed</b>						
P	-2.21 (2.65)	-1.11 (1.03)	Genotype: $F_{(1,21)} = 0.53$ , $p = .475$	.025		
S	-1.03 (1.86)	-1.52 (1.79)	Condition: $F_{(1.8,37.6)} = 3.69$ , $p = .039^*$	.150	$\tau_{(PT)} < \tau_{(ST)}$ : <sup>b</sup> $T_{(22)} = 0.70$ , $p = .489$	
					$\tau_{(PT)} < \tau_{(NT)}$ : <sup>b</sup> $T_{(22)} = 3.22$ , $p = .004^*$	
					$\tau_{(ST)} < \tau_{(NT)}$ : <sup>b</sup> $T_{(22)} = 1.76$ , $p = .091^+$	
N	-0.79 (1.81)	-0.26 (0.36)	Interaction: $F_{(1.8,37.6)} = 1.80$ , $p = .182$	.079		
<b>Discrimination analyses (LDA)</b>						
	ACC (%) <sup>c</sup>	p (uncorr.) <sup>d</sup>	Class. robustness (%) Mean (SD) <sup>e</sup>		$\chi^2$ - statistics	
P	78.26	.003	76.49 (10.19)		10.48, $p = .005^*$	
S	56.52	.418	59.75 (12.21)		2.99, $p = .224$	
N	52.17	.590	56.77 (12.64)		2.03, $p = .362$	

<sup>a</sup>T-test for independent samples, <sup>b</sup>T-test for dependent samples, <sup>c</sup> original data and, <sup>d</sup> k-fold, split-half, cross-validated means  $\pm$  SDs with  $k = 9999$ , <sup>e</sup>estimated using 9999 permutation operations, \* significant at  $p < .05$ ; + statistical trend  $p < .1$ . For inference statistics,  $\rho$ -values were Fisher z-scaled. Degrees of freedom Greenhouse-Geisser corrected for sphericity violations; all tests were performed two-tailed. Abbreviations: P = practiced stimuli, S = shuffled stimuli, N = novel stimuli, LDA = linear discriminant analyses, ACC = discrimination accuracy.

**Table S4: Monte-Carlo-simulation based estimation of corrected cluster sizes**

Cluster Size	Frequency	Cum Prop	p/Voxel	Max Freq	Alpha
<b>Brain response</b>					
1	10674	0.592769	0.042716	0	1
2	3472	0.785583	0.030144	10	1
3	1505	0.869162	0.021965	66	0.99
4	879	0.917976	0.016647	132	0.924
5	494	0.94541	0.012505	156	0.792
6	317	0.963014	0.009596	134	0.636
7	202	0.974232	0.007356	124	0.502
8	131	0.981507	0.00569	90	0.378
9	116	0.987949	0.004456	91	0.288
10	65	0.991559	0.003226	56	0.197
11	45	0.994058	0.002461	39	0.141
12	34	0.995946	0.001878	31	0.102
13	15	0.996779	0.001397	14	0.071
14	18	0.997779	0.001167	18	0.057
<b>15</b>	<b>10</b>	<b>0.998334</b>	<b>0.00087</b>	<b>9</b>	<b>0.039</b>
<b>Sustained Functional connectivity</b>					
1	5985	0.516973	0.035555	1	1
2	2332	0.718407	0.027882	28	0.999
3	1126	0.815669	0.021903	69	0.971
4	695	0.875702	0.017572	102	0.902
5	405	0.910685	0.014008	119	0.8
6	281	0.934957	0.011412	120	0.681
7	219	0.953874	0.00925	120	0.561
8	142	0.96614	0.007285	102	0.441
9	114	0.975987	0.005828	85	0.339
10	78	0.982724	0.004513	66	0.254
11	57	0.987648	0.003513	51	0.188
12	37	0.990844	0.002709	33	0.137
13	34	0.993781	0.00214	33	0.104
14	13	0.994904	0.001573	12	0.071
15	18	0.996458	0.00134	18	0.059
<b>16</b>	<b>10</b>	<b>0.997322</b>	<b>0.000994</b>	<b>10</b>	<b>0.041</b>

Note: Monte-Carlo-simulation using of AlphaSim as implemented in the software package RESTplus (<http://www.restfmri.net/forum/REST>). Voxel alpha threshold of  $P < .05$ ., Number of Monte Carlo simulations = 1000. The size of the first cluster with a probability of occurrence less than 5% was used to threshold the corresponding statistical map.

**Table S5:** Group comparison of parameter estimates ( $\tau, \alpha$ ) derived from sFC

	Val/Val (N = 11)	Met-carrier (N = 10)	T-statistics (2 sample t-test)
Mean $\tau$ (SD)	-3.6364e <sup>-05</sup> (0.1448)	-0.1532 (0.2248)	T <sub>(19)</sub> = 1.86, p = .008 <sup>+</sup>
Mean $\alpha$ (SD)	0.0970 (0.0355)	0.1151 (0.0468)	T <sub>(19)</sub> = -1.01, p = .327

Note: Parameter estimates (derived from the DLPFC cluster) were z-scaled; T-test for independent samples, <sup>+</sup> statistical trend P < .1; Abbreviations: sFC = sustained functional connectivity, DLPFC = dorsolateral prefrontal cortex

**Table S6:** Sample characteristics and data quality measures.

	Val/Val (N = 11)	Met-carrier (N = 12)	T, $\chi^2$ or F value	P-value
<b>Demographic information</b>				
Age (year)	27.00 ± 5.422	28.67 ± 9.58	-0.51	0.62
Sex (male / female)	4/7	3/9	0.35	0.44
Education (year)	16.00 ± 1.00	15.20 ± 1.30	1.62	0.12
<b>Head motion parameters</b>				
Mean translation(mm)	0.41 ± 0.15	0.38 ± 0.11	0.41	0.53
Mean rotation(degree)	0.32 ± 0.08	0.37 ± 0.03	0.24	0.63
Mean frame-wise displacement (mm)	0.13 ± 0.01	0.15 ± 0.00	0.57	0.46
<b>fMRI image quality</b>				
Signal-to-noise ratio	290.84 ± 13.6	290.60 ± 3.47	0.32	0.58
Number of spikes	6.88 ± 2.77	11.62 ± 7.60	0.83	0.37

Note: Characteristics are displayed as mean ± standard deviation of the mean. T-test for independent samples, significance level at P < 0.05. Abbreviations: Val = Valine, Met = Methionine.

## 7. Curriculum vitae

### Personal Information

**Name:** Lena Sophie Geiger-Primo (geb. Geiger)

**Date of Birth:** 23.10.1985

**Place of Birth:** Tscheljabinsk, Russia

### Academic and Professional Career

- 02/2020 - present    **Central Institute of Mental Health, Mannheim, Germany**  
Residency in Psychiatry
- 12/2011 - present    **Central Institute of Mental Health, Mannheim, Germany**  
Graduate student and research associate in the Research Group: Systems Neuroscience in Psychiatry (SNIP)
- 08/2010 – 11/2011    **Max Planck Institute for Biological Cybernetics, Centre for Integrative Neuroscience, Tübingen, Germany**  
Scientific diploma thesis “Lip-reading: Decoding the neural correlates.”

### Education

- 10/2013 – 12/2019    **Ruprecht-Karls University, Heidelberg, Germany**  
Study of Medicine at the Medical Faculty Mannheim. 3. State examination in 11/2019 (grade 2,0); 2. State examination 10/2018 (grade 3,0); 1. State examination 09/2015 (grade 3,0)
- 11/2018 – 02/2019    **University of Cape Town, Cape Town, South Africa**  
Final year internship in General Internal Medicine at Department of Medicine, Groote Schuur Hospital, Cape Town.
- 10/2005 – 09/2011    **Eberhard-Karls University, Tübingen, Germany**  
Study of Psychology (Diploma, MSc equivalent) at the Department of Psychology (Faculty of Science) (grade: 1,3); Diploma thesis: “Lip-reading: Decoding the neural correlates” (grade: 1,0)
- 07/2008 – 12/2008    **Stellenbosch University, South Africa**  
Elective studies at the Department of Psychology (Faculty of Arts and Social Science) an exchange program with Tübingen University
- 09/2002 – 07/2005    **Wirtschaftsgymnasium Hechingen, Germany**  
High school diploma (Abitur)

## Publications

- Geiger, L. S.**, Zang, Z., Melzer, M., Witt, S., Rietschel, M., van Raalten, T. R., Meyer-Lindenberg, A., Moessnang, C., Wüstenberg, T. & Tost, H. (2021). Longitudinal behavioral and brain functional effects of a plasticity-related variant in *BDNF* on verbal working memory learning. In presubmission to *Proc Natl Acad Sci U S A*.
- Fritze, S., Harneit, A., Waddington, J. L., Kubera, K. M., Schmitgen, M. M., Otte, M. L., **Geiger, L. S.**, Tost, H., Meyer-Lindenberg, A., Wolf, R. C., & Hirjak, D. (in press). Structural alterations in brainstem, basal ganglia and thalamus associated with parkinsonism in schizophrenia spectrum disorders. *European Neuropsychopharmacology*.
- Wolf, R. C., Kubera, K. M., Waddington, J. L., Schmitgen, M. M., Fritze, S., Rashidi, M., Thieme, C. E., Sambataro, F., **Geiger, L. S.**, Tost, H., & Hirjak, D. (2021). A neurodevelopmental signature of parkinsonism in schizophrenia. *Schizophrenia Research*, 231, 54-60. doi: 10.1016/j.schres.2021.03.004
- Zhang, X., Braun, U., Harneit, A., Zang, Z., **Geiger, L. S.**, Betzel, R. F., Chen, J., Schweiger, J. I., Schwarz, K., Reinwald, J. R., Fritze, S., Witt, S., Rietschel, M., Nothen, M. M., Degenhardt, F., Schwarz, E., Hirjak, D., Meyer-Lindenberg, A., Bassett, D. S., & Tost, H. (2021). Generative network models of altered structural brain connectivity in schizophrenia. *Neuroimage*, 225, 117510. doi:10.1016/j.neuroimage.2020.117510
- Wolf, R. C., Rashidi, M., Fritze, S., Kubera, K. M., Northoff, G., Sambataro, F., Calhoun, V. D., **Geiger, L. S.**, Tost, H., & Hirjak, D. (2020). A Neural Signature of Parkinsonism in Patients With Schizophrenia Spectrum Disorders: A Multimodal MRI Study Using Parallel ICA. *Schizophr Bull*, 46(4), 999-1008. doi:10.1093/schbul/sbaa007
- Wasserthal, J., Maier-Hein, K. H., Neher, P. F., Northoff, G., Kubera, K. M., Fritze, S., Harneit, A., **Geiger, L. S.**, Tost, H., Wolf, R. C., & Hirjak, D. (2020). Multiparametric mapping of white matter microstructure in catatonia. *Neuropsychopharmacology*, 45(10), 1750-1757. doi:10.1038/s41386-020-0691-2
- Kremer, T., Braun, U., Chen, J., Harneit, A., Zang, Z., Schweiger, J. I., Gan, G., Reichert, M., Zhang, X., Berhe, O., Ma, R., **Geiger, L.**, Schwarz, K., Mößnang, C., Streit, F., et al. (2020). Epigenetic Signature of FKBP5 is Associated With Structural Variance in Emotion Regulatory Brain Circuits. *Biological Psychiatry*, 87(9, Supplement), S391. doi: 10.1016/j.biopsych.2020.02.1001
- Chen, J., Zang, Z., Braun, U., Schwarz, K., Harneit, A., Kremer, T., Ma, R., Schweiger, J., Moessnang, C., **Geiger, L.**, Cao, H., Degenhardt, F., Nothen, M. M., Tost, H., Meyer-Lindenberg, A., & Schwarz, E. (2020). Association of a Reproducible Epigenetic Risk Profile for Schizophrenia With Brain Methylation and Function. *JAMA Psychiatry*, 77(6), 628-636. doi:10.1001/jama psychiatry.2019.4792
- Hirjak, D., Rashidi, M., Fritze, S., Bertolino, A. L., **Geiger, L. S.**, Zang, Z., Kubera, K. M., Schmitgen, M. M., Sambataro, F., Calhoun, V. D., Weisbrod, M., Tost, H., & Wolf, R. C. (2019). Patterns of co-altered brain structure and function underlying neurological soft signs in schizophrenia spectrum disorders. *Hum Brain Mapp*, 40(17), 5029-5041. doi:10.1002/hbm.24755
- Harneit, A., Braun, U., **Geiger, L. S.**, Zang, Z., Hakobjan, M., van Donkelaar, M. M. J., Schweiger, J. I., Schwarz, K., Gan, G., Erk, S., Heinz, A., Romanczuk-Seiferth, N., Witt, S., Rietschel, M., Walter, H., Franke, B., Meyer-Lindenberg, A., & Tost, H. (2019). MAOA-VNTR genotype affects structural and functional connectivity in distributed brain networks. *Hum Brain Mapp*, 40(18), 5202-5212. doi:10.1002/hbm.24766

- Geiger, L. S.**, Moessnang, C., Schafer, A., Zang, Z., Zangl, M., Cao, H., van Raalten, T.R., Meyer-Lindenberg, A., & Tost, H. (2018). Novelty modulates human striatal activation and prefrontal-striatal effective connectivity during working memory encoding. *Brain Struct Funct.* doi:10.1007/s00429-018-1679-0
- Zang, Z., **Geiger, L. S.**, Braun, U., Cao, H., Zangl, M., Schafer, A., Moessnang, C., Ruf, M., Reis, J., Schweiger, J. I., Dixon, L., Moscicki, A., Schwarz, E., Meyer-Lindenberg, A., & Tost, H. (2018). Resting-state brain network features associated with short-term skill learning ability in humans and the influence of N-methyl-d-aspartate receptor antagonism. *Netw Neurosci*, 2(4), 464-480. doi:10.1162/netn\_a\_00045
- Cao, H., Harneit, A., Walter, H., Erk, S., Braun, U., Moessnang, C., **Geiger, L. S.**, Zang, Z., Mohnke, S., Heinz, A., Romanczuk-Seiferth, N., Muhleisen, T., Mattheisen, M., Witt, S. H., Cichon, S., Nothen, M. M., Rietschel, M., Meyer-Lindenberg, A., & Tost, H. (2018). The 5-HTTLPR Polymorphism Affects Network-Based Functional Connectivity in the Visual-Limbic System in Healthy Adults. *Neuropsychopharmacology*, 43(2), 406-414. doi:10.1038/npp.2017.121
- Braun, U., Schafer, A., Bassett, D. S., Rausch, F., Schweiger, J. I., Bilek, E., Erk, S., Romanczuk-Seiferth, N., Grimm, O., **Geiger, L. S.**, Haddad, L., Otto, K., Mohnke, S., Heinz, A., Zink, M., Walter, H., Schwarz, E., Meyer-Lindenberg, A., & Tost, H. (2016). Dynamic brain network reconfiguration as a potential schizophrenia genetic risk mechanism modulated by NMDA receptor function. *Proc Natl Acad Sci U S A*, 113(44), 12568-12573. doi:10.1073/pnas.1608819113

## 8. Acknowledgments

To begin, I would like to thank Prof. Dr. Dr. Heike Tost and Prof. Dr. Andreas Meyer-Lindenberg for giving me this excellent opportunity to carry out such interesting and exciting research. I truly appreciate the outstanding guidance and advice of Prof. Dr. Dr. Heike Tost throughout the years, and I will always value the extraordinary support during my medical studies.

Then, I would like to thank Dr. Carolin Moessnang for her constant and overwhelming help and support over the last couple of years. Her advice in manuscript writing, methods, and analyses was invaluable. Besides, she always motivated me to carry on.

Furthermore, I would like to thank Dr. Jamila Andoh, who joined the SNIP research group only a few years ago, for her excellent advice towards the end. Where were you hiding before? This thesis would not have been the same without your precious comments.

Further, I would like to thank all of my colleagues from the research group SNiP. A special thanks to Dr. Zhenxiang (John) Zang, my “cellmate” with whom I shared my office, many thoughts, laughter, complaints, and many more experiences, e.g., endless times at the MRI scanner, poster presentations, and conference meetings. Thank you, John, for your trust and support over the years. I would like to thank Janina Schweiger, who became a close friend, for all her help and support during my long time in the SNiP research group and for helping me during my studies, especially with the preparations for my last state exam. Another person who became a close friend is Dr. Ceren Akdeniz, who I thank for her endless help and support, even after leaving the SNiP research group. I would have given up without her support. Further, I would like to thank Mirjam Melzer for her moral, strategical and physical support through data acquisition and running the “BMBF – project.” I would have been lost without you. Further, I would like to thank Dr. Axel Schäfer and Dr. Torsten Wüstenberg for their statistical and computational advice. Me and Matlab would be far worse off without your patience and help in scripting.

Then, I would like to thank my “Medschool-Group” for their lovely company and support over the years. I will never forget the endless hours we have spent in the library, preparing for endless amounts of exams.

Finally, I would like to thank my family. My parents and grandparents for all their love and for believing in me. My big sister, Anna, for her love and support from different parts of the world. Last but not least, I would like to thank my husband, Alphonso, for always understanding my unpredictable “work,” including the endless hours at the MRI scanner, office, library, or clinic. Thank you for your endless love and undying support.